

Utility Theory of Synthetic Data Generation

Shirong Xu* Will Wei Sun[†] Guang Cheng[‡]

Abstract

Synthetic data algorithms are widely employed in industries to generate artificial data for downstream learning tasks. While existing research primarily focuses on empirically evaluating utility of synthetic data, its theoretical understanding is largely lacking. This paper bridges the practice-theory gap by establishing relevant utility theory in a statistical learning framework. It considers two utility metrics: generalization and ranking of models trained on synthetic data. The former is defined as the generalization difference between models trained on synthetic and on real data. By deriving analytical bounds for this utility metric, we demonstrate that the synthetic feature distribution does not need to be similar as that of real data for ensuring comparable generalization of synthetic models, provided proper model specifications in downstream learning tasks. The latter utility metric studies the relative performance of models trained on synthetic data. In particular, we discover that the distribution of synthetic data is not necessarily similar as the real one to ensure consistent model comparison. Interestingly, consistent model comparison is still achievable even when synthetic responses are not well generated, as long as downstream models are separable by a generalization gap. Finally, extensive experiments on non-parametric models and deep neural networks have been conducted to validate these theoretical findings.

Keywords: Feature Fidelity, Generative Models, Statistical Learning Theory, Synthetic Data, Utility Metrics

*Department of Statistics, University of California, Los Angeles. Email: shirong@stat.ucla.edu.

[†]Mitchell E. Daniels, Jr. School of Business, Purdue University. Email: sun244@purdue.edu. Corresponding author.

[‡]Department of Statistics, University of California, Los Angeles. Email: guangcheng@ucla.edu.

1 Introduction

In recent years, there has been a growing interest in synthetic data generation due to its versatility in a wide range of applications, including financial data (Assefa et al., 2020; Dogariu et al., 2022) and medical data (Frid-Adar et al., 2018; Benaim et al., 2020; Chen et al., 2021). The core idea of data synthesis is to generate a synthetic surrogate of the real dataset that can either replace real data for protecting privacy or supplement real data for training, e.g., (Xing et al., 2022). For instance, synthetic data has enabled financial institutions to share their data while ensuring compliance with data sharing restrictions (Assefa et al., 2020). It has also been used to augment financial datasets for fraud detection purposes (Charitou et al., 2021; Cheng et al., 2023). Similarly, in the medical field, synthetic data has been utilized to improve data privacy and the performance of predictive models for disease diagnosis (Chen et al., 2021). In the literature, significant progress has been made in developing synthetic data algorithms, including classical marginal-based methods (McKenna et al., 2021; Bi and Shen, 2022; Li et al., 2023), generative adversarial networks (Arjovsky et al., 2017; Goodfellow et al., 2020; Zhou et al., 2022), and diffusion models (Song et al., 2021; Ouyang et al., 2022).

An important evaluation of synthetic data is the generalization ability of downstream tasks trained based on synthetic data, i.e., utility of synthetic models. Specifically, we are interested in comparing statistical results derived from synthetic data with those from real data. For example, Karr et al. (2006) calculated the averaged overlap between the confidence intervals of coefficients estimated from synthetic and real data, while their standardized difference are adopted by Woo and Slavkovic (2015) and Nowok et al. (2016) as a utility measure in linear regression. These utility metrics focus on the extent to which statistical results from synthetic data align with those from real data. Similar task-specific utility metrics have also been proposed for supervised learning, aiming to compare the generalization performance of models trained on synthetic and real data (Beaulieu-Jones et al., 2019; Hittmeir et al., 2019;

Rankin et al., 2020; El Emam et al., 2021). While numerous studies have introduced and evaluated utility metrics for synthetic data, theoretical relationship between these metrics and the synthetic data distributions has never been precisely characterized.

With this context, this paper aims to theoretically understand how a synthetic data algorithm affects the generalization performance of models learned from synthetic data and explicates what properties a synthetic data algorithm should possess for generating a good synthetic dataset for downstream learning tasks. We first consider a general utility metric (Hittmeir et al., 2019; El Emam et al., 2021), which is defined as the absolute difference between the generalization performances on test data between the models learned from the real and synthetic datasets. The rationale behind this utility metric is that a good synthetic dataset should produce a model with comparable performance to the real dataset.

In theory, we establish explicit generalization bounds for the utility metrics in both regression (Theorem 1) and classification (Theorem S6 in the supplementary file). Specifically, the analytic bound is decomposed into four major components, including the estimation error in the downstream learning task, the quality of synthetic features, the estimation of the regression function, and model specification in the downstream learning task. This decomposition enables us to identify key aspects that synthetic data algorithms should prioritize when generating high-quality synthetic datasets for downstream learning tasks.

There are two main theoretical findings regarding the convergence of the utility metrics. First, as long as synthetic features have perfect fidelity and the relationship between features and responses can be well approximated by synthetic data algorithms, the convergence of the utility metric to zero is guaranteed. The first result is expected since it is widely perceived that inferences from synthetic data will be valid if the distribution of synthetic data is not far from that of real data. Most importantly, the analytic bounds reveal an interesting phenomenon that if the model specification in the downstream learning task is correct in the sense that it can capture the relationship between features and responses, perfect fidelity

of feature is not needed for the convergence of utility metrics. This result shows that when the model specification is correct, the synthetic distribution is not required to be the same as the real distribution for producing a model with comparable generalization performance. This discovery contributes to our understanding of a surprising but frequently observed phenomenon: training models using synthetic data can improve generalization (Tremblay et al., 2018; Azizi et al., 2023). For example, Azizi et al. (2023) shows that using synthetic data generated from diffusion models can significantly improve the performance of ImageNet classification. Our result suggests that the reason behind this phenomenon is due to the high approximation powers of the function classes of downstream tasks. To better demonstrate this interesting argument, we use linear regression and LASSO as two illustrative examples and establish the corresponding explicit convergence rates under imperfect feature fidelity (refer to Theorems 2 and 3). Our simulation results for K -nearest neighbors (KNN; Coomans and Massart, 1982), random forest regressor (RF; Breiman, 2001), and deep neural networks (Farrell et al., 2021) empirically validate our theoretical findings, demonstrating that when the model specification is correct, the utility metrics converge to zero regardless of the disparity between synthetic and real features.

Another relevant metric for utility is relative performances of the downstream tasks trained on synthetic data (Jordon et al., 2019, 2022). Ideally, the relative performance of synthetic models should be consistent with that of models trained on real data. This will justify the use of synthetic data (for protecting privacy of real data) in data competitions such as Kaggle. To establish sufficient conditions on this “ranking” consistency result, we propose a new metric called (V, d) -fidelity level to measure the distribution difference between real and synthetic features. Specifically, we show that consistent model comparison is achievable on synthetic data (Theorem 4) as long as the generalization gap between two model classes is large enough to neutralize the distribution discrepancy between real and synthetic features, even in cases where synthetic labels are not well generated. To the best of our knowledge,

our work provides the first analytic solution to the question posed in [Jordon et al. \(2022\)](#) about when the relative performance of synthetic models is consistent with that of models trained on real data.

The remainder of the paper is organized as follows. In [Section 2](#), we introduce necessary notations and present background information and basic concepts related to supervised learning. In [Section 3](#), we introduce a framework for analyzing the utility of synthetic data based on the regression setting. [Section 4](#) establishes an analytic bound for the utility metric for regression and provides explicit sufficient conditions for their convergence. In [Section 5](#), we present several examples that illustrate the asymptotic behavior of the utility metrics under different conditions. Specifically, we apply the analytic bound to study the convergence of the utility metrics in linear regression and LASSO. In [Section 6](#), we study sufficient conditions on synthetic data to yield consistent results in comparing performances of different models. In [Section 7](#), we conduct extensive simulations and a real-world application to support our theoretical results. Finally, the supplementary file contains auxiliary results for the classification setting and the proofs of theoretical results in this paper.

2 Preliminaries

For a vector $\mathbf{x} \in \mathbb{R}^p$, we denote its l_1 -norm and l_2 -norm as $\|\mathbf{x}\|_1 = \sum_{i=1}^p |x_i|$ and $\|\mathbf{x}\|_2 = \left(\sum_{i=1}^p |x_i|^2\right)^{1/2}$, respectively. For a function $f : \mathcal{X} \rightarrow \mathbb{R}$, we denote its L_p -norm with respect to the probability measure μ as $\|f\|_{L^p(\mu)} = \left(\int_{\mathcal{X}} |f(\mathbf{x})|^p d\mu(\mathbf{x})\right)^{1/p}$. For two given sequences $\{A_n\}_{n \in \mathbb{N}}$ and $\{B_n\}_{n \in \mathbb{N}}$, we write $A_n \gtrsim B_n$ if there exists a constant $C > 0$ such that $A_n \geq CB_n$ for any $n \in \mathbb{N}$. Additionally, we write $A_n \asymp B_n$ if $A_n \gtrsim B_n$ and $A_n \lesssim B_n$. For a continuous random variable X , we let $P_X(x)$ denote its probability density function at x and \mathbb{P}_X denote the associated probability measure. Let \mathbb{E}_X denote the expectation taken with respect to the randomness of X . For a sequence of random variables $\{X_n\}_{n \in \mathbb{N}}$, we let $X_n = o_p(1)$ represent that X_n converges to zero in probability.

For clarity, we concentrate on the regression setting of supervised learning in the main paper. The classification setting is postponed to Section S.1 of the supplementary file. Let $\mathcal{D}_r = \{(\mathbf{x}_i, y_i)\}_{i=1}^n$ denote the typical dataset in regression problem, which are drawn from an unknown distribution of (\mathbf{X}, Y) with $\mathbf{X} \in \mathbb{R}^p$ and Y is a scalar response. It is usually assumed that y_i 's are generated according to $y_i = \mu(\mathbf{x}_i) + \epsilon_i, i = 1, \dots, n$, where $\mu(\mathbf{x}) = \mathbb{E}(Y|\mathbf{X} = \mathbf{x})$ is the conditional mean and ϵ_i is a noise term with mean 0 and variance σ^2 . We denote the risk under the squared loss as $R_r(f) = \mathbb{E}[(f(\mathbf{X}) - Y)^2]$, where the expectation is taken with respect to (\mathbf{X}, Y) . We denote the excess risk as $\Phi_r(f) = R_r(f) - R_r(\mu) = \mathbb{E}[(f(\mathbf{X}) - \mu(\mathbf{X}))^2]$. For a function class \mathcal{F} , we let $f_{\mathcal{F}}^* = \operatorname{argmin}_{f \in \mathcal{F}} R_r(f)$ denote the optimal function in \mathcal{F} to minimize $R_r(f)$. The estimated model via the regularized empirical risk minimization framework for regression is given as

$$\hat{f} = \operatorname{argmin}_{f \in \mathcal{F}} \frac{1}{n} \sum_{i=1}^n (f(\mathbf{x}_i) - y_i)^2 + \lambda_r J_r(f), \quad (1)$$

where \mathcal{F} is a class of functions for regression, λ_r is a tuning parameter controlling the weight of the penalty term, $J_r(f)$ is a penalty term.

3 Data Synthesis in Supervised Learning

In this paper, we consider a common framework for generating synthetic data for downstream learning tasks (Shoshan et al., 2023; Van Breugel et al., 2023). Based on a real dataset $\mathcal{D}_r = \{(\mathbf{x}_i, y_i)\}_{i=1}^n$, a generative model is trained on \mathcal{D}_r , and then a resulting synthetic dataset $\tilde{\mathcal{D}}_r = \{(\tilde{\mathbf{x}}_i, \tilde{y}_i)\}_{i=1}^{\tilde{n}}$ will be released to some downstream learning tasks, where \tilde{n} is the size of the synthetic dataset. As illustrated in Figure 1, a synthetic dataset $\tilde{\mathcal{D}}_r$ is usually generated for replacing \mathcal{D}_r for a downstream training task, which can be formulated as

$$\tilde{f} = \operatorname{argmin}_{f \in \mathcal{F}} \frac{1}{\tilde{n}} \sum_{i=1}^{\tilde{n}} (f(\tilde{\mathbf{x}}_i) - \tilde{y}_i)^2 + \lambda_r J_r(f), \quad (2)$$

where \mathcal{F} is the function class of interest in the downstream learning task and $J_r(f)$ is a regularization term.

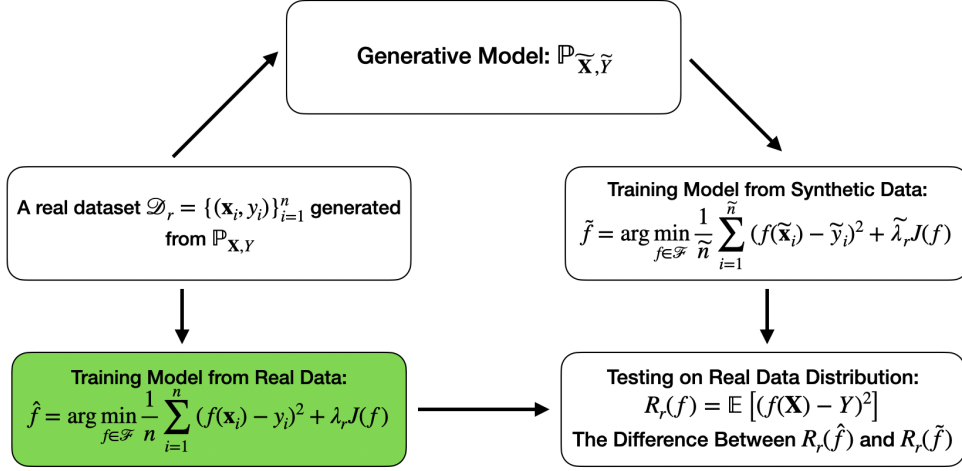


Figure 1: The architecture for generating and evaluating synthetic data in supervised learning: using regression as the example.

The central problem of data synthesis in supervised learning is whether \tilde{f} performs similarly to \hat{f} in terms of their generalization capabilities (Hittmeir et al., 2019; Rankin et al., 2020). Hence, we consider the following utility metric:

$$U_r(\tilde{f}, \hat{f}) = \left| R_r(\tilde{f}) - R_r(\hat{f}) \right|, \quad (3)$$

where $R_r(\tilde{f})$ denotes the generalization performance of \tilde{f} on unseen *real data*.

The rationale behind (3) is that the regression model trained from a synthetic dataset ought to possess similar performance in predicting unobserved samples (from real distribution) as that of the real dataset. For example, when \mathcal{D}_r and $\tilde{\mathcal{D}}_r$ are independently generated from the same distribution, the convergence of utility function is guaranteed by convergence of its the upper-bounding terms. Note that,

$$U_r(\tilde{f}, \hat{f}) \leq \left| R_r(\tilde{f}) - R_r(f_{\mathcal{F}}^*) \right| + \left| R_r(\hat{f}) - R_r(f_{\mathcal{F}}^*) \right|,$$

where $f_{\mathcal{F}}^* = \operatorname{argmin}_{f \in \mathcal{F}} R_r(f)$ denotes the optimal function in \mathcal{F} to approximate the true regression function μ . The right-hand side can be viewed as twice of the estimation errors in

statistical learning theory, of which the convergence in probability is supported by a vast body of literature (Bousquet, 2003; Vapnik, 1999).

4 Analytic Utility Bound

In this section, we establish an analytic upper bound for the utility metric as defined in (3). This metric aims to quantify the influence of the model specification in the downstream learning task \mathcal{F} and the synthetic data distribution $\mathbb{P}_{\tilde{\mathbf{X}}, \tilde{\mathbf{Y}}}$ on the convergence of $U_r(\tilde{f}, \hat{f})$.

Through our analytic bounds, we show that the impacts of \mathcal{F} and $\mathbb{P}_{\tilde{\mathbf{X}}, \tilde{\mathbf{Y}}}$ are interactive. Specifically, it is unnecessary for $\mathbb{P}_{\tilde{\mathbf{X}}, \tilde{\mathbf{Y}}}$ to resemble $\mathbb{P}_{\mathbf{X}, Y}$ under some specific model specifications for achieving the convergence of the proposed utility metric.

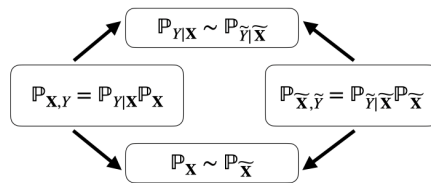


Figure 2: The similarity between $\mathbb{P}_{\mathbf{X}, Y}$ and $\mathbb{P}_{\tilde{\mathbf{X}}, \tilde{\mathbf{Y}}}$ can be decomposed into two key aspects: (1) feature fidelity: quantifying the proximity between $\mathbb{P}_{\mathbf{X}}$ and $\mathbb{P}_{\tilde{\mathbf{X}}}$; and (2) functional relationship estimation: assessing the effectiveness of $\mathbb{P}_{\tilde{\mathbf{Y}}|\tilde{\mathbf{X}}}$ in capturing the underlying functional relationship inherent in $\mathbb{P}_{Y|\mathbf{X}}$.

As depicted in Figure 2, rather than directly assessing the similarity between $\mathbb{P}_{\mathbf{X}, Y}$ and $\mathbb{P}_{\tilde{\mathbf{X}}, \tilde{\mathbf{Y}}}$, the examination of the impact of the synthetic data distribution $\mathbb{P}_{\tilde{\mathbf{X}}, \tilde{\mathbf{Y}}}$ is decomposed into two distinct components: feature fidelity and functional relationship estimation. In this study, feature fidelity is defined as the similarity between real and synthetic features, while functional relationship estimation pertains to how well the relationship between features and responses within $\mathbb{P}_{\tilde{\mathbf{X}}, \tilde{\mathbf{Y}}}$ approximates that of $\mathbb{P}_{\mathbf{X}, Y}$. To analyze the quality of functional relationship estimation, we consider the generated synthetic responses $\tilde{Y} = \hat{\mu}(\tilde{\mathbf{X}}) + \tilde{\epsilon}$, where $\tilde{\epsilon}$ denotes some implicit noise term with mean zero and finite variance and $\hat{\mu}$ is the underlying estimator for μ within the synthetic data generative model. Therefore, the functional relationship estimation will be evaluated via the difference between μ and $\hat{\mu}$.

To assess the similarity between distributions of real and synthetic features, we employ the integral probability metric, a widely used measure in synthetic data generation (Bousquet et al., 2020). This metric is defined as follows.

Definition 1. *The Integral Probability Metric (IPM) between two probability measures $\mathbb{P}_{\mathbf{X}}$ and $\mathbb{P}_{\widetilde{\mathbf{X}}}$ with respect to a function class \mathcal{H} is defined as*

$$D_{\mathcal{H}}(\mathbb{P}_{\mathbf{X}}, \mathbb{P}_{\widetilde{\mathbf{X}}}) = \sup_{h \in \mathcal{H}} \left| \mathbb{E}_{\mathbf{X} \sim \mathbb{P}_{\mathbf{X}}} [h(\mathbf{X})] - \mathbb{E}_{\widetilde{\mathbf{X}} \sim \mathbb{P}_{\widetilde{\mathbf{X}}}} [h(\widetilde{\mathbf{X}})] \right|,$$

where \mathcal{H} is a set of real-valued measurable functions on \mathcal{X} such that $\sup_{h \in \mathcal{H}} \mathbb{E}_{\mathbf{X} \sim \mathbb{P}_{\mathbf{X}}} [h(\mathbf{X})] < \infty$ and $\sup_{h \in \mathcal{H}} \mathbb{E}_{\widetilde{\mathbf{X}} \sim \mathbb{P}_{\widetilde{\mathbf{X}}}} [h(\widetilde{\mathbf{X}})] < \infty$.

We define the risk and the excess risk under the synthetic distribution as

$$\widetilde{R}_r(f) = \mathbb{E} \left[(f(\widetilde{\mathbf{X}}) - \widetilde{Y})^2 \right] \text{ and } \widetilde{\Phi}_r(f) = \mathbb{E} \left[(f(\widetilde{\mathbf{X}}) - \widehat{\mu}(\widetilde{\mathbf{X}}))^2 \right],$$

respectively, where the expectation is taken with respect to the randomness of $(\widetilde{\mathbf{X}}, \widetilde{Y})$. Let $\widetilde{f}_{\mathcal{F}}^* = \operatorname{argmin}_{f \in \mathcal{F}} \widetilde{\Phi}_r(f)$ denote the optimal function in \mathcal{F} to approximate $\widehat{\mu}$ under the synthetic distribution $\mathbb{P}_{\widetilde{\mathbf{X}}, \widetilde{Y}}$. In this paper, we assume that $f_{\mathcal{F}}^*$ and $\widetilde{f}_{\mathcal{F}}^*$ are both unique.

Theorem 1. *Let \widehat{f} and \widetilde{f} be the functions defined in (1) and (2), respectively. we have*

$$\begin{aligned} U_r(\widetilde{f}, \widehat{f}) \leq & |R_r(\widehat{f}) - R_r(f_{\mathcal{F}}^*)| + |\widetilde{R}_r(\widetilde{f}) - \widetilde{R}_r(\widetilde{f}_{\mathcal{F}}^*)| + 4D_{\mathcal{H}}(\mathbb{P}_{\mathbf{X}}, \mathbb{P}_{\widetilde{\mathbf{X}}}) \\ & + 2 \left(\sqrt{\Phi_r(\widetilde{f})} + 2\sqrt{\Phi_r(\widetilde{f}_{\mathcal{F}}^*)} + \sqrt{\Phi_r(f_{\mathcal{F}}^*)} \right) \sqrt{\Phi_r(\widehat{\mu})} + 4\Phi_r(\widehat{\mu}), \end{aligned} \quad (4)$$

where $\mathcal{H} = \left\{ h(\mathbf{x}) = (f(\mathbf{x}) - \widehat{\mu}(\mathbf{x}))^2 : f \in \{\widetilde{f}, f_{\mathcal{F}}^*, \widetilde{f}_{\mathcal{F}}^*\} \right\}$.

Theorem 1 provides an upper bound for $U_r(\widetilde{f}, \widehat{f})$, allowing us to specify sufficient conditions for the convergence of $U_r(\widetilde{f}, \widehat{f})$. Here it is worth noting that the upper bound in (4) is conditional on \mathcal{D}_r and $\widetilde{\mathcal{D}}_r$ and imposes no assumption on how synthetic data is generated. In statistical learning theory, the first term on the right-hand side of (4) is known as the estimation error, and its convergence in probability is generally assured under mild conditions

about the complexity of \mathcal{F} (Vapnik, 1999; De Mello and Ponti, 2018). The second term $|\tilde{R}_r(\tilde{f}) - \tilde{R}_r(\tilde{f}_{\mathcal{F}}^*)|$ represents the estimation error of \tilde{f} under the synthetic distribution. It is important to note that, $|\tilde{R}_r(\tilde{f}) - \tilde{R}_r(\tilde{f}_{\mathcal{F}}^*)|$ contains two sources of randomness from \mathcal{D}_r and $\tilde{\mathcal{D}}_r$, making $|\tilde{R}_r(\tilde{f}) - \tilde{R}_r(\tilde{f}_{\mathcal{F}}^*)|$ different from $|R_r(\hat{f}) - R_r(f_{\mathcal{F}}^*)|$. Nevertheless, the convergence of $|\tilde{R}_r(\tilde{f}) - \tilde{R}_r(\tilde{f}_{\mathcal{F}}^*)|$ can be generally guaranteed if the convergence is distribution-free.

With the convergence of the first two terms, achieving a small value of $U_r(\tilde{f}, \hat{f})$ entails the convergences of $D_{\mathcal{H}}(\mathbb{P}_{\mathbf{X}}, \mathbb{P}_{\tilde{\mathbf{X}}})$ and $\Phi_r(\hat{\mu})$. Here $\Phi_r(\hat{\mu})$ quantifies the approximation error to the true regression function μ provided by $\hat{\mu}$. This shows that achieving a high utility of synthetic data requires $\mathbb{P}_{\tilde{Y}|\tilde{\mathbf{X}}}$ and $\mathbb{P}_{Y|\mathbf{X}}$ have similar regression functions instead of aligning $\mathbb{P}_{\tilde{Y}|\tilde{\mathbf{X}}}$ with $\mathbb{P}_{Y|\mathbf{X}}$ precisely. Furthermore, $D_{\mathcal{H}}(\mathbb{P}_{\mathbf{X}}, \mathbb{P}_{\tilde{\mathbf{X}}})$ measures the closeness between $\mathbb{P}_{\mathbf{X}}$ and $\mathbb{P}_{\tilde{\mathbf{X}}}$ over a specific function class \mathcal{H} , which only comprises three functions. Consider a simple scenario where $\mathbb{P}_{\mathbf{X}}$ and $\mathbb{P}_{\tilde{\mathbf{X}}}$ have bounded density ratio, then the convergence of $D_{\mathcal{H}}(\mathbb{P}_{\mathbf{X}}, \mathbb{P}_{\tilde{\mathbf{X}}})$ can be analyzed in the following two cases:

1. **Perfect Feature Fidelity:** If $\mathbb{P}_{\mathbf{X}} = \mathbb{P}_{\tilde{\mathbf{X}}}$, we have $D_{\mathcal{H}}(\mathbb{P}_{\mathbf{X}}, \mathbb{P}_{\tilde{\mathbf{X}}}) = 0$ regardless of \mathcal{F} .
2. **Correct Model Specification:** If the model specification in the downstream task is correct such that $\mu \in \mathcal{F}$ and unlimited synthetic data is released for training ($\tilde{f} = \tilde{f}_{\mathcal{F}}^*$), then we have $D_{\mathcal{H}}(\mathbb{P}_{\mathbf{X}}, \mathbb{P}_{\tilde{\mathbf{X}}}) \lesssim \Phi_r(\hat{\mu})$ for any $\mathbb{P}_{\tilde{\mathbf{X}}}$.

Above we present two simplified scenarios where $D_{\mathcal{H}}(\mathbb{P}_{\mathbf{X}}, \mathbb{P}_{\tilde{\mathbf{X}}}) = 0$ is achievable. The first case is called perfect feature fidelity such that $\mathbb{P}_{\mathbf{X}} = \mathbb{P}_{\tilde{\mathbf{X}}}$. In this scenario, given that $\hat{\mu} = \mu$, we have $D_{\mathcal{H}}(\mathbb{P}_{\mathbf{X}}, \mathbb{P}_{\tilde{\mathbf{X}}}) = 0$ regardless of the downstream task \mathcal{F} . Conversely, the second scenario illustrates that achieving perfect feature fidelity is *not* necessary for the downstream task when the downstream function class \mathcal{F} is substantially large such that $\mu \in \mathcal{F}$. In this scenario, where $f_{\mathcal{F}}^* = \mu$, the convergence in probability of $\Phi_r(\hat{\mu})$ directly implies the convergence of $D_{\mathcal{H}}(\mathbb{P}_{\mathbf{X}}, \mathbb{P}_{\tilde{\mathbf{X}}})$. Our theoretical findings explain a prevalent phenomenon (Tremblay et al., 2018; Azizi et al., 2023) wherein synthetic data can significantly enhance the performance of downstream tasks. This enhancement stems from the inherent flexibility

of the downstream function class, facilitating improved generalization.

5 Examples for Utility Metrics

In this section, we provide several examples to illustrate the validity of the proposed utility bound established in Section 4. Firstly, we provide a one-dimensional regression example to demonstrate that imperfect feature fidelity may result in a shift in optimality of generalization when the model specification is incorrect. That is, the generalization performance of a model trained from synthetic data may depend on the marginal distribution of synthetic features, and thus the convergence of $U_r(\tilde{f}, \hat{f})$ may not be achieved. However, if the model specification is accurate, the proposed utility metric can converge, indicating that perfect feature fidelity is not necessary when sharing synthetic data for supervised learning. Secondly, we will apply the analytical bound to the linear regression to demonstrate the convergence of the proposed utility metrics even with imperfect feature fidelity. Specifically, we provide the explicit form of its associated bound, and show that its convergence in probability under double asymptotics can be analytically derived. Thirdly, we apply the analytical bound to the LASSO problem to highlight the versatility of the proposed utility bound in high-dimensional settings. Analogous results for the classification setting are included in the supplementary file.

5.1 Suboptimality with Imperfect Features

Theorems 1 demonstrates that the upper bound established in the previous section does not converge if the model specification is inaccurate and the feature fidelity is imperfect ($\mathbb{P}_{\mathbf{X}} \neq \mathbb{P}_{\tilde{\mathbf{X}}}$). In this section, we provide a toy regression example to further illustrate that this phenomenon also applies to the utility metrics.

One-dimensional regression. Assume that $\mathcal{X} = [-1, 1]$ and the regression function is $\mu(x) = |x|$. We assume that the observed responses are noise-free, that is $y = \mu(x)$. Furthermore, we assume that the true feature X and the synthetic feature \tilde{X} follow the

corresponding distributions:

$$P_X(x) = 1/2, x \in [-1, 1] \text{ and } P_{\tilde{X}}(x) = \begin{cases} \alpha, & \text{if } x \in [0, 1], \\ 1 - \alpha, & \text{if } x \in [-1, 0). \end{cases} \quad (5)$$

To simplify our analysis, we assume that the estimation model $\hat{\mu}$ is identical to the true regression function $\mu(x) = |x|$. Moreover, we consider a scenario where there are infinitely many samples in both the true dataset and the synthetic dataset. This means that the estimated models \hat{f} and \tilde{f} can be obtained by minimizing the risks directly with $\lambda_r = 0$.

Incorrect Model Specification. Under the model specification $\mathcal{F} = \{f(x) = \beta x : \beta \in \mathbb{R}\}$, the risks under the true and synthetic distributions are given as

$$R_r(f) = \frac{1 + \beta^2}{3} \text{ and } \tilde{R}_r(f) = \frac{\beta^2 + (2 - 4\alpha)\beta + 1}{3}.$$

The above calculations show that the estimated models can be obtained analytically as $\hat{f}(x) = 0$ and $\tilde{f}(x) = (2\alpha - 1)x$. Using these, $U_r(\hat{f}, \tilde{f})$ can be computed as

$$U_r(\hat{f}, \tilde{f}) = |R_r(\hat{f}) - R_r(\tilde{f})| = \frac{(2\alpha - 1)^2}{3} > 0, \quad (6)$$

for any $\alpha \in (0, 1/2) \cup (1/2, 1)$. The proposed utility metric in this case is always greater than 0 if $\mathbb{P}_X \neq \mathbb{P}_{\tilde{X}}$ ($\alpha \neq 1/2$). This demonstrates that, in the case of an inaccurate model specification, the discrepancy between the true and synthetic distributions results in a gap between the generalization capabilities of models estimated from real and synthetic datasets. Such sub-optimality gap does not converge to zero even we have infinite samples.

Correct Model Specification: If the true model μ is correctly specified with $\mathcal{F} = \{f(x) = \beta|x| : \beta \in \mathbb{R}\}$, we have

$$R_r(f) = \frac{(1 - \beta)^2}{3} \text{ and } \tilde{R}_r(f) = \frac{(1 - \beta)^2}{3}.$$

Clearly, the utility metric $U_r(\hat{f}, \tilde{f}) = 0$ regardless of the value of α . This validates the second conclusion stated in Section 4 that perfect synthetic feature is not a prerequisite for the convergence of $U_r(\hat{f}, \tilde{f})$ if the function class used in the downstream learning task is large

enough to cover $\mu(x)$. Similarly, an example for classification is provided in the supplementary file for demonstrating the same phenomenon.

5.2 Example: Linear Regression

This section provides an example using linear regression to illustrate the theoretical results presented in Section 4. The key point is that the convergence of $U_r(\tilde{f}, \hat{f})$ does not require perfect feature fidelity, as long as the regression function μ is correctly specified.

Assumption 1. For the random feature vectors $\mathbf{X} = (X_1, \dots, X_p)$ and $\tilde{\mathbf{X}} = (\tilde{X}_1, \dots, \tilde{X}_p)$, we assume that (1) $\mathbb{E}(X_i) = \mathbb{E}(\tilde{X}_i) = 0$; (2) the synthetic features are sampled from a fixed distribution $\mathbb{P}_{\tilde{\mathbf{X}}}$ that is independent of $\{\mathbf{x}_i\}_{i=1}^n$.

For an observed dataset $\mathcal{D}_r = \{(\mathbf{x}_i, y_i)\}_{i=1}^n$, we assume $y_i = \mu(\mathbf{x}_i) + \epsilon_i = \mathbf{x}_i^T \boldsymbol{\beta}^* + \epsilon_i$ for $i = 1, \dots, n$, where $\boldsymbol{\beta}^*$ denotes the true coefficient vector. Furthermore, for the synthetic dataset $\tilde{\mathcal{D}}_r = \{(\tilde{\mathbf{x}}_i, \tilde{y}_i)\}_{i=1}^{\tilde{n}}$, we assume the generation of the synthetic response \tilde{y}_i employs the ordinal least squares (OLS) estimator $\tilde{y}_i = \hat{\mu}(\tilde{\mathbf{x}}_i) + \tilde{\epsilon}_i = \hat{\boldsymbol{\beta}}^T \tilde{\mathbf{x}}_i + \tilde{\epsilon}_i$ for $i = 1, \dots, \tilde{n}$, where $\hat{\boldsymbol{\beta}} = (\mathbb{X}^T \mathbb{X})^{-1} \mathbb{X}^T \mathbb{Y}$, $\mathbb{X} = (\mathbf{x}_1, \mathbf{x}_2, \dots, \mathbf{x}_n)^T$, $\mathbb{Y} = (y_1, y_2, \dots, y_n)^T$, and $\tilde{\epsilon}_i$ is synthetic noise with variance $\tilde{\sigma}^2$.

For illustration purpose, we assume that the model specification in the downstream regression task is correct, that is $\mathcal{F} = \{f(\mathbf{x}) = \boldsymbol{\beta}^T \mathbf{x} : \boldsymbol{\beta} \in \mathbb{R}^p\}$. With this, the estimated models based on $\mathcal{D}_r = \{(\mathbf{x}_i, y_i)\}_{i=1}^n$ and $\tilde{\mathcal{D}}_r = \{(\tilde{\mathbf{x}}_i, \tilde{y}_i)\}_{i=1}^{\tilde{n}}$, respectively, are given as

$$\hat{f}_{LR}(\mathbf{x}) = \mathbf{x}^T (\mathbb{X}^T \mathbb{X})^{-1} \mathbb{X}^T \mathbb{Y} \text{ and } \tilde{f}_{LR}(\mathbf{x}) = \mathbf{x}^T (\tilde{\mathbb{X}}^T \tilde{\mathbb{X}})^{-1} \tilde{\mathbb{X}}^T \tilde{\mathbb{Y}},$$

where $\tilde{\mathbb{X}} = (\tilde{\mathbf{x}}_1, \tilde{\mathbf{x}}_2, \dots, \tilde{\mathbf{x}}_{\tilde{n}})^T$ and $\tilde{\mathbb{Y}} = (\tilde{y}_1, \tilde{y}_2, \dots, \tilde{y}_{\tilde{n}})^T$.

Assumption 2. Assume that $\tilde{\mathbb{X}}^T \tilde{\mathbb{X}}$ and $\mathbb{X}^T \mathbb{X}$ are both invertible almost surely. Moreover, $\mathbb{E}_{\mathbb{X}}[(n^{-1} \mathbb{X}^T \mathbb{X})^{-1}]$ and $\mathbb{E}_{\tilde{\mathbb{X}}}[(\tilde{n}^{-1} \tilde{\mathbb{X}}^T \tilde{\mathbb{X}})^{-1}]$ are both positive semidefinite.

Theorem 2. Denote that $\text{Var}(\mathbf{X}) = \mathbf{\Lambda}$ and $\text{Var}(\widetilde{\mathbf{X}}) = \widetilde{\mathbf{\Lambda}}$. Under Assumptions 1-2, the analytic bound established in Theorem 1 becomes

$$\begin{aligned} U_r(\widehat{f}_{LR}, \widetilde{f}_{LR}) \leq & 18 \text{trace}(\boldsymbol{\epsilon} \boldsymbol{\epsilon}^T \mathbf{Q} \mathbf{\Lambda} \mathbf{Q}^T) + 5 \text{trace}(\widetilde{\boldsymbol{\epsilon}} \widetilde{\boldsymbol{\epsilon}}^T \widetilde{\mathbf{Q}} \widetilde{\mathbf{\Lambda}} \widetilde{\mathbf{Q}}^T) \\ & + 4 \text{trace}(\boldsymbol{\epsilon} \boldsymbol{\epsilon}^T \mathbf{Q} \widetilde{\mathbf{\Lambda}} \mathbf{Q}^T) + 6 \text{trace}(\widetilde{\boldsymbol{\epsilon}} \widetilde{\boldsymbol{\epsilon}}^T \widetilde{\mathbf{Q}} \mathbf{\Lambda} \widetilde{\mathbf{Q}}^T), \end{aligned} \quad (7)$$

where $\mathbf{Q} = \mathbb{X}(\mathbb{X}^T \mathbb{X})^{-1}$, $\widetilde{\mathbf{Q}} = \widetilde{\mathbb{X}}(\widetilde{\mathbb{X}}^T \widetilde{\mathbb{X}})^{-1}$, $\text{trace}(\cdot)$ is the trace of a matrix, $\boldsymbol{\epsilon} = (\epsilon_1, \dots, \epsilon_n)^T$, and $\widetilde{\boldsymbol{\epsilon}} = (\widetilde{\epsilon}_1, \dots, \widetilde{\epsilon}_{\widetilde{n}})^T$. Furthermore, for any $\delta > 0$, it holds that

$$U_r(\widehat{f}_{LR}, \widetilde{f}_{LR}) \lesssim \frac{\widetilde{n} \sigma^2 \sum_{i=1}^p (\rho_i + \widetilde{\rho}_i) \kappa_i + n \widetilde{\sigma}^2 \sum_{i=1}^p (\rho_i + \widetilde{\rho}_i) \widetilde{\kappa}_i}{\widetilde{n} n \delta},$$

with probability at least $1 - \delta$, where ρ_i , $\widetilde{\rho}_i$, κ_i , and $\widetilde{\kappa}_i$ denote the i -th largest eigenvalues of $\mathbf{\Lambda}$, $\widetilde{\mathbf{\Lambda}}$, $\mathbb{E}_{\mathbb{X}}[(n^{-1} \mathbb{X}^T \mathbb{X})^{-1}]$, and $\mathbb{E}_{\widetilde{\mathbb{X}}}[(\widetilde{n}^{-1} \widetilde{\mathbb{X}}^T \widetilde{\mathbb{X}})^{-1}]$, respectively.

Theorem 2 first explicates the utility bound in (4) under the setting of linear regression with correct model specification, showing the utility metric $U_r(\widetilde{f}_{LR}, \widehat{f}_{LR})$ converges to 0 when n and \widetilde{n} both increase to infinity regardless the difference between \mathbf{X} and $\widetilde{\mathbf{X}}$ in distribution. This result suggests that even if the distributions of the real and synthetic features are different, models trained on these datasets can still perform similarly if the correct model specification is used. This is an important finding, as it implies that perfect feature fidelity is not necessary for effective synthetic data generation. This finding is consistent with our earlier conclusion in Section 4, implicitly indicating that the function class used in the downstream learning task is more important than feature fidelity for achieving good performance.

5.3 Example: LASSO Regression

In this section, we intend to show that the utility bound established in (4) is also valid for high-dimensional regression. For illustration, we use LASSO as an example where the dimension of \mathbf{X} may grow exponentially with the sample size n , i.e., $p \gg n$. Suppose the dataset $\mathcal{D}_r = \{(\mathbf{x}_i, y_i)\}_{i=1}^n$ is drawn from the distribution satisfying $Y = \mathbf{X}^T \boldsymbol{\beta}^* + \epsilon$, where $\boldsymbol{\beta}^* = (\beta_1^*, \dots, \beta_p^*)$ is a sparse coefficient vector with $\|\boldsymbol{\beta}^*\|_0 = s$ and $\epsilon \sim N(0, \sigma^2)$.

The synthetic data generator first estimates β^* using LASSO to generate synthetic datasets. The estimation process is carried out as follows:

$$\widehat{\beta}(\lambda_r) = \operatorname{argmin}_{\beta \in \mathbb{R}^p} \frac{1}{n} \sum_{i=1}^n (y_i - \mathbf{x}_i^T \beta)^2 + \lambda_r \|\beta\|_1. \quad (8)$$

Regarding the generation of synthetic features $\widetilde{\mathbf{X}}$, we follow the assumption as in Section 5.2 that synthetic features are independently generated from the real dataset. The primary objective of this assumption is to verify that feature fidelity becomes less important when the model specification is accurate. Denote that $\mathcal{A} = \{i : \beta_i^* \neq 0\}$ and $\widehat{\mathcal{A}} = \{i : \widehat{\beta}_i(\lambda_r) \neq 0\}$ with $\widehat{\beta}_i(\lambda_r)$ being the i -th element of $\widehat{\beta}(\lambda_r)$. We generate synthetic responses via $\widetilde{y}_i = \widehat{\mu}(\widetilde{\mathbf{x}}_i) + \widetilde{\epsilon}_i = \widetilde{\mathbf{x}}_i^T \widehat{\beta}(\lambda_r) + \widetilde{\epsilon}_i$, where $\widehat{\beta}(\lambda_r)$ is the sparse coefficient vector as defined in (8) and $\widetilde{\epsilon}_i \sim N(0, \widetilde{\sigma}^2)$ for imitating noise contained in synthetic generation methods.

In the downstream task, we assume a correct model specification where the LASSO technique is also considered, and the estimated coefficient vector the synthetic dataset $\widetilde{\mathcal{D}}_r = \{(\widetilde{\mathbf{x}}_i, \widetilde{y}_i)\}_{i=1}^{\widetilde{n}}$ is given as

$$\widetilde{\beta}(\widetilde{\lambda}_r) = \operatorname{argmin}_{\beta \in \mathbb{R}^p} \frac{1}{\widetilde{n}} \sum_{i=1}^{\widetilde{n}} (\widetilde{y}_i - \widetilde{\mathbf{x}}_i^T \beta)^2 + \widetilde{\lambda}_r \|\beta\|_1. \quad (9)$$

The difference between (8) and (9) lies in the choice of the tuning parameter and the dataset for training. Under the proposed utility metric, we are interested in the generalization performance between $\widehat{f}_{lasso}(\mathbf{x}) = \mathbf{x}^T \widehat{\beta}(\lambda_r)$ and $\widetilde{f}_{lasso}(\mathbf{x}) = \mathbf{x}^T \widetilde{\beta}(\widetilde{\lambda}_r)$ on test data.

We first make several common assumptions for studying the generalization performance of LASSO estimators. Specifically, Assumption 3 refers to as the restricted eigenvalue condition for LASSO estimators (Bickel et al., 2009), establishing the quantitative relationship between parameter estimation and empirical risk in the LASSO problem.

Assumption 3. *The real and synthetic design matrices \mathbb{X} and $\widetilde{\mathbb{X}}$ satisfy that there exists a positive constant κ such that for any $\mathcal{J} \subset \mathcal{A}$, we have $n^{-1} \|\mathbb{X}\mathbf{v}\|_2^2 \geq \kappa \|\mathbf{v}\|_2^2$ and $\widetilde{n}^{-1} \|\widetilde{\mathbb{X}}\mathbf{v}\|_2^2 \geq \kappa \|\mathbf{v}\|_2^2$ for any vector $\mathbf{v} \in \mathbb{C}(\mathcal{J})$ with $\mathbb{C}(\mathcal{J}) = \{\mathbf{v} \in \mathbb{R}^p : \|\mathbf{v}_{\mathcal{J}^c}\|_1 \leq 3\|\mathbf{v}_{\mathcal{J}}\|_1\}$ almost surely,*

where $\mathbf{v}_{\mathcal{J}} = (v_i)_{i \in \mathcal{J}}$ and \mathcal{J}^c is the complete of \mathcal{J} .

Assumption 4. Assume that the supports of \mathbf{X} and $\widetilde{\mathbf{X}}$ are both compact sets, and each element of \mathbf{X} and $\widetilde{\mathbf{X}}$ is bounded by $C_{\mathcal{X}}$.

Assumption 4 is the bounded support assumption for real and synthetic features, which is commonly assumed in studying the risk consistency of LASSO estimators (Chatterjee and Lahiri, 2011; Homrighausen and McDonald, 2017).

Assumption 5. Assume that the real design matrix \mathbb{X} satisfies the following conditions almost surely: (1) the smallest eigenvalue of $\mathbb{X}_{\mathcal{A}}^T \mathbb{X}_{\mathcal{A}}/n$ is lower bounded by c_1 ; (2) There exists a constant $\alpha \in [0, 1)$ such that $\max_{j \in \mathcal{A}^c} \|(\mathbb{X}_{\mathcal{A}}^T \mathbb{X}_{\mathcal{A}})^{-1} \mathbb{X}_{\mathcal{A}}^T \mathbb{X}_j\|_1 \leq \alpha$.

Assumption 5 is primarily used for ensuring no false inclusion within $\widehat{\mathcal{A}}(\lambda_r)$, i.e., $\widehat{\mathcal{A}} \subset \mathcal{A}$. Specifically, condition (1) assumes the absence of multicollinearity in \mathbb{X} , ensuring the identifiability of the model (Wainwright, 2019). Meanwhile, condition (2) assumes that the space spanned by the columns of $\mathbb{X}_{\mathcal{A}} = (\mathbb{X}_i)_{i \in \mathcal{A}}$ should exhibit approximate orthogonality characterized by α to \mathbb{X}_j for $j \in \mathcal{A}^c$, where \mathbb{X}_i denotes the i -th column of \mathbb{X} .

Theorem 3. Under Assumptions 3-5, the analytic bound established in Theorem 1 becomes

$$U_r(\widehat{f}_{lasso}, \widetilde{f}_{lasso}) \lesssim s(\widetilde{\lambda}_r^2 + \lambda_r^2), \quad (10)$$

where λ_r and $\widetilde{\lambda}_r$ satisfy the following conditions:

$$(I) \quad \lambda_r \geq 2 \max\{\|n^{-1} \sum_{i=1}^n \epsilon_i \mathbf{x}_i\|_{\infty}, (1-\alpha)^{-1} \|\mathbb{X}_{\mathcal{A}^c} (I_n - \mathbb{Q}_{\mathcal{A}} \mathbb{X}_{\mathcal{A}}^T) \boldsymbol{\epsilon}/n\|_{\infty}\} \text{ with } \mathbb{Q}_{\mathcal{A}} = \mathbb{X}_{\mathcal{A}} (\mathbb{X}_{\mathcal{A}}^T \mathbb{X}_{\mathcal{A}})^{-1};$$

$$(II) \quad \widetilde{\lambda}_r \geq 2 \|\widetilde{n}^{-1} \sum_{i=1}^{\widetilde{n}} \widetilde{\epsilon}_i \widetilde{\mathbf{x}}_i\|_{\infty}.$$

Furthermore, we have

$$U_r(\widehat{f}_{lasso}, \widetilde{f}_{lasso}) \lesssim s \log p \left(\frac{\sigma^2}{n} + \frac{\widetilde{\sigma}^2}{\widetilde{n}} \right), \quad (11)$$

with probability at least $1 - n^{-2} - \widetilde{n}^{-2}$.

Theorem 3 presents the precise form of the utility bound in (10) when applied to the LASSO problem, given appropriate choices of λ_r and $\tilde{\lambda}_r$. To ensure the convergence of the utility metric during synthetic data generation, the primary challenge lies in preventing any false inclusion of useless features within $\hat{\mathcal{A}}$, while also establishing a quantitative relationship between risk consistency and parameter estimation consistency regardless of the randomness from the real dataset. To this end, Assumptions 3 and 5 are imposed on the real dataset \mathcal{D}_r and condition (I) is imposed on the choice of λ_r . Specifically, condition (I) indicates that λ_r should be chosen appropriately such that $\hat{\mu}$ converges to μ . Under this condition, we can ensure that when using $\hat{\beta}(\lambda_r)$ to generate any synthetic dataset, the convergence of $\tilde{R}_r(\tilde{f}_{lasso}) - \tilde{R}_r(\tilde{f}_{\mathcal{F}}^*)$ can be established irrespective of the randomness inherent in the real dataset. Furthermore, condition (II) is employed to ensure consistent estimation in the downstream task, whether based on the real or synthetic dataset. Subsequently, Theorem 3 establishes the convergence in probability of the utility bound for the LASSO problem under a specific sample complexity constraint.

There are several interesting conclusions from (11) regarding improving the utility of synthetic datasets. First, when compared with existing results regarding the risk consistency of LASSO estimators, our analytic bound consists of two sources of randomness originating from real and synthetic data. A key difference of our analytic bound is its dependence on the variable selection during the synthetic data generation step for ensuring the utility of synthetic data. Clearly, the utility can be improved by either reducing noise, i.e., $\tilde{\sigma}^2$, in the synthetic label generation or increasing synthetic samples, i.e., \tilde{n} , for downstream training.

Second, the sparsity in the synthetic dataset is varying and depends on the real dataset and choice of λ_r . Our result indicates that, under the same sample sizes n and \tilde{n} , it is easier to achieve good utility of synthetic datasets if the informative real features indexed by \mathcal{A} are orthogonal to unrelated real features indexed by \mathcal{A}^c . Finally, the upper bound in (11) remains unaffected by the similarity between the distributions of \mathbf{X} and $\tilde{\mathbf{X}}$, showing that

perfect feature fidelity is unnecessary for ensuring the utility of synthetic data when the model specification is correctly specified in the downstream task. As both n and \tilde{n} approach infinity, the utility metric $U_r(\hat{f}_{lasso}, \tilde{f}_{lasso})$ can be controlled to reach any small value given the correct model specification.

6 Model Comparison Based on Synthetic Data

Another use of synthetic data involves ranking model performances solely based on synthetic data (Jordon et al., 2018, 2022). This necessitates consistency in the ranking of model performances between synthetic and real data, which is especially crucial when synthetic data is employed in competitions, such as Kaggle. In this section, we study sufficient conditions on the synthetic data distribution that ensure that the relative generalization performance of models trained from synthetic data remains consistent with that of models trained from real data. We consider the regression setting in the main paper, while similar findings in the classification setting can be examined in Section S.1.4 of the supplementary file.

We first present a definition for consistent model comparison based on synthetic data.

Definition 2. (*Consistent Model Comparison for Regression*) Let $(\mathcal{F}_1, \mathcal{F}_2)$ be a pair classes of models for comparison in the downstream learning task. We say the synthetic distribution $\mathbb{P}_{\tilde{\mathbf{X}}, \tilde{\mathbf{Y}}}$ preserves the utility of consistent model comparison if

$$\left(R_r(f_{\mathcal{F}_1}^*) - R_r(f_{\mathcal{F}_2}^*) \right) \left(R_r(\tilde{f}_{\mathcal{F}_1}^*) - R_r(\tilde{f}_{\mathcal{F}_2}^*) \right) > 0,$$

where $\tilde{f}_{\mathcal{F}_i}^* = \operatorname{argmin}_{f \in \mathcal{F}_i} \tilde{R}_r(f)$ for $i = 1, 2$.

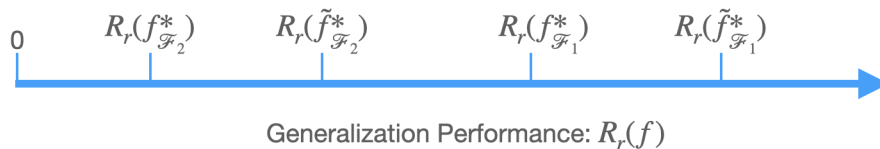


Figure 3: An illustrative example for consistent model comparison when the synthetic and real distributions are not the same.

Particularly, when the synthetic and real distributions are identical, the optimal models will necessarily be the same. As a result, it is straightforward to derive a consistent model comparison based on synthetic data. However, more interestingly, consistent model comparison can still be achieved using synthetic data even if the synthetic and real distributions are not identical. To illustrate this phenomenon, we provide an intuitive example in Figure 3. In this example, we assume that $f_{\mathcal{F}_2}^*$ outperforms $f_{\mathcal{F}_1}^*$ in generalization performance, i.e., $R_r(f_{\mathcal{F}_2}^*) < R_r(f_{\mathcal{F}_1}^*)$. According to the analytic bound established in Theorem 1, the gap between $R_r(f_{\mathcal{F}_1}^*)$ and $R_r(\tilde{f}_{\mathcal{F}_1}^*)$ resulting from the difference between the synthetic and real distributions will vanish as the synthetic distribution becomes more similar to the real one.

This example demonstrates that consistent model comparison is possible if the synthetic distribution is constructed such that $R_r(\tilde{f}_{\mathcal{F}_2}^*)$ falls in the interval $[R_r(f_{\mathcal{F}_2}^*), R_r(f_{\mathcal{F}_1}^*)]$, providing a sufficient condition for consistent comparison on synthetic data. Therefore, consistent generalization does not necessarily imply consistent model comparison based on synthetic data. Motivated by this example, we aim to explicate the sufficient conditions for synthetic data to yield identical model comparison as that of real data.

6.1 Examples for Inconsistent Model Comparison

In this section, we present an illustrative example for regression to demonstrate that the dissimilarity between the marginal distributions of the synthetic and real features sometimes might lead to distinctive optimal models under the same model specification, which results in inconsistent model comparison. Similar results for classification are provided in the supplementary file. In this example, we denote the support of synthetic and real features as $\mathcal{X} = [-1, 1]$ and let the regression function be $\mu(x) = x$. The true feature X and the synthetic feature \tilde{X} are further assumed to follow the corresponding distributions,

$$P_X(x) = \begin{cases} 1 - \alpha, & \text{if } x \in [0, 1], \\ \alpha, & \text{if } x \in [-1, 0). \end{cases} \quad \text{and} \quad P_{\tilde{X}}(x) = \begin{cases} \alpha, & \text{if } x \in [0, 1], \\ 1 - \alpha, & \text{if } x \in [-1, 0). \end{cases} \quad (12)$$

We further assume that the estimation model $\hat{\mu}$ and $\hat{\eta}$ are the same as μ and η , respectively.

For the regression task, we suppose there are two model specifications $\mathcal{F}_1 = \{f(x) = \beta : \beta \in [-1/2, 1/2]\}$ and $\mathcal{F}_2 = \{f(x) = \beta : \beta \in [-1/4, 1/4]\}$, the risks under the true and synthetic distributions are, respectively, given as

$$R_r(f) = \frac{1}{3} - \beta + \beta^2 + 2\alpha\beta \text{ and } \tilde{R}_r(f) = \frac{1}{3} + \beta + \beta^2 - 2\alpha\beta.$$

Let $\alpha = 5/6$, we have $R_r(f) = \beta^2 + 2\beta/3 + 1/3$ and $\tilde{R}_r(f) = \beta^2 - 2/3\beta + 1/3$. Then we can verify that $f_{\mathcal{F}_1}^*(x) = -1/3$ and $f_{\mathcal{F}_2}^*(x) = -1/4$, which leads to $R_r(f_{\mathcal{F}_2}^*) > R_r(f_{\mathcal{F}_1}^*)$. Conversely, $\tilde{f}_{\mathcal{F}_1}^*(x) = 1/3$ and $\tilde{f}_{\mathcal{F}_2}^*(x) = 1/4$, which leads to $R_r(\tilde{f}_{\mathcal{F}_1}^*) > R_r(\tilde{f}_{\mathcal{F}_2}^*)$.

The example provided illustrates how changes in the marginal distribution of features can influence the optimal model for minimizing risk under a given model specification. While a more flexible model specification can offer better generalization performance by capturing complex relationships between features and the target variable, it also increases the possibility of estimating an inferior model based on synthetic data with low feature fidelity.

6.2 Consistent Model Comparison

In this section, we examine how the quality of synthetic data influences the results of model comparisons. Our objective is to shed light on the conditions necessary for ensuring that the relative performance of optimal models derived from synthetic data aligns with those derived from real data. As seen in Figure 2, our analysis of these sufficient conditions will be grounded in the relationships between $\mathbb{P}_{Y|\mathbf{X}}$ and $\mathbb{P}_{\tilde{Y}|\tilde{\mathbf{X}}}$, as well as between $\mathbb{P}_{\mathbf{X}}$ and $\mathbb{P}_{\tilde{\mathbf{X}}}$.

To begin with, we present a novel metric called (V, d) -fidelity level that evaluates the differences between synthetic and real feature distributions. Our proposed metric resembles f -divergences (Rényi, 1961) in essence, as both rely on density ratios for characterizing distributional difference. The proposed (V, d) -fidelity level offers an alternative means of gauging the disparity between two distributions. In essence, by utilizing the (V, d) -fidelity level, we can carry out a more intricate analysis of how the deviation of the synthetic distribution from the real distribution influences downstream model comparison.

Definition 3 ((V, d) -fidelity level). Let \mathcal{X} be the union of supports of $\mathbb{P}_{\mathbf{X}}$ and $\mathbb{P}_{\widetilde{\mathbf{X}}}$. We say the distributions $\mathbb{P}_{\mathbf{X}}$ and $\mathbb{P}_{\widetilde{\mathbf{X}}}$ satisfy (V, d) -fidelity level if there exist $V \geq 0$ and $0 < d \leq \infty$ such that for any $C > 0$,

$$\max \left\{ \int_{\mathcal{X}_C} P_{\mathbf{X}}(\mathbf{x}) d\mathbf{x}, \int_{\mathcal{X}'_C} P_{\widetilde{\mathbf{X}}}(\mathbf{x}) d\mathbf{x} \right\} \leq V \cdot C^{-d}, \quad (13)$$

where $\mathcal{X}_C = \{\mathbf{x} \in \mathcal{X} : P_{\mathbf{X}}(\mathbf{x})/P_{\widetilde{\mathbf{X}}}(\mathbf{x}) \geq C\}$ and $\mathcal{X}'_C = \{\mathbf{x} \in \mathcal{X} : P_{\widetilde{\mathbf{X}}}(\mathbf{x})/P_{\mathbf{X}}(\mathbf{x}) \geq C\}$.

It should be noted that the proposed metric in (13) is symmetric and utilizes two parameters V and d to describe the probabilities of areas with high density ratio values. A greater value of d or a smaller value of V signifies a higher degree of similarity between the two distributions. A notable attribute of (V, d) -fidelity levels is their capacity to accommodate different supports between real and synthetic feature distributions, a scenario where many f -divergence metrics encounter limitations.

Lemma 1. *The following are some examples of (V, d) -fidelity level.*

- 1 If $\mathbb{P}_{\mathbf{X}} = \mathbb{P}_{\widetilde{\mathbf{X}}}$, then $\mathbb{P}_{\mathbf{X}}$ and $\mathbb{P}_{\widetilde{\mathbf{X}}}$ satisfy $(1, \infty)$ -fidelity level.
- 2 If $M_1 \leq P_{\mathbf{X}}(\mathbf{x})/P_{\widetilde{\mathbf{X}}}(\mathbf{x}) \leq M_2$ for some positive constants $M_1 \in [0, 1]$ and $M_2 \in [1, \infty]$, then $P_{\mathbf{X}}$ and $P_{\widetilde{\mathbf{X}}}$ satisfy $(\max\{M_2^d, M_1^{-d}\}, d)$ -fidelity level for any $d > 0$.

In Lemma 1, the second example assumes that the ratio of densities is bounded, which is a common assumption in transfer learning (Kpotufe, 2017) and density ratio estimation (Kato and Teshima, 2021).

Theorem 4. *Let $(\mathcal{F}_1, \mathcal{F}_2)$ be a pair of model classes with $R_r(f_{\mathcal{F}_2}^*) < R_r(f_{\mathcal{F}_1}^*)$. For a synthetic data distribution $\mathbb{P}_{\widetilde{\mathbf{X}}}$ satisfying (V, d) -fidelity level, we define*

$$\begin{aligned} \mathcal{W}(\mathcal{F}_1, \mathcal{F}_2) &= \sqrt{\Phi_r(f_{\mathcal{F}_1}^*)} - C_{d,V,U} \left(\sqrt{\Phi_r(f_{\mathcal{F}_2}^*)} \right)^{\frac{d^2}{(d+1)^2}}, \\ \mathcal{B}(\widehat{\mu}, \mu) &= \|\widehat{\mu} - \mu\|_{L^2(\mathbb{P}_{\mathbf{X}})} + C_{d,V,U} \|\widehat{\mu} - \mu\|_{L^2(\mathbb{P}_{\mathbf{X}})}^{\frac{d^2}{(d+1)^2}}, \end{aligned}$$

where $C_{d,V,U} = (d^{\frac{1}{d+1}} + d^{-\frac{d}{d+1}})^{\frac{3d+1}{2(d+1)}} V^{\frac{2d+1}{2(d+1)^2}} U^{\frac{2d+1}{(d+1)^2}}$ and $U = \max\{\|f_{\mathcal{F}_2}^* - \hat{\mu}\|_{L^\infty(\mathbb{P}_{\mathbf{X}})}, \|\tilde{f}_{\mathcal{F}_2}^* - \hat{\mu}\|_{L^\infty(\mathbb{P}_{\mathbf{X}})}\}$. If $\mathcal{B}(\hat{\mu}, \mu) \leq \mathcal{W}(\mathcal{F}_1, \mathcal{F}_2)$, then we have consistent model comparison based on synthetic data, i.e., $\left(R_r(f_{\mathcal{F}_2}^*) - R_r(f_{\mathcal{F}_1}^*)\right)\left(R_r(\tilde{f}_{\mathcal{F}_2}^*) - R_r(\tilde{f}_{\mathcal{F}_1}^*)\right) > 0$.

Theorem 4 sheds light on the sufficient conditions that $\mathbb{P}_{\tilde{\mathbf{X}}, \tilde{\mathbf{Y}}}$ must fulfill to guarantee consistent model comparison in the downstream task. In this theorem, $\mathcal{B}(\hat{\mu}, \mu)$ characterizes the approximation error of $\hat{\mu}$ to μ , while $\mathcal{W}(\mathcal{F}_1, \mathcal{F}_2)$ characterizes the generalization performance gap between the optimal models of \mathcal{F}_1 and \mathcal{F}_2 . An intriguing observation is that achieving consistent model comparison only entails $\mathcal{B}(\hat{\mu}, \mu)$ to be smaller than $\mathcal{W}(\mathcal{F}_1, \mathcal{F}_2)$. This result implies that even in a situation where synthetic responses are not well generated ($\|\hat{\mu} - \mu\|_{L^2(\mathbb{P}_{\mathbf{X}})}$ is large), consistent model comparison remains attainable as long as $\mathcal{W}(\mathcal{F}_1, \mathcal{F}_2)$ is large enough. Additionally, (V, d) -fidelity level affects the difficulty to meet the condition $\mathcal{B}(\hat{\mu}, \mu) \leq \mathcal{W}(\mathcal{F}_1, \mathcal{F}_2)$. Specifically, the quantity $C_{d,V,U}$ converges to 1 as d approaches infinity (larger similarity between $\mathbb{P}_{\mathbf{X}}$ and $\mathbb{P}_{\tilde{\mathbf{X}}}$) irrespective of the specific values of V and U .

In what follows, we provide several examples explicating the condition $\mathcal{W}(\mathcal{F}_1, \mathcal{F}_2) > \mathcal{B}(\hat{\mu}, \mu)$ under varying (V, d) -fidelity levels and the condition that synthetic responses are generated well ($\hat{\mu} = \mu$).

Example 1. If $\Phi_r(f_{\mathcal{F}_2}^*) = 0$ and $\Phi_r(f_{\mathcal{F}_1}^*) > 0$, then $\mathcal{W}(\mathcal{F}_1, \mathcal{F}_2) = \sqrt{\Phi_r(f_{\mathcal{F}_1}^*)} > 0$ automatically holds true.

Example 2. If $\mathbb{P}_{\mathbf{X}} = \mathbb{P}_{\tilde{\mathbf{X}}}$, then $\mathcal{W}(\mathcal{F}_1, \mathcal{F}_2) = \sqrt{\Phi_r(f_{\mathcal{F}_1}^*)} - \sqrt{\Phi_r(f_{\mathcal{F}_2}^*)} > 0$, where $\mathcal{W}(\mathcal{F}_1, \mathcal{F}_2) > 0$ automatically holds true by the assumption that $R_r(f_{\mathcal{F}_2}^*) < R_r(f_{\mathcal{F}_1}^*)$.

Example 3. If $M_1 \leq P_{\mathbf{X}}(\mathbf{x})/P_{\tilde{\mathbf{X}}}(\mathbf{x}) \leq M_2$ for some positive constants $M_1 \in [0, 1]$ and $M_2 \in [1, \infty]$ with $M_2 > M_1^{-1}$, then $\mathcal{W}(\mathcal{F}_1, \mathcal{F}_2) > 0$ if $M_2^2 \Phi_r(f_{\mathcal{F}_2}^*) \leq \Phi_r(f_{\mathcal{F}_1}^*)$.

Theorem 5. For any $v > 0$, let $\mathcal{H}(v) = \{(\mathcal{F}_1, \mathcal{F}_2) : \mathcal{W}(\mathcal{F}_1, \mathcal{F}_2) \geq v\}$ denote a class of function pairs $(\mathcal{F}_1, \mathcal{F}_2)$. Assume that (1) $\mathbb{P}_{\tilde{\mathbf{X}}}$ and $\mathbb{P}_{\mathbf{X}}$ satisfy (V, d) -fidelity level; (2) $\hat{\mu}$ is a consistent estimator of μ such that for some positive sequence $\{a_n\}_{n=1}^\infty$ tending towards infinity, for any

$n \geq 1$ and any $\delta > 0$, $\mathbb{P}(\|\widehat{\mu} - \mu\|_{L^2(\mathbb{P}_{\mathbf{X}})} > \delta) \leq C_1 \exp(-C_2 a_n \delta)$, for some positive constants C_1 and C_2 . Then, for any $v > 0$,

$$\begin{aligned} & \sup_{(\mathcal{F}_1, \mathcal{F}_2) \in \mathcal{H}(v)} \mathbb{P} \left((R_r(f_{\mathcal{F}_2}^*) - R_r(f_{\mathcal{F}_1}^*)) (R_r(\widetilde{f}_{\mathcal{F}_2}^*) - R_r(\widetilde{f}_{\mathcal{F}_1}^*)) < 0 \right) \\ & \leq C_1 \left\{ \exp \left(-C_2 a_n \right) + \exp \left(-C_2 a_n v^{\frac{(d+1)^2}{d^2}} (C_{d,V,U} + 1)^{-\frac{(d+1)^2}{d^2}} \right) \right\}, \end{aligned}$$

where the randomness results from the training dataset \mathcal{D}_r used for estimating μ .

Theorem 5 shows that consistent model comparison is guaranteed with a high probability for any pair of model classes $(\mathcal{F}_1, \mathcal{F}_2)$ within $\mathcal{H}(v)$ under suitable conditions. Notably, assumption (2) in Theorem 5 indicates as n approaches infinity, the synthetic conditional distribution $\mathbb{P}_{\widetilde{Y}|\widetilde{\mathbf{X}}}$ accurately captures the relationship between features and response in $\mathbb{P}_{Y|\mathbf{X}}$. This assumption is mild and is generally attainable through some non-parametric regression techniques (Fan and Gijbels, 1992; Fan et al., 1997; Zhao and Lai, 2019) or neural networks (Nakada and Imaizumi, 2020; Kohler and Langer, 2021).

Corollary 1. *Under the assumptions of Theorem 5, if \mathcal{F}_2 is chosen appropriately such that $\Phi_r(f_{\mathcal{F}_2}^*) = 0$, then we have*

$$\begin{aligned} & \mathbb{P} \left((R_r(f_{\mathcal{F}_2}^*) - R_r(f_{\mathcal{F}_1}^*)) (R_r(\widetilde{f}_{\mathcal{F}_2}^*) - R_r(\widetilde{f}_{\mathcal{F}_1}^*)) < 0 \right) \\ & \leq C_1 \left\{ \exp \left(-C_2 a_n \right) + \exp \left(-C_2 a_n [\Phi_r(f_{\mathcal{F}_1}^*)]^{\frac{(d+1)^2}{2d^2}} (C_{d,V,U} + 1)^{-\frac{(d+1)^2}{d^2}} \right) \right\}. \quad (14) \end{aligned}$$

Corollary 1 considers a specific scenario where \mathcal{F}_2 is the optimal function class with $\Phi_r(f_{\mathcal{F}_2}^*) = 0$. In this special case, consistent model comparison holds true for any \mathcal{F}_1 with $\Phi_r(f_{\mathcal{F}_1}^*) > 0$ under different (V, d) -fidelity levels, provided that $\|\widehat{\mu} - \mu\|_{L^2(\mathbb{P}_{\mathbf{X}})} = o_p(1)$. Furthermore, the inequality in (14) aligns with the intuition that a larger value of $\Phi_r(f_{\mathcal{F}_1}^*)$ corresponds to a greater probability of ensuring consistent model comparison under varying (V, d) -fidelity levels. This result unveils an intriguing observation: the optimal model from the correct model specification under synthetic data consistently outperforms other optimal models derived from inferior model specifications, irrespective of the distribution of

synthetic features. Moreover, Corollary 1 demonstrates that consistent model comparison can be achievable across varying degrees of dissimilarity between real and synthetic feature distributions, provided that one downstream model class exhibits the best generalization performance, i.e. $\Phi_r(f_{\mathcal{F}_2}^*) = 0$.

7 Numerical Experiments

7.1 Simulation

Consistent Generalization. In this section, we present a series of simulations aimed at validating our theoretical findings. Specifically, the simulations focus on verifying the convergence of the utility metric as described in (3) and investigating how the convergence of the utility metric is affected by various factors such as model specification, feature fidelity, and the estimation models used. Our experimental results are in line with our theoretical findings, thereby confirming the tightness and effectiveness of the analytic bounds established in (4). We consider some practical scenarios in which non-parametric methods are used as the estimation model under different model specifications. The generation of real dataset $\{(\mathbf{x}_i, y_i)\}_{i=1}^n$ for regression is structured as follows. First, we generate the real features \mathbf{x}_i 's via a truncated multivariate normal distribution (Botev, 2017) with lower bounds set at $\mathbf{l} = (-2, -2)$, upper bounds set at $\mathbf{u} = (2, 2)$, and a mean vector of $\mathbf{m} = (1, 1)$. We set $\mu(\mathbf{x}_i) = \exp(x_{i1}) - \exp(x_{i2})$ and generate true responses y_i as $y_i = \mu(\mathbf{x}_i) + \epsilon_i$, where ϵ_i is Gaussian noise with mean 0 and variance 1

We consider two non-parametric methods, namely K -nearest neighbors (KNN; Coomans and Massart, 1982) and random forest regressor (RF; Breiman, 2001), as well as deep neural networks (Farrell et al., 2021) for generating synthetic responses. For the hyperparameters, we set the number of neighbors K at the order of $n^{2/(2+p)}$ (Hall et al., 2008) in KNN. For random forests, we set the numbers of trees and the maximum depth of each tree as $3/2n^{1/2}$ and $\log(n)$, respectively. For the deep neural network, we consider the 4-layer perceptron

with hidden units being 10 and ReLU activation function. With the estimation models, we then generate synthetic responses following the procedure illustrated in Figure 1.

We consider the following three specifications of training models: (1) $\mathcal{F}_1 = \{f(\mathbf{x}) = \beta_1 x_1 + \beta_2 x_2 : \boldsymbol{\beta} \in \mathbb{R}^2\}$; (2) $\mathcal{F}_2 = \{f(\mathbf{x}) = \beta_1 x_1 + \beta_2 x_2 + \beta_3 x_1^2 + \beta_4 x_2^2 : \boldsymbol{\beta} \in \mathbb{R}^4\}$; (3) $\mathcal{F}_3 = \{f(\mathbf{x}) = \beta_1 \exp(x_1) + \beta_2 \exp(x_2) : \boldsymbol{\beta} \in \mathbb{R}^2\}$. Clearly, \mathcal{F}_1 is a class of linear models of real features and can be included as a special case by \mathcal{F}_2 . Additionally, \mathcal{F}_3 refers to as the correct model specification that achieves the optimal generalization error. We generate a testing dataset of 50,000 samples to estimate the risks of the estimated models.

To investigate the effect of feature fidelity on the utility metrics, we consider two scenarios. In Scenario I, the synthetic and real feature distributions are assumed to be the same, and the convergence of utility metrics is analyzed under various model assumptions and estimation methods. In Scenario II, the synthetic feature distribution is a uniform distribution over the same support, and the behavior of utility metrics is studied under three different model specifications. The sample size is set as $n \in \{1000 \times 2^i, i = 1, 2, 3, 4, 5\}$, and each setting is replicated 100 times to evaluate the convergence of utility metrics. We reports the average estimated utility metrics and their 95% confidence intervals for both scenarios in Figure 4.

As can be seen in Figure 4, with perfect feature fidelity, the utility metric $U_r(\hat{f}, \tilde{f})$ with different model specifications and estimation methods decrease to zero simultaneously as expected. In stark contrast, the utility metrics of wrong model specifications \mathcal{F}_1 and \mathcal{F}_2 converge to some fixed positive constants as n increases and finally stay unchanged. Conversely, for the correct model specification \mathcal{F}_3 , the utility metrics with different estimation models converge to zero as n increases. These results empirically support our theories.

In this paper, our primary emphasis lies in theoretical understanding of learning utility of synthetic data. In this experiment, we extend our analysis by employing three additional utility metrics to evaluate the efficacy of diverse estimation models. Our objective is to ascertain whether analogous phenomena can be discerned across multiple utility metrics,

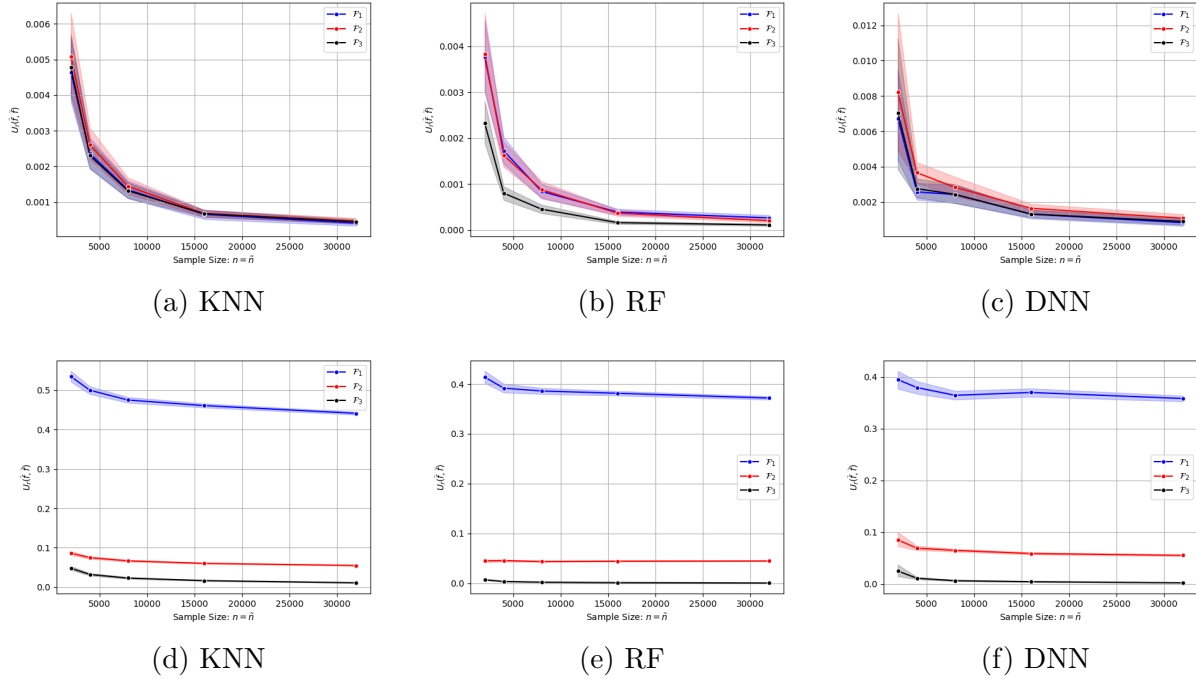


Figure 4: The estimated utility metrics with perfect features (a)-(c) and imperfect features (d)-(f) for Scenarios I and II, respectively.

encompassing absolute coefficient differences (ACD) (Raghuathan, 2021), the standardized coefficient difference (SCD) (Snok et al., 2018), and the overlap of 95% confidence intervals (CIO) in percentage (Karr et al., 2006; Woo and Slavkovic, 2015; Azizi et al., 2021). The SCD is computed as $|\hat{\beta} - \tilde{\beta}|/se(\hat{\beta})$, where $\hat{\beta}$ and $\tilde{\beta}$ denote estimates derived from real and synthetic data, respectively. The term $se(\hat{\beta})$ represents the standard error of $\hat{\beta}$. The confidence interval overlap assesses the percentage of overlap in the confidence intervals of $\hat{\beta}$ and $\tilde{\beta}$.

In Tables 1 and 2, we present the averaged absolute and standardized coefficient differences, along with confidence interval overlaps across three model specifications and three estimation models in Scenarios I and II. Table 1 reveals that, given perfect feature fidelity, random forests outperform the other two estimation models across three utility metrics under all three model specifications simultaneously. As depicted in Table 2, in scenarios with poor feature fidelity, all utility metrics degrade under all estimation models and model specifications. It is noteworthy that the improvement of utility metrics is evident as the downstream function

Table 1: The averaged absolute coefficient differences, standardized coefficient differences, confidence interval overlaps of all cases in Scenario I with $n = \tilde{n} = 2,000$.

Model Specification	Metrics	DNN	KNN	RF
\mathcal{F}_1	ACD	0.0523	0.0638	0.0507
	SCD	1.4744	1.7995	1.4299
	CIO	64.66%	55.82%	64.59%
\mathcal{F}_2	ACD	0.0410	0.0418	0.0407
	SCD	1.1776	1.1791	1.1417
	CIO	70.95%	70.63%	71.74%
\mathcal{F}_3	ACD	0.0179	0.0304	0.0142
	SCD	1.6837	2.8678	1.3384
	CIO	63.99%	30.29%	66.63%

Table 2: The averaged absolute coefficient differences, standardized coefficient differences, confidence interval overlaps of all cases in Scenario II with $n = \tilde{n} = 2,000$.

Model Specification	Metrics	DNN	KNN	RF
\mathcal{F}_1	ACD	0.6374	0.7467	0.6562
	SCD	17.9880	21.0732	18.5208
	CIO	0.00%	0.00%	0.00%
\mathcal{F}_2	ACD	0.2205	0.1660	0.1857
	SCD	6.5822	5.2813	5.4796
	CIO	1.74%	17.22%	1.02%
\mathcal{F}_3	ACD	0.0417	0.0973	0.0297
	SCD	3.9324	9.1877	2.8143
	CIO	28.05%	0.44 %	36.52%

class becomes larger ($\mathcal{F}_1 \prec \mathcal{F}_2 \prec \mathcal{F}_3$). Specifically, ACD, SCD, and CIO of \mathcal{F}_3 surpass those of \mathcal{F}_1 and \mathcal{F}_2 when using DNN and RF to generate synthetic responses. Notably, the ACD of \mathcal{F}_3 exhibits minimal deterioration compared to the scenario with perfect feature fidelity. This result is consistent with our theoretical findings regarding the proposed utility metrics, indicating that the downstream model specification also significantly influences the utility of synthetic data.

Consistent Model Comparison. In this part, we conduct an experiment to validate two phenomenon of model comparison based on synthetic data. Specifically, consistency of model comparison based on synthetic data is achievable when one of the models accurately specifies the regression function, or when the generalization gap between two model specifications is

wide enough to offset any differences in distribution between synthetic and real features.

We generate real data as follows. First, we generate real features as $x_i \sim \text{Unif}(0, 2)$ for $i = 1, \dots, n$. Then we consider the regression function $y_i = \mathbf{u}_i^T \boldsymbol{\beta}$, where $\mathbf{u}_i = ((x_i + 0.1)^{-1}, x_i, x_i^2, x_i^3)$ and $\boldsymbol{\beta} = (1, -2, -2, 1)$. For the downstream learning tasks, we consider the following four specifications of training models: (1) $\mathcal{F}_0 = \{f(x) = \beta_1 x + \beta_2 x^3 : \boldsymbol{\beta} \in \mathbb{R}^2\}$; (2) $\mathcal{F}_1 = \{f(\mathbf{x}) = \beta_1(x + 0.1)^{-1} + \beta_2 x^3 : \boldsymbol{\beta} \in \mathbb{R}^2\}$; (3) $\mathcal{F}_2 = \{f(\mathbf{x}) = \beta_1 x^2 + \beta_2 x^3 : \boldsymbol{\beta} \in \mathbb{R}^2\}$; (4) $\mathcal{F}_3 = \{f(\mathbf{x}) = \beta_1(x + 0.1)^{-1} + \beta_2 x + \beta_3 x^2 + \beta_4 x^3 : \boldsymbol{\beta} \in \mathbb{R}^4\}$. Here \mathcal{F}_3 is considered the correct model specification. To generate synthetic features \tilde{x}_i , we use the density function $P_{\tilde{X}}(x) = \alpha(x - 1) + 1$ for $x \in [0, 2]$, where $\alpha \in [0, 1/2]$ is a parameter that controls the distribution similarity between X and \tilde{X} . As α increases, the distribution of \tilde{X} becomes less similar to that of X . The case where $\alpha = 0$ corresponds to $X = \tilde{X}$. It's important to note that we assume the estimation model is perfect, meaning that $\tilde{y}_i = \tilde{\mathbf{u}}_i^T \boldsymbol{\beta}$, where $\tilde{\mathbf{u}}_i = ((\tilde{x}_i + 0.1)^{-1}, \tilde{x}_i, \tilde{x}_i^2, \tilde{x}_i^3)$. For each setting, we generate 10,000 real samples and 10,000 synthetic samples for training and evaluate the fitted models on 50,000 real samples. The generalization performances of fitted models from real and synthetic data over 100 replications are reported in Figure 5.

Figure 5 demonstrates that the black dashed curve consistently lies below the other dashed curves for various values of α , indicating that consistent model comparison is achieved when one of the models for comparison is accurate. This result aligns with Theorem 4. Additionally, as the synthetic feature distribution becomes less similar to the real feature distribution, the generalization performances of models trained on synthetic data worsen. Among the blue, red, and grey dashed curves, the blue curve appears to be the most affected by changes in the synthetic feature distribution, and eventually leads to inconsistent model comparison between \mathcal{F}_1 and \mathcal{F}_0 , where $R_r(\tilde{f}_{\mathcal{F}_1}^*)$ becomes greater than $R_r(\tilde{f}_{\mathcal{F}_0}^*)$. Nevertheless, $R_r(\tilde{f}_{\mathcal{F}_1}^*)$ remains below $R_r(\tilde{f}_{\mathcal{F}_2}^*)$ due to the wide gap between $R_r(f_{\mathcal{F}_1}^*)$ and $R_r(f_{\mathcal{F}_2}^*)$. This finding confirms our theoretical results in Section 6 that consistent model comparison based

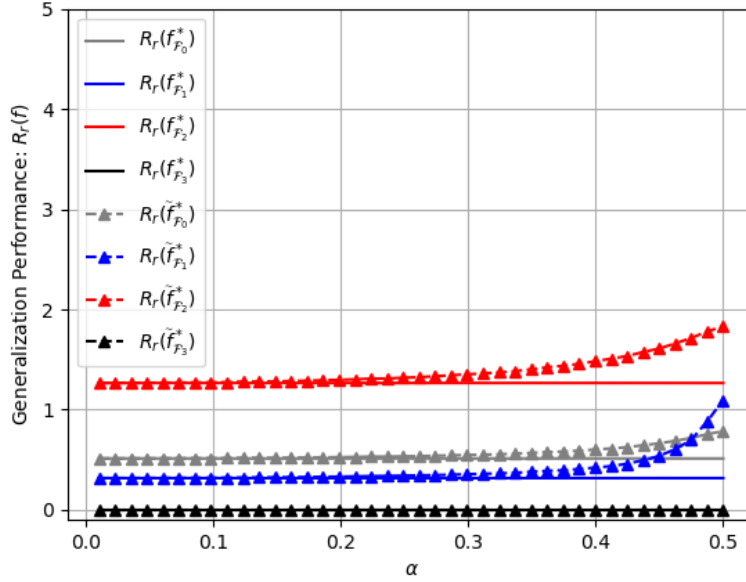


Figure 5: The generalization performances of models estimated from synthetic data and real data under different model specifications.

on synthetic data requires a substantial generalization gap between two model specifications to offset the impact of any differences between distributions of synthetic and actual features.

7.2 Real Experiment: MNIST Dataset

In this section, we use the MNIST dataset (LeCun, 1998) as an example to demonstrate how models trained on synthetic data can generalize well on real data with appropriate model specification, even when the quality of the synthetic data is subpar. The MNIST dataset comprises 60,000 training images and 10,000 testing images, with each sample being a 28×28 grey-scale pixel image of one of the 10 digits. We utilize a generative adversarial network (GAN; Goodfellow et al. 2014) to generate synthetic images. The generator and discriminator both have three-layer perceptrons with a LeakyReLU activation function. We randomly generate 100-dimensional Gaussian samples as input for the generator. Under the supervision of the discriminator, the generator will be trained to find the mapping between Gaussian samples and 784-dimensional vectors, which are then reshaped into 28×28 synthetic images.

We employ the Adam optimizer with a learning rate of 0.0002 and use generators trained for 100 and 400 epochs to generate synthetic images representing different feature fidelity levels.

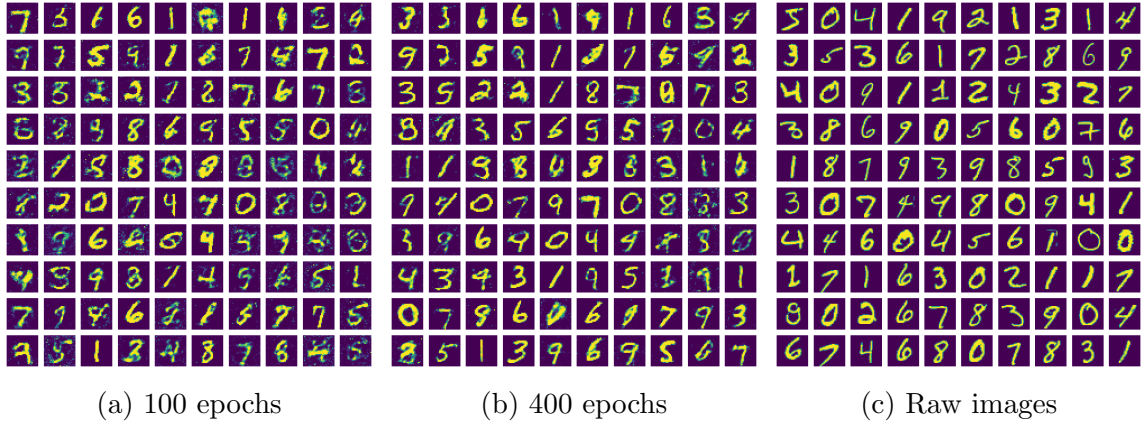


Figure 6: Synthetic images generated by GANs at different epochs and real images. As the training epoch increases, synthetic images become clearer and resemble real images more.

In this experiment, we utilize a neural network consisting of two convolution layers with ReLU activation and two fully-connected layers to generate responses for synthetic images. The kernel sizes and the number of channels for the convolution layers are set as 4×4 and 28, respectively, and each convolution layer is followed by a max pooling layer with size 2×2 . The first fully-connected layer comprises 128 hidden units with ReLU activation, while the last layer utilizes softmax activation to output the probability for each class. The neural network is trained using the Adam optimizer with a learning rate of 0.0003, achieving nearly 98.5% accuracy on testing samples. To highlight the significance of model specification, we suppose three distinct downstream model specifications: (1) a single-layer perceptron that takes flattened images as input and produces the probability of each class as output; (2) a two-layer perceptron with 40 hidden units; and (3) a model that is identical to the one employed to generate synthetic responses. The accuracies on testing samples have been reported in Figure 7, which have been averaged over 30 replications.

Figure 7 depicts the impact of increasing training epochs on the performance of all three model specifications, which demonstrates that higher quality synthetic images lead to improved model performance. Notably, Model 1 and Model 2 exhibit a significant drop in

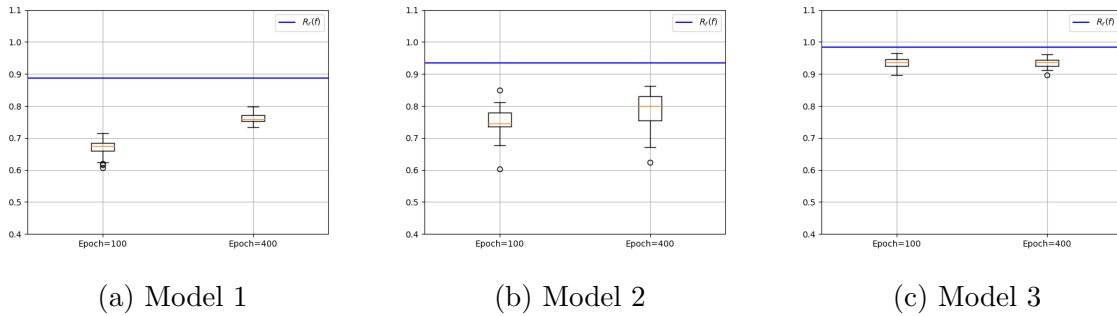


Figure 7: The testing accuracies on 10,000 real images of different model specifications and two generators trained in 100 and 400 epochs, respectively. The blue line denotes the testing accuracy of the model trained on the raw training dataset under the same model specification.

generalization accuracy on testing samples when the real dataset is substituted with synthetic data. Conversely, the drop in generalization accuracy is less severe for Model 3, which aligns with our theoretical findings that an accurate model specification is more important than the feature fidelity of synthetic data in yielding comparable performance to real data.

References

- Arjovsky, M., Chintala, S., and Bottou, L. (2017). Wasserstein generative adversarial networks. In *International Conference on Machine Learning*, pages 214–223. PMLR.
- Assefa, S. A., Dervovic, D., Mahfouz, M., Tillman, R. E., Reddy, P., and Veloso, M. (2020). Generating synthetic data in finance: opportunities, challenges and pitfalls. In *Proceedings of the First ACM International Conference on AI in Finance*, pages 1–8.
- Azizi, S., Kornblith, S., Saharia, C., Norouzi, M., and Fleet, D. J. (2023). Synthetic data from diffusion models improves imagenet classification. *arXiv preprint arXiv:2304.08466*.
- Azizi, Z., Zheng, C., Mosquera, L., Pilote, L., and El Emam, K. (2021). Can synthetic data be a proxy for real clinical trial data? a validation study. *BMJ open*, 11(4):e043497.
- Beaulieu-Jones, B. K., Wu, Z. S., Williams, C., Lee, R., Bhavnani, S. P., Byrd, J. B., and Greene, C. S. (2019). Privacy-preserving generative deep neural networks support clinical data sharing. *Circulation: Cardiovascular Quality and Outcomes*, 12(7):e005122.
- Benaim, A. R., Almog, R., Gorelik, Y., Hochberg, I., Nassar, L., Mashiach, T., Khamaisi, M., Lurie, Y., Azzam, Z. S., Khoury, J., et al. (2020). Analyzing medical research results based on synthetic data and their relation to real data results: systematic comparison from five observational studies. *JMIR medical informatics*, 8(2):e16492.
- Bi, X. and Shen, X. (2022). Distribution-invariant differential privacy. *Journal of Econometrics*.

- Bickel, P. J., Ritov, Y., and Tsybakov, A. B. (2009). Simultaneous analysis of Lasso and Dantzig selector. *The Annals of Statistics*, 37(4):1705 – 1732.
- Botev, Z. I. (2017). The normal law under linear restrictions: simulation and estimation via minimax tilting. *Journal of the Royal Statistical Society: Series B (Statistical Methodology)*, 79(1):125–148.
- Bousquet, O. (2003). New approaches to statistical learning theory. *Annals of the Institute of Statistical Mathematics*, 55(2):371–389.
- Bousquet, O., Livni, R., and Moran, S. (2020). Synthetic data generators—sequential and private. *Advances in Neural Information Processing Systems*, 33:7114–7124.
- Breiman, L. (2001). Random forests. *Machine learning*, 45(1):5–32.
- Charitou, C., Dragicevic, S., and Garcez, A. d. (2021). Synthetic data generation for fraud detection using gans. *arXiv preprint arXiv:2109.12546*.
- Chatterjee, A. and Lahiri, S. (2011). Strong consistency of lasso estimators. *Sankhya A*, 73:55–78.
- Chen, R. J., Lu, M. Y., Chen, T. Y., Williamson, D. F., and Mahmood, F. (2021). Synthetic data in machine learning for medicine and healthcare. *Nature Biomedical Engineering*, 5(6):493–497.
- Cheng, Yinan, W. C.-H., K Potluru, V., Balch, T., and Cheng, G. (2023). Downstream task-oriented generative model selections on synthetic data training for fraud detection models. In *ACM International Conference on AI in Finance – Workshop*.
- Coomans, D. and Massart, D. L. (1982). Alternative k-nearest neighbour rules in supervised pattern recognition: Part 1. k-nearest neighbour classification by using alternative voting rules. *Analytica Chimica Acta*, 136:15–27.
- De Mello, R. F. and Ponti, M. A. (2018). Statistical learning theory. *Rodrigo Fernandes de Mello*, page 75.
- Dogariu, M., Ștefan, L.-D., Boteanu, B. A., Lamba, C., Kim, B., and Ionescu, B. (2022). Generation of realistic synthetic financial time-series. *ACM Transactions on Multimedia Computing, Communications, and Applications (TOMM)*, 18(4):1–27.
- El Eman, K., Mosquera, L., Jonker, E., and Sood, H. (2021). Evaluating the utility of synthetic covid-19 case data. *JAMIA open*, 4(1):o0ab012.
- Fan, J., Gasser, T., Gijbels, I., Brockmann, M., and Engel, J. (1997). Local polynomial regression: Optimal kernels and asymptotic minimax efficiency. *Annals of the Institute of Statistical Mathematics*, 49:79–99.
- Fan, J. and Gijbels, I. (1992). Variable bandwidth and local linear regression smoothers. *The Annals of Statistics*, pages 2008–2036.

- Farrell, M. H., Liang, T., and Misra, S. (2021). Deep neural networks for estimation and inference. *Econometrica*, 89(1):181–213.
- Frid-Adar, M., Klang, E., Amitai, M., Goldberger, J., and Greenspan, H. (2018). Synthetic data augmentation using gan for improved liver lesion classification. In *2018 IEEE 15th International Symposium on Biomedical Imaging (ISBI 2018)*, pages 289–293. IEEE.
- Goodfellow, I., Pouget-Abadie, J., Mirza, M., Xu, B., Warde-Farley, D., Ozair, S., Courville, A., and Bengio, Y. (2014). Generative adversarial nets. *Advances in neural information processing systems*, 27.
- Goodfellow, I., Pouget-Abadie, J., Mirza, M., Xu, B., Warde-Farley, D., Ozair, S., Courville, A., and Bengio, Y. (2020). Generative adversarial networks. *Communications of the ACM*, 63(11):139–144.
- Hall, P., Park, B. U., and Samworth, R. J. (2008). Choice of neighbor order in nearest-neighbor classification. *the Annals of Statistics*, 36(5):2135–2152.
- Hittmeir, M., Ekelhart, A., and Mayer, R. (2019). On the utility of synthetic data: An empirical evaluation on machine learning tasks. In *Proceedings of the 14th International Conference on Availability, Reliability and Security*, pages 1–6.
- Homrighausen, D. and McDonald, D. J. (2017). Risk consistency of cross-validation with lasso-type procedures. *Statistica Sinica*, pages 1017–1036.
- Jordon, J., Szpruch, L., Houssiau, F., Bottarelli, M., Cherubin, G., Maple, C., Cohen, S. N., and Weller, A. (2022). Synthetic data—what, why and how? *arXiv preprint arXiv:2205.03257*.
- Jordon, J., Yoon, J., and van der Schaar, M. (2018). Measuring the quality of synthetic data for use in competitions. *arXiv preprint arXiv:1806.11345*.
- Jordon, J., Yoon, J., and Van Der Schaar, M. (2019). Pate-gan: Generating synthetic data with differential privacy guarantees. In *International Conference on Learning Representations*.
- Karr, A. F., Kohnen, C. N., Oganian, A., Reiter, J. P., and Sanil, A. P. (2006). A framework for evaluating the utility of data altered to protect confidentiality. *The American Statistician*, 60(3):224–232.
- Kato, M. and Teshima, T. (2021). Non-negative bregman divergence minimization for deep direct density ratio estimation. In *International Conference on Machine Learning*, pages 5320–5333. PMLR.
- Kohler, M. and Langer, S. (2021). On the rate of convergence of fully connected deep neural network regression estimates. *The Annals of Statistics*, 49(4):2231–2249.
- Kpotufe, S. (2017). Lipschitz density-ratios, structured data, and data-driven tuning. In *Artificial Intelligence and Statistics*, pages 1320–1328. PMLR.
- LeCun, Y. (1998). The mnist database of handwritten digits. <http://yann.lecun.com/exdb/mnist/>.

- Li, X., Wang, C., and Cheng, G. (2023). Statistical theory of differentially private marginal-based data synthesis algorithms. *arXiv preprint arXiv:2301.08844*.
- Mann, H. B. and Wald, A. (1943). On stochastic limit and order relationships. *The Annals of Mathematical Statistics*, 14(3):217–226.
- McKenna, R., Pradhan, S., Sheldon, D. R., and Miklau, G. (2021). Relaxed marginal consistency for differentially private query answering. *Advances in Neural Information Processing Systems*, 34:20696–20707.
- Nakada, R. and Imaizumi, M. (2020). Adaptive approximation and generalization of deep neural network with intrinsic dimensionality. *The Journal of Machine Learning Research*, 21(1):7018–7055.
- Nowok, B., Raab, G. M., and Dibben, C. (2016). synthpop: Bespoke creation of synthetic data in r. *Journal of Statistical Software*, 74:1–26.
- Ouyang, Y., Xie, L., and Cheng, G. (2022). Improving adversarial robustness by contrastive guided diffusion process. *arXiv preprint arXiv:2210.09643*.
- Raghunathan, T. E. (2021). Synthetic data. *Annual Review of Statistics and Its Application*, 8:129–140.
- Rankin, D., Black, M., Bond, R., Wallace, J., Mulvenna, M., Epelde, G., et al. (2020). Reliability of supervised machine learning using synthetic data in health care: Model to preserve privacy for data sharing. *JMIR medical informatics*, 8(7):e18910.
- Rényi, A. (1961). On measures of entropy and information. In *Proceedings of the Fourth Berkeley Symposium on Mathematical Statistics and Probability, Volume 1: Contributions to the Theory of Statistics*, volume 4, pages 547–562. University of California Press.
- Shoshan, A., Bhonker, N., Kviatkovsky, I., Fintz, M., and Medioni, G. (2023). Synthetic data for model selection. In *International Conference on Machine Learning*, pages 31633–31656. PMLR.
- Snoke, J., Raab, G. M., Nowok, B., Dibben, C., and Slavkovic, A. (2018). General and specific utility measures for synthetic data. *Journal of the Royal Statistical Society. Series A (Statistics in Society)*, 181(3):663–688.
- Song, Y., Durkan, C., Murray, I., and Ermon, S. (2021). Maximum likelihood training of score-based diffusion models. *Advances in Neural Information Processing Systems*, 34:1415–1428.
- Tremblay, J., Prakash, A., Acuna, D., Brophy, M., Jampani, V., Anil, C., To, T., Cameracci, E., Boochoon, S., and Birchfield, S. (2018). Training deep networks with synthetic data: Bridging the reality gap by domain randomization. In *Proceedings of the IEEE conference on computer vision and pattern recognition workshops*, pages 969–977.
- Van Breugel, B., Qian, Z., and van der Schaar, M. (2023). Synthetic data, real errors: how (not) to publish and use synthetic data. *arXiv preprint arXiv:2305.09235*.

- Vapnik, V. N. (1999). An overview of statistical learning theory. *IEEE Transactions on Neural Networks*, 10(5):988–999.
- Wainwright, M. J. (2019). *High-dimensional statistics: A non-asymptotic viewpoint*, volume 48. Cambridge university press.
- Woo, Y. M. J. and Slavkovic, A. (2015). Generalised linear models with variables subject to post randomization method. *Statistica Applicata-Italian Journal of Applied Statistics*, 24(1):29–56.
- Xing, Y., Song, Q., and Cheng, G. (2022). Why do artificially generated data help adversarial robustness. In Koyejo, S., Mohamed, S., Agarwal, A., Belgrave, D., Cho, K., and Oh, A., editors, *Advances in Neural Information Processing Systems*, volume 35, pages 954–966. Curran Associates, Inc.
- Zhang, T. (2004). Statistical behavior and consistency of classification methods based on convex risk minimization. *The Annals of Statistics*, 32(1):56–85.
- Zhao, P. and Lai, L. (2019). Analysis of knn information estimators for smooth distributions. *IEEE Transactions on Information Theory*, 66(6):3798–3826.
- Zhou, X., Jiao, Y., Liu, J., and Huang, J. (2022). A deep generative approach to conditional sampling. *Journal of the American Statistical Association*, pages 1–12.

Supplementary Materials

“Utility Theory of Synthetic Data Generation”

This Appendix provides auxiliary results for the classification setting and detailed proofs for all theorems and lemmas. For theoretical proofs in the following, we introduce the concept of ϵ -covering set. If \mathcal{C} is a ϵ -covering set of a function class \mathcal{F} with metric $\|\cdot\|_{L^2(\mathbb{P}_{\mathbf{X}})}$, then for any $f \in \mathcal{F}$, there exists $f' \in \mathcal{C}$ such that $\|f' - f\|_{L^2(\mathbb{P}_{\mathbf{X}})} < \epsilon$. For real and synthetic feature distributions $\mathbb{P}_{\mathbf{X}}$ and $\mathbb{P}_{\tilde{\mathbf{X}}}$, we let \mathcal{X} denote the union of their supports.

S.1 Auxiliary Results for Classification

In this section, we provide results in the classification setting. The section is organized as follows: Section [S.1.1](#) introduces necessary notations and provides background information on classification. In Section [S.1.2](#), we introduce a utility metric for classification and establish an analytical bound to analyze the convergence behavior of the proposed metric. In Section [S.1.3](#), we offer several classification examples to demonstrate that imperfect synthetic features may result in the divergence of the utility metric. However, this challenge can be addressed if the downstream function class is highly flexible. To illustrate, we present a linear classification case with logistic loss. Section [S.1.4](#) sheds light on the sufficient conditions for ensuring consistent model comparison in the classification setting.

S.1.1 Preliminaries

Let $\mathcal{D}_c = \{(\mathbf{x}_i, z_i)\}_{i=1}^n$ denote the dataset in binary classification, where z_i takes values in $\{-1, 1\}$ and

$$z_i = \begin{cases} 1 & \text{with probability } \eta(\mathbf{x}_i), \\ -1 & \text{with probability } 1 - \eta(\mathbf{x}_i), \end{cases}$$

where $\eta(\mathbf{x}_i) = \mathbb{P}(Z = 1 | \mathbf{X} = \mathbf{x}_i)$ and Z denotes the response variable in classification. Denote the classification risk under the 0-1 loss by $R_{0-1}(g) = \mathbb{E} \left[I(\text{sign}(g(\mathbf{X})) \neq Z) \right]$, where $I(\cdot)$ is an indicator function. The optimal classifier minimizing $R_{0-1}(g)$ is the Bayes classifier, which is given as $g^*(\mathbf{X}) = \text{sign}(\eta(\mathbf{X}) - 1/2)$. The excess risk in classification is defined as

$$\Phi_{0-1}(g) = R_{0-1}(g) - R_{0-1}(g^*) = \mathbb{E} \left[I(\text{sign}(g(\mathbf{X})) \neq g^*(\mathbf{X})) | 2\eta(\mathbf{X}) - 1 \right],$$

where the expectation is taken with respect to \mathbf{X} . For a function class \mathcal{G} , we let $g_{\mathcal{G}}^* = \text{argmin}_{g \in \mathcal{G}} R_{0-1}(g)$ denote the optimal function in \mathcal{G} to minimize $R_{0-1}(g)$.

The estimated models resulting from the regularized empirical risk minimization framework for classification is given as

$$\hat{g} = \text{argmin}_{g \in \mathcal{G}} \frac{1}{n} \sum_{i=1}^n \phi(\mathbf{x}_i z_i) + \lambda_c J_c(g), \quad (\text{S1})$$

where \mathcal{G} is a class of functions for classification, λ_c is a regularization parameter controlling the weight of the penalty term, $J_c(g)$ is a penalty terms, and ϕ is a margin loss for classification, such as hinge loss and logistic loss.

S.1.2 Data Synthesis and Utility Bound for Classification

Let $\tilde{\mathcal{D}}_c = \{(\tilde{\mathbf{x}}_i, \tilde{z}_i)\}_{i=1}^{\tilde{n}}$ be a synthetic dataset generated based on \mathcal{D}_c , respectively. Based on $\tilde{\mathcal{D}}_c$, the classifier is derived from

$$\tilde{g} = \text{argmin}_{g \in \mathcal{G}} \frac{1}{\tilde{n}} \sum_{i=1}^{\tilde{n}} \phi(g(\tilde{\mathbf{x}}_i) \tilde{z}_i) + \lambda_c J_c(g). \quad (\text{S2})$$

Then we consider a similar utility metric for classification.

$$U_c(\tilde{g}, \hat{g}) = \left| R_{0-1}(\tilde{g}) - R_{0-1}(\hat{g}) \right|.$$

Let \tilde{Z} denote the random variable of the synthetic responses $\{\tilde{z}_i\}_{i=1}^{\tilde{n}}$. For any g , we define its 0-1 risk and excess 0-1 risk under the synthetic distribution $P_{\tilde{\mathbf{X}}, \tilde{Z}}$ as

$$\tilde{R}_{0-1}(g) = \mathbb{E} \left[I(\text{sign}(g(\tilde{\mathbf{X}})) \neq \tilde{Z}) \right] \text{ and } \tilde{\Phi}_{0-1}(g) = \mathbb{E} \left[I(\text{sign}(g(\tilde{\mathbf{X}})) \neq \tilde{g}^*(\tilde{\mathbf{X}})) \cdot |2\tilde{\eta}(\tilde{\mathbf{X}}) - 1| \right],$$

respectively, where $\tilde{g}^*(\mathbf{x}) = \text{sign}(\hat{\eta}(\mathbf{x}) - 1/2)$.

Theorem S6. Denote $\tilde{g}_{\mathcal{G}}^* = \text{argmin}_{g \in \mathcal{G}} \tilde{R}_{0-1}(g)$ and $g_{\mathcal{G}}^* = \text{argmin}_{g \in \mathcal{G}} R_{0-1}(g)$. Let \hat{g} and \tilde{g} be the functions defined in (S1) and (S2), respectively.

$$U_c(\tilde{g}, \hat{g}) \leq |R_{0-1}(\hat{g}) - R_{0-1}(g_{\mathcal{G}}^*)| + |\tilde{R}_{0-1}(\tilde{g}) - \tilde{R}_{0-1}(\tilde{g}_{\mathcal{G}}^*)| + 16\|\hat{\eta} - \eta\|_{L^2(\mathbb{P}_{\mathbf{X}})} + 4D_{\mathcal{K}}(\mathbb{P}_{\mathbf{X}}, \mathbb{P}_{\tilde{\mathbf{X}}}) \quad (\text{S3})$$

where $\mathcal{K} = \{k(\mathbf{x}) = |2\hat{\eta}(\mathbf{x}) - 1|I(g(\mathbf{x})(\hat{\eta}(\mathbf{x}) - 1/2) < 0), g \in \{\tilde{g}, g_{\mathcal{G}}^*, \tilde{g}_{\mathcal{G}}^*\}\}$.

Theorem S6 establishes an upper bound for $U_c(\tilde{g}, \hat{g})$. Drawing on this utility bound, we derive sufficient conditions for the convergence of $U_c(\tilde{g}, \hat{g})$. The first two terms of (S3) represent estimation errors under the real and synthetic distributions, with their convergence assured by statistical literature. The third term, $\|\hat{\eta} - \eta\|_{L^2(\mathbb{P}_{\mathbf{X}})}$, quantifies the accuracy of synthetic label generators in approximating the underlying decision boundary η . Furthermore, $D_{\mathcal{K}}(\mathbb{P}_{\mathbf{X}}, \mathbb{P}_{\tilde{\mathbf{X}}})$ gauges the distributional disparity between synthetic and real feature distributions through the Integrated Probability Metric (IPM). It is noteworthy that the function class \mathcal{K} comprises only three functions. Specifically, if \mathcal{G} is chosen appropriately such that $g_{\mathcal{G}}^*(\mathbf{x})(\hat{\eta}(\mathbf{x}) - 1/2) > 0$ and $\tilde{g}_{\mathcal{G}}^*(\mathbf{x})(\hat{\eta}(\mathbf{x}) - 1/2) > 0$ almost surely, $D_{\mathcal{K}}(\mathbb{P}_{\mathbf{X}}, \mathbb{P}_{\tilde{\mathbf{X}}})$ converges to zero in probability.

S.1.3 Examples of Utility Metric: Classification

S.1.3.1 Suboptimality with Imperfect Features: Classification

In this part, we offer an illustrative example of classification as a supplement to Section 5. The purpose is to demonstrate that the utility metric of classification does not converge when there is imperfect feature fidelity and an incorrect model specification. The example we consider is one-dimensional linear classification. We assume $\mathcal{X} = [-1, 1]$ and define the classification function $\eta(x)$ such that $\eta(x) = 1$ for any $x \in (0, 1]$ and $\eta(x) = 0$ otherwise. Let X and \tilde{X} follow the distributions as

$$P_X(x) = \begin{cases} 1 - \alpha, & \text{if } x \in [0, 1], \\ \alpha, & \text{if } x \in [-1, 0). \end{cases} \quad \text{and} \quad P_{\tilde{X}}(x) = \begin{cases} \alpha, & \text{if } x \in [0, 1], \\ 1 - \alpha, & \text{if } x \in [-1, 0). \end{cases}$$

Incorrect Model Specification: In the downstream classification task, we suppose that the class of classifiers $\mathcal{G} = \{g(x) = \text{sign}(\beta|x|) : \beta \in \{-1, 1\}\}$ is considered. The risks of any $g \in \mathcal{G}$ under the true and synthetic distributions can be written as

$$R_{0-1}(g) = (1 - \alpha)I(\beta \leq 0) + \alpha I(\beta \geq 0) \quad \text{and} \quad \tilde{R}_{0-1}(g) = (1 - \alpha)I(\beta \geq 0) + \alpha I(\beta \leq 0).$$

Suppose there are infinite samples in the real and synthetic datasets, then we have

$$\hat{g}(x) = \begin{cases} \text{sign}(-x), & \text{if } \alpha > 1/2, \\ \text{sign}(x), & \text{if } \alpha < 1/2. \end{cases} \quad \text{and} \quad \tilde{g}(x) = \begin{cases} \text{sign}(x), & \text{if } \alpha > 1/2, \\ \text{sign}(-x), & \text{if } \alpha < 1/2. \end{cases}$$

Therefore, we obtain

$$U_c(\hat{g}, \tilde{g}) = |R_{0-1}(\hat{g}) - R_{0-1}(\tilde{g})| = |2\alpha - 1| > 0, \tag{S4}$$

for any $\alpha \in (0, 1/2) \cup (1/2, 1)$. As can be seen in (S4), the utility metric $U_c(\hat{g}, \tilde{g})$ for classification can be bounded away from 0 given inaccurate model specification and imperfect feature fidelity.

Correct Model Specification: If \mathcal{G} includes the Bayes classifier, say $\mathcal{G} = \{g(x) = \text{sign}(\beta x) : \beta \in \{-1, 1\}\}$. The risks of any $g \in \mathcal{G}$ are given as

$$R_{0-1}(g) = I(\beta \leq 0) \quad \text{and} \quad \tilde{R}_{0-1}(g) = I(\beta \leq 0).$$

This result shows that even though the distribution of \tilde{X} is not identical to that of X , $U_c(\hat{g}, \tilde{g}) \equiv 0$ for any α in $\mathbb{P}_{\tilde{X}}$. This example also validates the second conclusion for classification as stated in Section 4.

S.1.3.2 Linear Classifier with Logistic Loss

This section aims to demonstrate our theoretical results for classification using logistic loss, as discussed in Section 5.2. We consider a scenario where $\mathbb{P}_{\tilde{X}}$ is fixed and independent of $\{\mathbf{x}_i\}_{i=1}^n$. We denote the real and synthetic datasets in the logistic regression as $\mathcal{D}_c = \{(\mathbf{x}_i, z_i)\}_{i=1}^n$ and $\tilde{\mathcal{D}}_c = \{(\tilde{\mathbf{x}}_i, \tilde{z}_i)\}_{i=1}^n$, respectively. For any given feature \mathbf{x}_i , we suppose its associated response

z_i is generated as follows:

$$z_i = \begin{cases} 1, & \text{with probability } \eta(\mathbf{x}_i), \\ -1, & \text{with probability } 1 - \eta(\mathbf{x}_i), \end{cases}$$

where $\eta(\mathbf{x}_i) = 1/(1 + \exp(-\mathbf{x}_i^T \boldsymbol{\beta}^*))$.

To generate synthetic responses \tilde{z}_i 's, we assume that the maximum likelihood estimator (MLE) is employed to generate synthetic responses and given as follow

$$\hat{\boldsymbol{\beta}} = \operatorname{argmin}_{\boldsymbol{\beta} \in \mathbb{R}^p} \frac{1}{n} \sum_{i=1}^n \log \left(1 + \exp(-z_i \mathbf{x}_i^T \boldsymbol{\beta}) \right).$$

With $\hat{\boldsymbol{\beta}}$, for any given synthetic feature $\tilde{\mathbf{x}}_i$, the synthetic response \tilde{z}_i is generated via the following distribution.

$$\tilde{z}_i = \begin{cases} 1, & \text{with probability } \hat{\eta}(\tilde{\mathbf{x}}_i), \\ -1, & \text{with probability } 1 - \hat{\eta}(\tilde{\mathbf{x}}_i), \end{cases}$$

where $\hat{\eta}(\tilde{\mathbf{x}}_i) = 1/(1 + \exp(-\tilde{\mathbf{x}}_i^T \hat{\boldsymbol{\beta}}))$.

In the downstream classification task, we suppose the model specification is correct with $\mathcal{G} = \{g(\mathbf{x}) = \mathbf{x}^T \boldsymbol{\beta} : \boldsymbol{\beta} \in [-B, B]^p\}$, where B is a constant chosen to satisfy $\|\boldsymbol{\beta}^*\|_\infty < B/2$. Then the estimated models based on \mathcal{D}_c and $\tilde{\mathcal{D}}_c$, respectively, are given as

$$\begin{aligned} \hat{g}_{log} &= \operatorname{argmin}_{g \in \mathcal{G}} \frac{1}{n} \sum_{i=1}^n \log \left(1 + \exp(-z_i g(\mathbf{x}_i)) \right), \\ \tilde{g}_{log} &= \operatorname{argmin}_{g \in \mathcal{G}} \frac{1}{n} \sum_{i=1}^n \log \left(1 + \exp(-\tilde{z}_i g(\tilde{\mathbf{x}}_i)) \right). \end{aligned}$$

It is straightforward to verify that $1/(1 + \exp(-\hat{g}_{log}))$ is identical to the estimation model $\hat{\eta}$ used to generate synthetic responses if $\|\hat{\boldsymbol{\beta}}\|_\infty \leq B$.

Theorem S7. *Suppose that \mathcal{X} is a compact set and there exists a positive constants M_1, M_2 such that $M_1 \leq P_{\tilde{\mathbf{X}}}(\mathbf{x})/P_{\mathbf{X}}(\mathbf{x}) \leq M_2$ for any $\mathbf{x} \in \mathcal{X}$. Then, for any $\delta > 0$,*

$$\lim_{n \rightarrow \infty} \lim_{\tilde{n} \rightarrow \infty} \mathbb{P}(U_c(\tilde{\mathcal{G}}_{log}, \hat{g}_{log}) > \delta) = 0.$$

In Theorem S7, we present a result regarding the convergence of the utility metric in

logistic regression, but we do not provide the explicit forms of the analytic bound because the analytic solution of logistic regression is not obtainable. Theorem S7 shows that the utility metric $U_c(\tilde{g}_{log}, \hat{g}_{log})$ approaches 0 with a high probability, and this convergence becomes more certain as both n and \tilde{n} increase to infinity. Importantly, this result does not require the distributions of \mathbf{X} and $\tilde{\mathbf{X}}$ to be the same, which is consistent with the second conclusion in Section 4.

S.1.4 Model Comparison Based on Synthetic Data: Classification

In this section, we consider the model comparison problem in classification. In the following, we provide a formal definition of consistent model comparison in classification.

Definition 4. (*Consistent Model Comparison for Classification*) Let $(\mathcal{G}_1, \mathcal{G}_2)$ be a pair classes of classification models for comparison in the downstream learning task. We say the synthetic distribution $\mathbb{P}_{\tilde{\mathbf{X}}, \tilde{\mathbf{Z}}}$ preserves the utility of consistent model comparison if

$$\left(R_{0-1}(g_{\mathcal{G}_1}^*) - R_{0-1}(g_{\mathcal{G}_2}^*) \right) \left(R_{0-1}(\tilde{g}_{\mathcal{G}_1}^*) - R_{0-1}(\tilde{g}_{\mathcal{G}_2}^*) \right) > 0,$$

where $\tilde{g}_{\mathcal{G}_i}^* = \operatorname{argmin}_{g \in \mathcal{G}_i} \tilde{R}_{0-1}(g)$ for $i = 1, 2$.

Examples for Inconsistent Model Comparison. Here we present an illustrative example for classification to demonstrate that the dissimilarity between the marginal distributions of the synthetic and real features sometimes might lead to distinctive optimal models under the same model specification, which results in inconsistent model comparison. We denote the support of synthetic and real features as $\mathcal{X} = [-1, 1]$. Let the decision rule function in classification be $\eta(x) = 1$ for $x \in [0, 1]$ and -1 otherwise. The true feature X and the synthetic feature \tilde{X} are further assumed to follow the corresponding distributions,

$$P_X(x) = \begin{cases} 1 - \alpha, & \text{if } x \in [0, 1], \\ \alpha, & \text{if } x \in [-1, 0). \end{cases} \quad \text{and} \quad P_{\tilde{X}}(x) = \begin{cases} \alpha, & \text{if } x \in [0, 1], \\ 1 - \alpha, & \text{if } x \in [-1, 0). \end{cases}$$

We further assume that the estimation model $\hat{\mu}$ and $\hat{\eta}$ are the same as μ and η , respectively.

For the classification task, we also suppose there are two model specifications $\mathcal{G}_1 = \{g(x) =$

$\text{sign}(|x| - \beta) : \beta \in [0, 1/2]$ and $\mathcal{G}_2 = \{g(x) = \text{sign}(|x| - \beta) : \beta \in [1/4, 1/3]\}$, the risks of the true and synthetic distributions are, respectively, given as

$$R_{0-1}(g) = 1 - \alpha + (2\alpha - 1)\beta \text{ and } \tilde{R}_{0-1}(g) = \alpha - (2\alpha - 1)\beta.$$

For any $\alpha > 1/2$, we have $g_{\mathcal{G}_1}^*(x) = \text{sign}(|x|)$ and $g_{\mathcal{G}_2}^*(x) = \text{sign}(|x| - 1/4)$, while $\tilde{g}_{\mathcal{G}_1}^*(x) = \text{sign}(|x| - 1/2)$ and $\tilde{g}_{\mathcal{G}_2}^*(x) = \text{sign}(|x| - 1/3)$. Clearly, the model comparison is inconsistent since $R_{0-1}(\tilde{g}_{\mathcal{G}_1}^*) < R_{0-1}(\tilde{g}_{\mathcal{G}_2}^*)$. Similar to the case in regression, the change in the marginal distribution of features can influence the optimal model for minimizing risk under a given model specification. While a more flexible model specification can offer better generalization performance by capturing complex relationships between features and the target variable, it also increases the possibility of estimating an inferior model based on synthetic data with low feature fidelity.

Theorem S8. *For any synthetic distribution $\mathbb{P}_{\tilde{\mathbf{X}}, \tilde{\mathbf{Z}}}$ and any pair of model classes $(\mathcal{G}_1, \mathcal{G}_2)$ with $R_{0-1}(g_{\mathcal{G}_2}^*) < R_{0-1}(g_{\mathcal{G}_1}^*)$ satisfying*

(a) $\mathbb{P}_{\tilde{\mathbf{X}}}$ and $\mathbb{P}_{\mathbf{X}}$ satisfy (V, d) -fidelity level,

(b) $4K_{d,V} \|\hat{\eta} - \eta\|_{L^2(\mathbb{P}_{\mathbf{X}})}^{\frac{d^2}{(d+1)^2}} + 4\|\hat{\eta} - \eta\|_{L^2(\mathbb{P}_{\mathbf{X}})} < \Phi_{0-1}(g_{\mathcal{G}_1}^*) - K_{d,V} (\Phi_{0-1}(g_{\mathcal{G}_2}^*))^{\frac{d^2}{(d+1)^2}},$

where $K_{d,V} = (d^{\frac{1}{d+1}} + d^{-\frac{d}{d+1}})^{\frac{2d+1}{d+1}} V^{\frac{2d+1}{(d+1)^2}}$. Then we have consistent model comparison based on synthetic data, i.e., $(R_{0-1}(g_{\mathcal{G}_1}^*) - R_{0-1}(g_{\mathcal{G}_2}^*)) (R_{0-1}(\tilde{g}_{\mathcal{G}_1}^*) - R_{0-1}(\tilde{g}_{\mathcal{G}_2}^*)) > 0$.

Theorem S9. *For any $v > 0$, let $\mathcal{H}_c(u) = \left\{ (\mathcal{G}_1, \mathcal{G}_2) : \Phi_{0-1}(g_{\mathcal{G}_1}^*) - K_{d,V} (\Phi_{0-1}(g_{\mathcal{G}_2}^*))^{\frac{d^2}{(d+1)^2}} \geq u \right\}$ denote a class of pairs of function classes $(\mathcal{G}_1, \mathcal{G}_2)$. Assume that (1) $P_{\tilde{\mathbf{X}}}$ and $P_{\mathbf{X}}$ satisfy (V, d) -fidelity level; (2) $\hat{\eta}$ is a consistent estimator η such that for some positive sequence $\{a_n\}_{n=1}^{\infty}$ tending towards infinity, for any $n \geq 1$ and any $\delta > 0$, $\mathbb{P}(\|\hat{\eta} - \eta\|_{L^2(\mathbb{P}_{\mathbf{X}})} > \delta) \leq C_1 \exp(-C_2 a_n \delta)$, for some positive constants C_1 and C_2 . Then, for any $g > 0$,*

$$\begin{aligned} & \sup_{(\mathcal{G}_1, \mathcal{G}_2) \in \mathcal{H}(u)} \mathbb{P} \left((R_{0-1}(g_{\mathcal{G}_2}^*) - R_{0-1}(g_{\mathcal{G}_1}^*)) (R_{0-1}(\tilde{g}_{\mathcal{G}_2}^*) - R_{0-1}(\tilde{g}_{\mathcal{G}_1}^*)) < 0 \right) \\ & \leq C_1 \exp \left(-C_2 a_n u^{\frac{(d+1)^2}{d^2}} (4K_{d,V} + 4)^{-\frac{(d+1)^2}{d^2}} \right), \end{aligned}$$

where the randomness results from the training dataset \mathcal{D}_c used for estimating η .

S.1.5 Additional Numerical Results

Correct Model Specification: Linear Regression and Logistic Regression. This part mainly studies the convergence of utility metrics for linear regression and logistic regression under imperfect feature fidelity. For both tasks, we generate true features \mathbf{x}_i 's via a truncated multivariate normal distribution with mean 0 (Botev, 2017), that is $\mathbf{x}_i \sim \text{TN}(\mathbf{0}, \mathbf{I}, \mathbf{l}, \mathbf{u})$, where $\mathbf{0}$ is the mean vector, \mathbf{I} is the identity covariance matrix, \mathbf{l} and \mathbf{u} are both d -dimensional vectors representing the lower bounds and upper bounds for all dimensions, respectively. As for synthetic features, we generate $\{\tilde{\mathbf{x}}_i\}_{i=1}^{\tilde{n}}$ via a uniform distribution with the same support $\tilde{\mathbf{x}}_i \sim \text{Unif}(\mathbf{l}, \mathbf{u})$. To generating synthetic responses in linear regression and logistic regression, we follow the settings in Section 5. Additionally, we generate 50,000 testing samples from the true distributions for estimating the risks in both regression and classification.

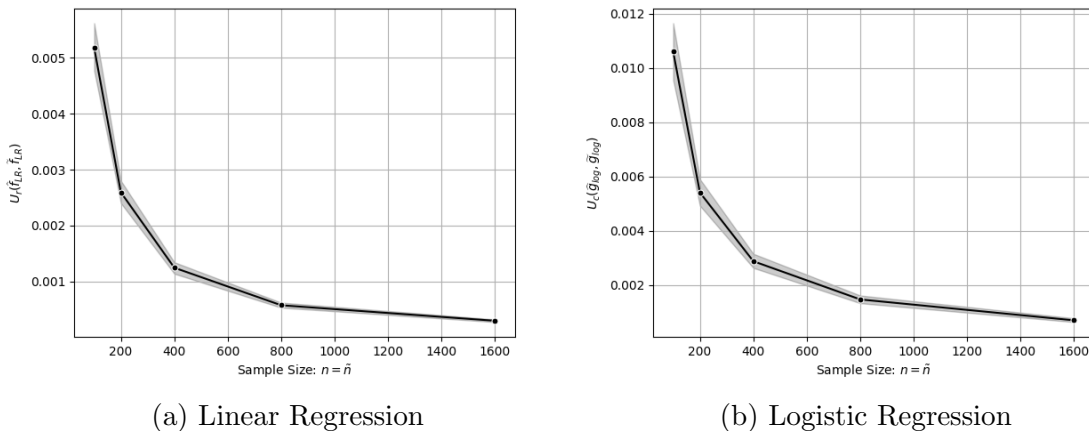


Figure 8: The estimated utility metrics in linear regression (Left) and logistic regression (Right) of different sample sizes.

We consider cases $n \in \{100 \times 2^i : i = 1, 2, 3, 4\}$ in both the linear regression and the logistic regression, with $\mathbf{l} = (-4, -4, -4, -4)$ and $\mathbf{u} = (4, 4, 4, 4)$, respectively. The averaged estimated utility metrics and their 95% confidence intervals are shown in Figure 8 after 500 replications of each scenario. The estimated utility metrics clearly converge to 0 as sample size

n grows, despite the fact that synthetic features and real features have distinct distributions. This indicates that correct model specification allows for the creation of synthetic datasets with high utility but poor feature fidelity.

S.2 Proof of Main Theorems

In this section, we present detailed proofs for all the theorems presented in both the main text and the supplementary file.

S.2.1 Proof of Theorem 1

By the triangle inequality, $U_r(\tilde{f}, \hat{f})$ can be upper bounded as

$$U_r(\tilde{f}, \hat{f}) \leq |R_r(\tilde{f}) - R_r(f_{\mathcal{F}}^*)| + |R_r(\hat{f}) - R_r(f_{\mathcal{F}}^*)|, \quad (\text{S5})$$

where $f_{\mathcal{F}}^* = \operatorname{argmin}_{f \in \mathcal{F}} R_r(f)$ denotes the optimal function in \mathcal{F} for approximating μ . Here $R_r(\hat{f}) - R_r(f_{\mathcal{F}}^*)$ basically measures the estimation error in statistical learning theory and is always positive due to the optimality of $f_{\mathcal{F}}^*$.

Next, we proceed to bound the term $|R_r(\tilde{f}) - R_r(f_{\mathcal{F}}^*)|$. By the fact that $R_r(f) = \Phi_r(f) + \sigma^2$ for any $f \in \mathcal{F}$, we have

$$\begin{aligned} & |R_r(\tilde{f}) - R_r(f_{\mathcal{F}}^*)| = |\Phi_r(\tilde{f}) - \Phi_r(f_{\mathcal{F}}^*)| \\ & \leq |\Phi_r(\tilde{f}) - \tilde{\Phi}_r(\tilde{f})| + |\tilde{\Phi}_r(\tilde{f}) - \tilde{\Phi}_r(\tilde{f}_{\mathcal{F}}^*)| + |\tilde{\Phi}_r(\tilde{f}_{\mathcal{F}}^*) - \Phi_r(\tilde{f}_{\mathcal{F}}^*)| + |\Phi_r(\tilde{f}_{\mathcal{F}}^*) - \Phi_r(f_{\mathcal{F}}^*)| \\ & \triangleq I_1 + I_2 + I_3 + I_4, \end{aligned}$$

where $\tilde{\Phi}_r(f) = \int_{\mathcal{X}} (f(\mathbf{x}) - \hat{\mu}(\mathbf{x}))^2 p_{\tilde{\mathbf{X}}}(\mathbf{x}) d\mathbf{x}$ and $\tilde{f}_{\mathcal{F}}^* = \operatorname{argmin}_{f \in \mathcal{F}} \mathbb{E}_{\tilde{\mathbf{X}}, \tilde{Y}} [(f(\tilde{\mathbf{X}}) - \tilde{Y})^2]$. Similar to $R_r(\hat{f}) - R_r(f_{\mathcal{F}}^*)$, $I_2 = |\tilde{\Phi}_r(\tilde{f}) - \tilde{\Phi}_r(\tilde{f}_{\mathcal{F}}^*)|$ also measures the estimation error of \tilde{f} under the synthetic distribution.

Next, we proceed to bound I_1 and I_3 by establishing a general upper bound for $|\Phi_r(f) -$

$\tilde{\Phi}_r(f)$. By the definitions of Φ_r and $\tilde{\Phi}_r$, we have

$$\begin{aligned} |\Phi_r(f) - \tilde{\Phi}_r(f)| &= \left| \int_{\mathcal{X}} (f(\mathbf{x}) - \mu(\mathbf{x}))^2 P_{\mathbf{X}}(\mathbf{x}) d\mathbf{x} - \int_{\mathcal{X}} (f(\mathbf{x}) - \hat{\mu}(\mathbf{x}))^2 P_{\tilde{\mathbf{X}}}(\mathbf{x}) d\mathbf{x} \right| \\ &\leq \left| \mathbb{E}_{\mathbf{X} \sim \mathbb{P}_{\mathbf{X}}} \left[(f(\mathbf{X}) - \mu(\mathbf{X}))^2 \right] - \mathbb{E}_{\mathbf{X} \sim \mathbb{P}_{\mathbf{X}}} \left[(f(\mathbf{X}) - \hat{\mu}(\mathbf{X}))^2 \right] \right| \\ &\quad + \left| \mathbb{E}_{\mathbf{X} \sim \mathbb{P}_{\mathbf{X}}} \left[(f(\mathbf{X}) - \hat{\mu}(\mathbf{X}))^2 \right] - \mathbb{E}_{\mathbf{X} \sim \mathbb{P}_{\tilde{\mathbf{X}}}} \left[(f(\mathbf{X}) - \hat{\mu}(\mathbf{X}))^2 \right] \right| \\ &\triangleq J_1(f) + J_2(f), \end{aligned}$$

where \mathcal{X} denotes the union of the supports of $\mathbb{P}_{\mathbf{X}}$ and $\mathbb{P}_{\tilde{\mathbf{X}}}$.

Next, we proceed to bound $J_1(f)$ and $J_2(f)$ separately. For $J_2(f)$, it can be reformulated as

$$J_2(f) = \sup_{g \in \mathcal{H}_0} \left| \mathbb{E}_{\mathbf{X} \sim \mathbb{P}_{\mathbf{X}}} [g(\mathbf{X})] - \mathbb{E}_{\mathbf{X} \sim \mathbb{P}_{\tilde{\mathbf{X}}}} [g(\mathbf{X})] \right| = D_{\mathcal{H}_0}(\mathbb{P}_{\mathbf{X}}, \mathbb{P}_{\tilde{\mathbf{X}}}),$$

where $\mathcal{H}_0 = \{g(\mathbf{x}) = (f(\mathbf{x}) - \hat{\mu}(\mathbf{x}))^2\}$ is a function class with only one function. For $J_1(f)$, it follows from Cauchy-Schwarz inequality that

$$\begin{aligned} J_1(f) &= \left| \int_{\mathcal{X}} (f(\mathbf{x}) - \hat{\mu}(\mathbf{x}))^2 P_{\mathbf{X}}(\mathbf{x}) d\mathbf{x} - \int_{\mathcal{X}} (f(\mathbf{x}) - \mu(\mathbf{x}))^2 P_{\mathbf{X}}(\mathbf{x}) d\mathbf{x} \right| \\ &\leq \mathbb{E}_{\mathbf{X}} \left[\left(2f(\mathbf{X}) - \hat{\mu}(\mathbf{X}) - \mu(\mathbf{X}) \right) \left(\hat{\mu}(\mathbf{X}) - \mu(\mathbf{X}) \right) \right] \\ &\leq \sqrt{\mathbb{E}_{\mathbf{X}} \left[\left(2f(\mathbf{X}) - \hat{\mu}(\mathbf{X}) - \mu(\mathbf{X}) \right)^2 \right]} \cdot \sqrt{\mathbb{E}_{\mathbf{X}} \left[\left(\hat{\mu}(\mathbf{X}) - \mu(\mathbf{X}) \right)^2 \right]} \\ &= \|2f - \hat{\mu} - \mu\|_{L^2(\mathbb{P}_{\mathbf{X}})} \cdot \sqrt{\Phi_r(\hat{\mu})} \leq 2\sqrt{\Phi_r(f)} \sqrt{\Phi_r(\hat{\mu})} + \Phi_r(\hat{\mu}). \end{aligned}$$

Combining the upper bounds for $J_1(f)$ and $J_2(f)$ yields that

$$|\Phi_r(f) - \tilde{\Phi}_r(f)| \leq D_{\mathcal{H}_0}(\mathbb{P}_{\mathbf{X}}, \mathbb{P}_{\tilde{\mathbf{X}}}) + 2\sqrt{\Phi_r(f)\Phi_r(\hat{\mu})} + \Phi_r(\hat{\mu}). \quad (\text{S6})$$

To sum up, we have

$$I_1 + I_3 \leq 2D_{\mathcal{H}_1}(P_{\mathbf{X}}, P_{\tilde{\mathbf{X}}}) + 2\sqrt{\Phi_r(\tilde{f})\Phi_r(\hat{\mu})} + 2\sqrt{\Phi_r(\tilde{f}_{\mathcal{F}}^*)\Phi_r(\hat{\mu})} + 2\Phi_r(\hat{\mu}),$$

where $\mathcal{H}_1 = \left\{ g(\mathbf{x}) = (f(\mathbf{x}) - \hat{\mu}(\mathbf{x}))^2 : f \in \{\tilde{f}, \tilde{f}_{\mathcal{F}}^*\} \right\}$.

We now consider bounding $I_4 = |\Phi_r(\tilde{f}_{\mathcal{F}}^*) - \Phi_r(f_{\mathcal{F}}^*)|$. Given the optimality of both $\tilde{f}_{\mathcal{F}}^*$ and

$f_{\mathcal{F}}^*$ in minimizing $\tilde{\Phi}_r(f)$ and $\Phi_r(f)$, respectively, we can conclude

$$\Phi_r(\tilde{f}_{\mathcal{F}}^*) - \Phi_r(f_{\mathcal{F}}^*) \geq 0 \text{ and } \tilde{\Phi}_r(f_{\mathcal{F}}^*) - \tilde{\Phi}_r(\tilde{f}_{\mathcal{F}}^*) \geq 0.$$

It then follows that

$$\begin{aligned} I_4 &= \left| \Phi_r(\tilde{f}_{\mathcal{F}}^*) - \Phi_r(f_{\mathcal{F}}^*) \right| \leq \left| \Phi_r(\tilde{f}_{\mathcal{F}}^*) - \tilde{\Phi}_r(\tilde{f}_{\mathcal{F}}^*) - \Phi_r(f_{\mathcal{F}}^*) + \tilde{\Phi}_r(f_{\mathcal{F}}^*) \right| \\ &\leq \left| \Phi_r(\tilde{f}_{\mathcal{F}}^*) - \tilde{\Phi}_r(\tilde{f}_{\mathcal{F}}^*) \right| + \left| \Phi_r(f_{\mathcal{F}}^*) - \tilde{\Phi}_r(f_{\mathcal{F}}^*) \right|. \end{aligned}$$

Applying the upper bound established in (S6) to $|\Phi_r(\tilde{f}_{\mathcal{F}}^*) - \tilde{\Phi}_r(\tilde{f}_{\mathcal{F}}^*)|$ and $|\Phi_r(f_{\mathcal{F}}^*) - \tilde{\Phi}_r(f_{\mathcal{F}}^*)|$, we get

$$I_4 \leq 2D_{\mathcal{H}_2}(P_{\mathbf{X}}, P_{\tilde{\mathbf{X}}}) + 2\sqrt{\Phi_r(\tilde{f}_{\mathcal{F}}^*)\Phi_r(\hat{\mu})} + 2\sqrt{\Phi_r(f_{\mathcal{F}}^*)\Phi_r(\hat{\mu})} + 2\Phi_r(\hat{\mu}),$$

where $\mathcal{H}_2 = \left\{ g(\mathbf{x}) = (f(\mathbf{x}) - \hat{\mu}(\mathbf{x}))^2 : f \in \{f_{\mathcal{F}}^*, \tilde{f}_{\mathcal{F}}^*\} \right\}$.

To sum up, we have

$$\begin{aligned} U_r(\tilde{f}, \hat{f}) &\leq \left| \tilde{R}_r(\tilde{f}) - \tilde{R}_r(\tilde{f}_{\mathcal{F}}^*) \right| + \left| R_r(\hat{f}) - R_r(f_{\mathcal{F}}^*) \right| + 4D_{\mathcal{H}}(P_{\mathbf{X}}, P_{\tilde{\mathbf{X}}}) \\ &\quad + 2\left(\sqrt{\Phi_r(\tilde{f})} + 2\sqrt{\Phi_r(\tilde{f}_{\mathcal{F}}^*)} + \sqrt{\Phi_r(f_{\mathcal{F}}^*)} \right) \sqrt{\Phi_r(\hat{\mu})} + 4\Phi_r(\hat{\mu}), \end{aligned}$$

where $\mathcal{H} = \left\{ g(\mathbf{x}) = (f(\mathbf{x}) - \hat{\mu}(\mathbf{x}))^2 : f \in \{\tilde{f}, f_{\mathcal{F}}^*, \tilde{f}_{\mathcal{F}}^*\} \right\}$. This completes the proof. \square

S.2.2 Proof of Theorem 2

In this proof, we analyze the explicit form of each component of the utility bound in (4) for linear regression.

Bounding Estimation Errors. Since the model specification is correct, we can easily verify that $f_{\mathcal{F}}^*(\mathbf{x}) = \mu(\mathbf{x}) = \mathbf{x}^T \boldsymbol{\beta}^*$ and $\tilde{f}_{\mathcal{F}}^*(\mathbf{x}) = \mathbf{x}^T (\mathbb{X}^T \mathbb{X})^{-1} \mathbb{X}^T \mathbb{Y}$. With this, the first term of the

right-hand side in (4) can be written as

$$\begin{aligned}
|R_r(\widehat{f}_{LR}) - R_r(f_{\mathcal{F}}^*)| &= \mathbb{E} \left[(\mathbf{X}^T (\mathbb{X}^T \mathbb{X})^{-1} \mathbb{X}^T \mathbb{Y} - Y)^2 \right] - \sigma^2 \\
&= \mathbb{E}_{\mathbf{X}, Y} \left[(\mathbf{X}^T (\mathbb{X}^T \mathbb{X})^{-1} \mathbb{X}^T (\mathbb{X} \boldsymbol{\beta}^* + \boldsymbol{\epsilon}) - Y)^2 \right] - \sigma^2 \\
&= \mathbb{E}_{\mathbf{X}, \boldsymbol{\epsilon}} \left[(\mathbf{X}^T (\mathbb{X}^T \mathbb{X})^{-1} \mathbb{X}^T \boldsymbol{\epsilon} - \boldsymbol{\epsilon})^2 \right] - \sigma^2 = \mathbb{E}_{\mathbf{X}} \left[\boldsymbol{\epsilon}^T \mathbb{X} (\mathbb{X}^T \mathbb{X})^{-1} \mathbf{X} \mathbf{X}^T (\mathbb{X}^T \mathbb{X})^{-1} \mathbb{X}^T \boldsymbol{\epsilon} \right] \\
&= \text{trace} \left(\boldsymbol{\epsilon} \boldsymbol{\epsilon}^T \mathbb{X} (\mathbb{X}^T \mathbb{X})^{-1} \boldsymbol{\Lambda} (\mathbb{X}^T \mathbb{X})^{-1} \mathbb{X}^T \right). \tag{S7}
\end{aligned}$$

Applying a similar argument for the second term of (4) yields that

$$|\widetilde{R}_r(\widetilde{f}_{LR}) - \widetilde{R}_r(\widetilde{f}_{\mathcal{F}}^*)| = \text{trace} \left(\widetilde{\boldsymbol{\epsilon}} \widetilde{\boldsymbol{\epsilon}}^T \widetilde{\mathbb{X}} (\widetilde{\mathbb{X}}^T \widetilde{\mathbb{X}})^{-1} \widetilde{\boldsymbol{\Lambda}} (\widetilde{\mathbb{X}}^T \widetilde{\mathbb{X}})^{-1} \widetilde{\mathbb{X}}^T \right). \tag{S8}$$

Bounding $\Upsilon_1 = \sqrt{\Phi_r(\widetilde{f}_{LR})} + 2\sqrt{\Phi_r(\widetilde{f}_{\mathcal{F}}^*)} + \sqrt{\Phi_r(f_{\mathcal{F}}^*)}$. First, by the fact that $\Phi_r(f_{\mathcal{F}}^*) = 0$ due to the correct model specification, we have

$$\Upsilon_1 = \sqrt{\Phi_r(\widetilde{f}_{LR})} + 2\sqrt{\Phi_r(\widetilde{f}_{\mathcal{F}}^*)} + \sqrt{\Phi_r(f_{\mathcal{F}}^*)} = \sqrt{\Phi_r(\widetilde{f}_{LR})} + 2\sqrt{\Phi_r(\widetilde{f}_{\mathcal{F}}^*)}.$$

It remains to analyze $\Phi_r(\widetilde{f}_{LR})$ and $\Phi_r(\widetilde{f}_{\mathcal{F}}^*)$. By the definition of \widetilde{f}_{LR} ,

$$\begin{aligned}
\widetilde{f}_{LR}(\mathbf{x}) &= \mathbf{x}^T (\widetilde{\mathbb{X}}^T \widetilde{\mathbb{X}})^{-1} \widetilde{\mathbb{X}}^T \widetilde{\mathbb{Y}} = \mathbf{x}^T (\widetilde{\mathbb{X}}^T \widetilde{\mathbb{X}})^{-1} \widetilde{\mathbb{X}}^T [(\widetilde{\mathbb{X}} (\mathbb{X}^T \mathbb{X})^{-1} \mathbb{X}^T \mathbb{Y} + \widetilde{\boldsymbol{\epsilon}})] \\
&= \mathbf{x}^T (\mathbb{X}^T \mathbb{X})^{-1} \mathbb{X}^T \mathbb{Y} + \mathbf{x}^T (\widetilde{\mathbb{X}}^T \widetilde{\mathbb{X}})^{-1} \widetilde{\mathbb{X}}^T \widetilde{\boldsymbol{\epsilon}} \\
&= \mathbf{x}^T \boldsymbol{\beta}^* + \mathbf{x}^T (\mathbb{X}^T \mathbb{X})^{-1} \mathbb{X}^T \boldsymbol{\epsilon} + \mathbf{x}^T (\widetilde{\mathbb{X}}^T \widetilde{\mathbb{X}})^{-1} \widetilde{\mathbb{X}}^T \widetilde{\boldsymbol{\epsilon}}. \tag{S9}
\end{aligned}$$

Therefore, we have $\widetilde{f}_{LR}(\mathbf{x}) - \widehat{f}_{LR}(\mathbf{x}) = \mathbf{x}^T (\widetilde{\mathbb{X}}^T \widetilde{\mathbb{X}})^{-1} \widetilde{\mathbb{X}}^T \widetilde{\boldsymbol{\epsilon}}$ for any \mathbf{x} . Substituting (S9) into $\Phi_r(\widetilde{f}_{LR})$ yields that

$$\begin{aligned}
\Phi_r(\widetilde{f}_{LR}) &= \mathbb{E}_{\mathbf{X}} \left[(\mathbf{X}^T (\mathbb{X}^T \mathbb{X})^{-1} \mathbb{X}^T \boldsymbol{\epsilon} + \mathbf{X}^T (\widetilde{\mathbb{X}}^T \widetilde{\mathbb{X}})^{-1} \widetilde{\mathbb{X}}^T \widetilde{\boldsymbol{\epsilon}})^2 \right] \\
&\leq 2\text{trace} \left(\boldsymbol{\epsilon} \boldsymbol{\epsilon}^T \mathbb{X} (\mathbb{X}^T \mathbb{X})^{-1} \boldsymbol{\Lambda} (\mathbb{X}^T \mathbb{X})^{-1} \mathbb{X}^T \right) + 2\text{trace} \left(\widetilde{\boldsymbol{\epsilon}} \widetilde{\boldsymbol{\epsilon}}^T \widetilde{\mathbb{X}} (\widetilde{\mathbb{X}}^T \widetilde{\mathbb{X}})^{-1} \boldsymbol{\Lambda} (\widetilde{\mathbb{X}}^T \widetilde{\mathbb{X}})^{-1} \widetilde{\mathbb{X}}^T \right),
\end{aligned}$$

where the inequality follows from the Cauchy–Schwarz inequality. Notice that $\widetilde{f}_{\mathcal{F}}^*(\mathbf{x}) =$

$\mathbf{x}^T(\mathbb{X}^T\mathbb{X})^{-1}\mathbb{X}^T\mathbb{Y}$, then

$$\Phi_r(\tilde{f}_{\mathcal{F}}^*) = \Phi_r(\hat{\mu}) = \text{trace}\left(\boldsymbol{\epsilon}\boldsymbol{\epsilon}^T\mathbb{X}(\mathbb{X}^T\mathbb{X})^{-1}\boldsymbol{\Lambda}(\mathbb{X}^T\mathbb{X})^{-1}\mathbb{X}^T\right).$$

To sum up, we get

$$\Upsilon_1 \leq \sqrt{2\text{trace}\left(\tilde{\boldsymbol{\epsilon}}\tilde{\boldsymbol{\epsilon}}^T\tilde{\mathbb{X}}(\tilde{\mathbb{X}}^T\tilde{\mathbb{X}})^{-1}\tilde{\boldsymbol{\Lambda}}(\tilde{\mathbb{X}}^T\tilde{\mathbb{X}})^{-1}\tilde{\mathbb{X}}^T\right)} + (2 + \sqrt{2})\sqrt{\text{trace}\left(\boldsymbol{\epsilon}\boldsymbol{\epsilon}^T\mathbb{X}(\mathbb{X}^T\mathbb{X})^{-1}\boldsymbol{\Lambda}(\mathbb{X}^T\mathbb{X})^{-1}\mathbb{X}^T\right)}.$$

Finally, the fourth term of (4) can be further bounded as

$$2\Upsilon_1\sqrt{\Phi_r(\hat{\mu})} \leq 2\text{trace}\left(\tilde{\boldsymbol{\epsilon}}\tilde{\boldsymbol{\epsilon}}^T\tilde{\mathbb{X}}(\tilde{\mathbb{X}}^T\tilde{\mathbb{X}})^{-1}\tilde{\boldsymbol{\Lambda}}(\tilde{\mathbb{X}}^T\tilde{\mathbb{X}})^{-1}\tilde{\mathbb{X}}^T\right) + 9\text{trace}\left(\boldsymbol{\epsilon}\boldsymbol{\epsilon}^T\mathbb{X}(\mathbb{X}^T\mathbb{X})^{-1}\boldsymbol{\Lambda}(\mathbb{X}^T\mathbb{X})^{-1}\mathbb{X}^T\right).$$

Bounding $D_{\mathcal{H}}(P_{\mathbf{X}}, P_{\tilde{\mathbf{X}}})$. Next, we turn to analyze the term $D_{\mathcal{H}}(P_{\mathbf{X}}, P_{\tilde{\mathbf{X}}})$, which can be written as

$$\begin{aligned} D_{\mathcal{H}}(P_{\mathbf{X}}, P_{\tilde{\mathbf{X}}}) &= \max \left\{ \left| \mathbb{E}_{\mathbf{X}} \left[(\tilde{f}_{LR}(\mathbf{X}) - \hat{f}_{LR}(\mathbf{X}))^2 \right] - \mathbb{E}_{\tilde{\mathbf{X}}} \left[(\tilde{f}_{LR}(\tilde{\mathbf{X}}) - \hat{f}_{LR}(\tilde{\mathbf{X}}))^2 \right] \right|, \right. \\ &\quad \left. \left| \mathbb{E}_{\mathbf{X}} \left[(\mu(\mathbf{X}) - \hat{f}_{LR}(\mathbf{X}))^2 \right] - \mathbb{E}_{\tilde{\mathbf{X}}} \left[(\mu(\mathbf{X})(\tilde{\mathbf{X}}) - \hat{f}_{LR}(\tilde{\mathbf{X}}))^2 \right] \right| \right\} \\ &= \max \left\{ \left| \text{trace}\left(\tilde{\boldsymbol{\epsilon}}\tilde{\boldsymbol{\epsilon}}^T\tilde{\mathbb{X}}(\tilde{\mathbb{X}}^T\tilde{\mathbb{X}})^{-1}(\boldsymbol{\Lambda} - \tilde{\boldsymbol{\Lambda}})(\tilde{\mathbb{X}}^T\tilde{\mathbb{X}})^{-1}\tilde{\mathbb{X}}^T\right) \right|, \right. \\ &\quad \left. \left| \text{trace}\left(\boldsymbol{\epsilon}\boldsymbol{\epsilon}^T\mathbb{X}(\mathbb{X}^T\mathbb{X})^{-1}(\boldsymbol{\Lambda} - \tilde{\boldsymbol{\Lambda}})(\mathbb{X}^T\mathbb{X})^{-1}\mathbb{X}^T\right) \right| \right\}. \end{aligned}$$

To sum up, the utility bound in linear regression can be written as

$$\begin{aligned} U_r(\hat{f}_{LR}, \tilde{f}_{LR}) &\leq 14\text{trace}\left(\boldsymbol{\epsilon}\boldsymbol{\epsilon}^T\mathbb{X}(\mathbb{X}^T\mathbb{X})^{-1}\boldsymbol{\Lambda}(\mathbb{X}^T\mathbb{X})^{-1}\mathbb{X}^T\right) + \text{trace}\left(\tilde{\boldsymbol{\epsilon}}\tilde{\boldsymbol{\epsilon}}^T\tilde{\mathbb{X}}(\tilde{\mathbb{X}}^T\tilde{\mathbb{X}})^{-1}\tilde{\boldsymbol{\Lambda}}(\tilde{\mathbb{X}}^T\tilde{\mathbb{X}})^{-1}\tilde{\mathbb{X}}^T\right) \\ &+ 2\text{trace}\left(\tilde{\boldsymbol{\epsilon}}\tilde{\boldsymbol{\epsilon}}^T\tilde{\mathbb{X}}(\tilde{\mathbb{X}}^T\tilde{\mathbb{X}})^{-1}\boldsymbol{\Lambda}(\tilde{\mathbb{X}}^T\tilde{\mathbb{X}})^{-1}\tilde{\mathbb{X}}^T\right) + 4D_{\mathcal{H}}(P_{\mathbf{X}}, P_{\tilde{\mathbf{X}}}). \end{aligned} \quad (\text{S10})$$

Next, we proceed to prove the convergence of components of the right-hand side in (S10) separately. For ease of notations, we denote that

$$\begin{aligned} I_1 &= \text{trace}\left(\boldsymbol{\epsilon}\boldsymbol{\epsilon}^T\mathbb{X}(\mathbb{X}^T\mathbb{X})^{-1}\boldsymbol{\Lambda}(\mathbb{X}^T\mathbb{X})^{-1}\mathbb{X}^T\right), & I_2 &= \text{trace}\left(\tilde{\boldsymbol{\epsilon}}\tilde{\boldsymbol{\epsilon}}^T\tilde{\mathbb{X}}(\tilde{\mathbb{X}}^T\tilde{\mathbb{X}})^{-1}\tilde{\boldsymbol{\Lambda}}(\tilde{\mathbb{X}}^T\tilde{\mathbb{X}})^{-1}\tilde{\mathbb{X}}^T\right), \\ I_3 &= \text{trace}\left(\boldsymbol{\epsilon}\boldsymbol{\epsilon}^T\mathbb{X}(\mathbb{X}^T\mathbb{X})^{-1}\tilde{\boldsymbol{\Lambda}}(\mathbb{X}^T\mathbb{X})^{-1}\mathbb{X}^T\right), & I_4 &= \text{trace}\left(\tilde{\boldsymbol{\epsilon}}\tilde{\boldsymbol{\epsilon}}^T\tilde{\mathbb{X}}(\tilde{\mathbb{X}}^T\tilde{\mathbb{X}})^{-1}\boldsymbol{\Lambda}(\tilde{\mathbb{X}}^T\tilde{\mathbb{X}})^{-1}\tilde{\mathbb{X}}^T\right). \end{aligned}$$

Then (S10) can be further bounded as

$$U_r(\widehat{f}_{LR}, \widetilde{f}_{LR}) \leq 14I_1 + I_2 + 2I_4 + 4 \max\{|I_3 - I_1|, |I_4 - I_2|\} \leq 18I_1 + 5I_2 + 4I_3 + 6I_4.$$

Next, we proceed to prove the convergence in probability of I_1 - I_4 . Take the expectation of I_1 with respect to $\boldsymbol{\epsilon}$ and \mathbb{X} , we have

$$\begin{aligned} \mathbb{E}_{\boldsymbol{\epsilon}, \mathbb{X}}[I_1] &= \mathbb{E}_{\boldsymbol{\epsilon}, \mathbb{X}} \left[\text{trace} \left(\boldsymbol{\epsilon} \boldsymbol{\epsilon}^T \mathbb{X} (\mathbb{X}^T \mathbb{X})^{-1} \boldsymbol{\Lambda} (\mathbb{X}^T \mathbb{X})^{-1} \mathbb{X}^T \right) \right] \\ &= \frac{\sigma^2}{n} \text{trace} \left(\boldsymbol{\Lambda} \mathbb{E}_{\mathbb{X}} \left[(n^{-1} \mathbb{X}^T \mathbb{X})^{-1} \right] \right) = \frac{\sigma^2}{n} \text{trace} \left(\boldsymbol{\Lambda} \mathbb{E}_{\mathbb{X}} \left[(n^{-1} \mathbb{X}^T \mathbb{X})^{-1} \right] \right), \end{aligned} \quad (\text{S11})$$

where the second equality follows from the fact that trace is a linear operator. Then, by the Markov's inequality, we have

$$\mathbb{P}(I_1 \geq \delta) \leq \delta^{-1} n^{-1} \sigma^2 \text{trace} \left(\boldsymbol{\Lambda} \mathbb{E}_{\mathbb{X}} \left[(n^{-1} \mathbb{X}^T \mathbb{X})^{-1} \right] \right). \quad (\text{S12})$$

Notice that $n^{-1} \mathbb{X}^T \mathbb{X}$ is the sample covariance matrix that converges to $\boldsymbol{\Lambda}$ in probability and the matrix inverse function is continuous. By the continuous mapping theorem (Mann and Wald, 1943), we have

$$\lim_{n \rightarrow \infty} \text{trace} \left(\boldsymbol{\Lambda} \mathbb{E}_{\mathbb{X}} \left[(n^{-1} \mathbb{X}^T \mathbb{X})^{-1} \right] \right) = p. \quad (\text{S13})$$

Combining (S12) and (S13), we have

$$\lim_{n \rightarrow \infty} \mathbb{P}(I_1 \geq \delta) = \lim_{n \rightarrow \infty} \delta^{-1} n^{-1} \sigma^2 \text{trace} \left(\boldsymbol{\Lambda} \mathbb{E}_{\mathbb{X}} \left[(n^{-1} \mathbb{X}^T \mathbb{X})^{-1} \right] \right) = 0. \quad (\text{S14})$$

Denote that $I_2 = \text{trace} \left(\widetilde{\boldsymbol{\epsilon}} \widetilde{\boldsymbol{\epsilon}}^T \widetilde{\mathbb{X}} (\widetilde{\mathbb{X}}^T \widetilde{\mathbb{X}})^{-1} \widetilde{\boldsymbol{\Lambda}} (\widetilde{\mathbb{X}}^T \widetilde{\mathbb{X}})^{-1} \widetilde{\mathbb{X}}^T \right)$ and $I_3 = \text{trace} \left(\boldsymbol{\epsilon} \boldsymbol{\epsilon}^T \mathbb{X} (\mathbb{X}^T \mathbb{X})^{-1} \widetilde{\boldsymbol{\Lambda}} (\mathbb{X}^T \mathbb{X})^{-1} \mathbb{X}^T \right)$.

Since the generation of $\widetilde{\boldsymbol{\epsilon}}$ and $\widetilde{\mathbb{X}}$ is independent of \mathcal{D}_r , therefore applying a similar argument to I_2 and I_3 as that for I_1 yields that

$$\lim_{\widetilde{n} \rightarrow \infty} \mathbb{P}(I_2 \geq \delta) = \lim_{\widetilde{n} \rightarrow \infty} \delta^{-1} \widetilde{n}^{-1} \widetilde{\sigma}^2 \text{trace} \left(\widetilde{\boldsymbol{\Lambda}} \mathbb{E}_{\widetilde{\mathbb{X}}} \left[(\widetilde{n}^{-1} \widetilde{\mathbb{X}}^T \widetilde{\mathbb{X}})^{-1} \right] \right) = 0, \quad (\text{S15})$$

$$\lim_{n \rightarrow \infty} \mathbb{P}(I_3 \geq \delta) = \lim_{n \rightarrow \infty} \delta^{-1} n^{-1} \sigma^2 \text{trace} \left(\widetilde{\boldsymbol{\Lambda}} \mathbb{E}_{\mathbb{X}} \left[(n^{-1} \mathbb{X}^T \mathbb{X})^{-1} \right] \right) = 0, \quad (\text{S16})$$

$$\lim_{\widetilde{n} \rightarrow \infty} \mathbb{P}(I_4 \geq \delta) = \lim_{\widetilde{n} \rightarrow \infty} \delta^{-1} \widetilde{n}^{-1} \widetilde{\sigma}^2 \text{trace} \left(\boldsymbol{\Lambda} \mathbb{E}_{\widetilde{\mathbb{X}}} \left[(\widetilde{n}^{-1} \widetilde{\mathbb{X}}^T \widetilde{\mathbb{X}})^{-1} \right] \right) = 0. \quad (\text{S17})$$

By Von Neumann's trace inequality, we have

$$\begin{aligned}\Lambda \mathbb{E}_{\tilde{\mathbb{X}}}[(\tilde{n}^{-1}\tilde{\mathbb{X}}^T\tilde{\mathbb{X}})^{-1}] &\leq \sum_{i=1}^p \rho_i \tilde{\kappa}_i, & \tilde{\Lambda} \mathbb{E}_{\tilde{\mathbb{X}}}[(\tilde{n}^{-1}\tilde{\mathbb{X}}^T\tilde{\mathbb{X}})^{-1}] &\leq \sum_{i=1}^p \tilde{\rho}_i \tilde{\kappa}_i, \\ \tilde{\Lambda} \mathbb{E}_{\mathbb{X}}[(n^{-1}\mathbb{X}^T\mathbb{X})^{-1}] &\leq \sum_{i=1}^p \tilde{\rho}_i \kappa_i, & \Lambda \mathbb{E}_{\mathbb{X}}[(n^{-1}\mathbb{X}^T\mathbb{X})^{-1}] &\leq \sum_{i=1}^p \rho_i \kappa_i,\end{aligned}$$

where ρ_i , $\tilde{\rho}_i$, κ_i , and $\tilde{\kappa}_i$ denote the i -th largest eigenvalues of Λ , $\tilde{\Lambda}$, $\mathbb{E}_{\mathbb{X}}[(n^{-1}\mathbb{X}^T\mathbb{X})^{-1}]$, and $\mathbb{E}_{\tilde{\mathbb{X}}}[(\tilde{n}^{-1}\tilde{\mathbb{X}}^T\tilde{\mathbb{X}})^{-1}]$, respectively. Finally, combining (S14)-(S17) will give the bound as

$$\mathbb{P}\left(U_r(\hat{f}_{LR}, \tilde{f}_{LR}) > \delta\right) \leq \mathbb{P}\left(\sum_{i=1}^4 I_i > \delta/18\right) \lesssim \frac{\tilde{n}\sigma^2 \sum_{i=1}^p (\rho_i + \tilde{\rho}_i)\kappa_i + n\tilde{\sigma}^2 \sum_{i=1}^p (\rho_i + \tilde{\rho}_i)\tilde{\kappa}_i}{\tilde{n}n\delta}.$$

Thus, we have $\lim_{n \rightarrow \infty} \lim_{\tilde{n} \rightarrow \infty} \mathbb{P}\left(U_r(\hat{f}_{LR}, \tilde{f}_{LR}) > \delta\right) = 0$ for any $\delta > 0$. This completes the proof. \square

S.2.3 Proof of Theorem 3

The proof of Theorem 3 consists of several steps. First, we provide a general result regarding the consistency in parameter estimation of LASSO estimator under Assumptions 3 and 4. Second, we establish no false inclusion of useless features, i.e., $\hat{\mathcal{A}} \subset \mathcal{A}$. Third, we establish the relation between the excess risk and the l_2 estimation error. Finally, we explicate the upper bound for the proposed utility metric.

1. Consistency of Parameter Estimation. In this part, we mainly use the estimator defined in (9) for illustration. Afterwards, similar results for $\tilde{\beta}(\tilde{\lambda}_r)$ can be derived accordingly. We first establish the quantitative connections of $\|\hat{\beta}(\lambda_r) - \beta^*\|_2^2$ to λ_r and the sparsity parameter s under the assumptions. Using the fact that $y_i = \mathbf{x}_i^T \beta^* + \epsilon_i$, we have

$$\frac{1}{n} \sum_{i=1}^n (y_i - \mathbf{x}_i^T \hat{\beta}(\lambda_r))^2 + \lambda_r \|\hat{\beta}(\lambda_r)\|_1 = \frac{1}{n} \sum_{i=1}^n [\epsilon_i + \mathbf{x}_i^T (\beta^* - \hat{\beta}(\lambda_r))]^2 + \lambda_r \|\hat{\beta}(\lambda_r)\|_1.$$

Next, by the optimality of $\widehat{\boldsymbol{\beta}}(\lambda_r)$, we have

$$\begin{aligned} & \frac{1}{n} \sum_{i=1}^n [\epsilon_i + \mathbf{x}_i^T (\boldsymbol{\beta}^* - \widehat{\boldsymbol{\beta}}(\lambda_r))]^2 + \lambda_r \|\widehat{\boldsymbol{\beta}}(\lambda_r)\|_1 \\ & \leq \frac{1}{n} \sum_{i=1}^n (y_i - \mathbf{x}_i^T \boldsymbol{\beta}^*)^2 + \lambda_r \|\boldsymbol{\beta}^*\|_1 = \frac{1}{n} \sum_{i=1}^n \epsilon_i^2 + \lambda_r \|\boldsymbol{\beta}^*\|_1. \end{aligned}$$

Following some algebra, we get

$$\frac{1}{n} \sum_{i=1}^n \left[\mathbf{x}_i^T (\boldsymbol{\beta}^* - \widehat{\boldsymbol{\beta}}(\lambda_r)) \right]^2 \leq \frac{1}{n} \sum_{i=1}^n \epsilon_i \mathbf{x}_i^T (\widehat{\boldsymbol{\beta}}(\lambda_r) - \boldsymbol{\beta}^*) + \lambda_r \|\boldsymbol{\beta}^*\|_1 - \lambda_r \|\widehat{\boldsymbol{\beta}}(\lambda_r)\|_1. \quad (\text{S18})$$

Applying Hölder inequality to the first term on the right-hand side of (S18), we get

$$\frac{1}{n} \sum_{i=1}^n \left[\mathbf{x}_i^T (\boldsymbol{\beta}^* - \widehat{\boldsymbol{\beta}}(\lambda_r)) \right]^2 \leq \|n^{-1} \sum_{i=1}^n \epsilon_i \mathbf{x}_i^T\|_\infty \|\boldsymbol{\beta}^* - \widehat{\boldsymbol{\beta}}(\lambda_r)\|_1 + \lambda_r \|\boldsymbol{\beta}^*\|_1 - \lambda_r \|\widehat{\boldsymbol{\beta}}(\lambda_r)\|_1.$$

Setting $\lambda_r \geq 2\|n^{-1} \sum_{i=1}^n \epsilon_i \mathbf{x}_i^T\|_\infty$ yields that

$$\begin{aligned} \frac{1}{n} \sum_{i=1}^n \left[\mathbf{x}_i^T (\boldsymbol{\beta}^* - \widehat{\boldsymbol{\beta}}(\lambda_r)) \right]^2 & \leq \frac{\lambda_r}{2} \|\boldsymbol{\beta}^* - \widehat{\boldsymbol{\beta}}(\lambda_r)\|_1 + \lambda_r \|\boldsymbol{\beta}^*\|_1 - \lambda_r \|\widehat{\boldsymbol{\beta}}(\lambda_r)\|_1 \\ & \leq \frac{3\lambda_r}{2} \|\boldsymbol{\beta}^*\|_1 - \frac{\lambda_r}{2} \|\widehat{\boldsymbol{\beta}}(\lambda_r)\|_1, \end{aligned}$$

where the last inequality follows from the triangle inequality. This also implies that $\|\widehat{\boldsymbol{\beta}}(\lambda_r)\|_1 \leq 3\|\boldsymbol{\beta}^*\|_1$ as long as $\lambda_r \geq 2\|n^{-1} \sum_{i=1}^n \epsilon_i \mathbf{x}_i^T\|_\infty > 0$. Therefore, we further have $\|\boldsymbol{\beta}^* - \widehat{\boldsymbol{\beta}}(\lambda_r)\|_1 \leq \|\boldsymbol{\beta}^*\|_1 + \|\widehat{\boldsymbol{\beta}}(\lambda_r)\|_1 \leq 4\|\boldsymbol{\beta}^*\|_1$.

Next, we denote that $\Delta = \widehat{\boldsymbol{\beta}}(\lambda_r) - \boldsymbol{\beta}^*$, and inequality (S18) can be written as

$$\frac{1}{n} \sum_{i=1}^n \left[\mathbf{x}_i^T (\boldsymbol{\beta}^* - \widehat{\boldsymbol{\beta}}(\lambda_r)) \right]^2 \leq \frac{\lambda_r}{2} \|\Delta\|_1 + \lambda_r (\|\boldsymbol{\beta}^*\|_1 - \|\boldsymbol{\beta}^* + \Delta\|_1) \leq \frac{3\lambda_r}{2} \|\Delta\|_1.$$

Additionally, we also have

$$\begin{aligned} \frac{1}{n} \sum_{i=1}^n \left[\mathbf{x}_i^T (\boldsymbol{\beta}^* - \widehat{\boldsymbol{\beta}}(\lambda_r)) \right]^2 & \leq \frac{\lambda_r}{2} \|\Delta\|_1 + \lambda_r \|\boldsymbol{\beta}^*\|_1 - \lambda_r \|\Delta + \boldsymbol{\beta}^*\|_1 \\ & = \frac{\lambda_r}{2} \|\Delta\|_1 + \lambda_r \|\boldsymbol{\beta}_{\mathcal{A}}^*\|_1 - \lambda_r \|\Delta_{\mathcal{A}} + \boldsymbol{\beta}_{\mathcal{A}}^*\|_1 - \lambda_r \|\Delta_{\mathcal{A}^c}\|_1 \\ & \leq \frac{3\lambda_r}{2} \|\Delta_{\mathcal{A}}\|_1 - \frac{1}{2} \lambda_r \|\Delta_{\mathcal{A}^c}\|_1, \end{aligned} \quad (\text{S19})$$

where \mathcal{A}^c denotes the complete of \mathcal{A} . Clearly, (S19) implies that $3\lambda_r\|\Delta_{\mathcal{A}}\|_1 > \lambda_r\|\Delta_{\mathcal{A}^c}\|_1$, and hence $\Delta \in \mathbb{C}(\mathcal{A})$. Therefore, by Assumption 3, we have

$$\frac{1}{n} \sum_{i=1}^n \left[\mathbf{x}_i^T \left(\boldsymbol{\beta}^* - \widehat{\boldsymbol{\beta}}(\lambda_r) \right) \right]^2 \geq \kappa \|\boldsymbol{\beta}^* - \widehat{\boldsymbol{\beta}}(\lambda_r)\|_2^2.$$

To sum up, we get $\kappa\|\boldsymbol{\beta}^* - \widehat{\boldsymbol{\beta}}(\lambda_r)\|_2^2 \leq \frac{3}{2}\lambda_r\|\boldsymbol{\beta}^* - \widehat{\boldsymbol{\beta}}(\lambda_r)\|_1 \leq \frac{3\sqrt{s}}{2}\lambda_r\|\boldsymbol{\beta}^* - \widehat{\boldsymbol{\beta}}(\lambda_r)\|_2$, which then implies $\|\boldsymbol{\beta}^* - \widehat{\boldsymbol{\beta}}(\lambda_r)\|_2^2 \leq \frac{9s\lambda_r^2}{4\kappa^2}$. Note that $\widehat{f}_{lasso}(\mathbf{x}) = \mathbf{x}^T \widehat{\boldsymbol{\beta}}(\lambda_r)$ is also estimated from the real dataset. By assuming $\lambda_r \geq 2\|n^{-1} \sum_{i=1}^n \epsilon_i \mathbf{x}_i\|_\infty$, we get $\|\boldsymbol{\beta}^* - \widehat{\boldsymbol{\beta}}(\lambda_r)\|_2^2 \leq \frac{9s\lambda_r^2}{4\kappa^2}$. Next, we apply the sub-Gaussian tail bound to $\|n^{-1} \sum_{i=1}^n \epsilon_i \mathbf{x}_i^T\|_\infty$, and will get

$$\mathbb{P} \left(\left\| n^{-1} \sum_{i=1}^n \epsilon_i \mathbf{x}_i \right\|_\infty > 4C_{\mathcal{X}} \sigma \sqrt{\frac{\log p}{n}} \right) \leq n^{-2}. \quad (\text{S20})$$

2. Variable Selection $\widehat{\mathcal{A}} \subset \mathcal{A}$. In this part, we intend to prove that we have $\|\widehat{\boldsymbol{\beta}}(\lambda_r)\|_0 \leq \|\boldsymbol{\beta}^*\|_0 = s$ under some appropriate choices of λ_r . To prove this, it suffices to prove $\widehat{\mathcal{A}} \subset \mathcal{A}$. First, by Theorem 7.21 of Wainwright (2019), we have $\widehat{\mathcal{A}} \subset \mathcal{A}$ given that $\lambda_r \geq \max_{j \in \mathcal{A}^c} \frac{2}{1-\alpha} \left| \mathbb{X}_j^T [I_n - \mathbb{X}_{\mathcal{A}}(\mathbb{X}_{\mathcal{A}}^T \mathbb{X}_{\mathcal{A}})^{-1} \mathbb{X}_{\mathcal{A}}^T] \boldsymbol{\epsilon} / n \right|$, where $j \in \mathcal{A}^c$, \mathbb{X}_j denotes the j -th column of \mathbb{X} , and α is defined in Assumption 5. Using the fact that $\|\mathbb{X}_j^T [I_n - \mathbb{X}_{\mathcal{A}}(\mathbb{X}_{\mathcal{A}}^T \mathbb{X}_{\mathcal{A}})^{-1} \mathbb{X}_{\mathcal{A}}^T]\|_2 \leq \|\mathbb{X}_j^T\|_2 \leq \sqrt{n}C_{\mathcal{X}}$, we have

$$\mathbb{P} \left(\left| \mathbb{X}_j^T [I_n - \mathbb{X}_{\mathcal{A}}(\mathbb{X}_{\mathcal{A}}^T \mathbb{X}_{\mathcal{A}})^{-1} \mathbb{X}_{\mathcal{A}}^T] \boldsymbol{\epsilon} / n \right| > \delta \mid \mathbb{X} \right) \leq 2 \exp \left(-\frac{n\delta^2}{2C_{\mathcal{X}}^2 \sigma^2} \right), \quad (\text{S21})$$

where the inequality follows from the sub-Gaussian tail bound. Notice that (S21) only requires the boundedness of \mathbb{X} , hence we have

$$\mathbb{P} \left(\max_{j \in \mathcal{A}^c} \left| \mathbb{X}_j^T [I_n - \mathbb{X}_{\mathcal{A}}(\mathbb{X}_{\mathcal{A}}^T \mathbb{X}_{\mathcal{A}})^{-1} \mathbb{X}_{\mathcal{A}}^T] \boldsymbol{\epsilon} / n \right| > \delta \right) \leq 2(p-s) \exp \left(-\frac{n\delta^2}{2C_{\mathcal{X}}^2 \sigma^2} \right).$$

Setting $\delta = \sqrt{2}C_{\mathcal{X}}\sigma \left(\sqrt{\frac{\log(p-s)}{n}} + t \right)$ with $t > 0$ yields that

$$\mathbb{P} \left(\max_{j \in \mathcal{A}^c} \left| \mathbb{X}_j^T [I_n - \mathbb{X}_{\mathcal{A}}(\mathbb{X}_{\mathcal{A}}^T \mathbb{X}_{\mathcal{A}})^{-1} \mathbb{X}_{\mathcal{A}}^T] \boldsymbol{\epsilon} / n \right| > \sqrt{2}C_{\mathcal{X}}\sigma \left(\sqrt{\frac{\log(p-s)}{n}} + t \right) \right) \leq \exp(-nt^2).$$

We further set $t = \sqrt{\frac{2\log n}{n}}$, which then gives

$$\mathbb{P}\left(\max_{j \in \mathcal{A}^c} |\mathbb{X}_j^T [I_n - \mathbb{X}_{\mathcal{A}}(\mathbb{X}_{\mathcal{A}}^T \mathbb{X}_{\mathcal{A}})^{-1} \mathbb{X}_{\mathcal{A}}^T] \boldsymbol{\epsilon}/n| > \sqrt{2} C_{\mathcal{X}} \sigma \left(\sqrt{\frac{2\log(p-s)}{n}} + \frac{2\log n}{n} \right)\right) \leq n^{-2}.$$

By the condition $n \ll p$, we have

$$\mathbb{P}\left(\max_{j \in \mathcal{A}^c} |\mathbb{X}_j^T [I_n - \mathbb{X}_{\mathcal{A}}(\mathbb{X}_{\mathcal{A}}^T \mathbb{X}_{\mathcal{A}})^{-1} \mathbb{X}_{\mathcal{A}}^T] \boldsymbol{\epsilon}/n| > 4C_{\mathcal{X}} \sigma \sqrt{\frac{\log p}{n}}\right) \leq n^{-2}.$$

This result implies that if we set $\lambda_r = \frac{8}{1-\alpha} C_{\mathcal{X}} \sigma \sqrt{\frac{\log p}{n}}$, then we have $\widehat{\mathcal{A}} \subset \mathcal{A}$ with probability at least $1 - n^{-2}$.

3 Convergence of excess risk. In this part, we prove the convergences of $\Phi_r(\widehat{\boldsymbol{\mu}})$, $R_r(\widehat{f}_{lasso}) - R_r(f_{\mathcal{F}}^*)$, and $\widetilde{R}_r(\widetilde{f}_{lasso}) - \widetilde{R}_r(\widetilde{f}_{\mathcal{F}}^*)$.

We first we turn to bound $\Phi_r(\widehat{\boldsymbol{\mu}})$ based on the upper bound for $\|\boldsymbol{\beta}^* - \widehat{\boldsymbol{\beta}}(\lambda_r)\|_2^2$. For any $f(\mathbf{x}) = \mathbf{x}^T \boldsymbol{\beta}$, the risk can be bounded as $R_r(f) \leq C_{\mathcal{X}}^2 \|\boldsymbol{\beta} - \boldsymbol{\beta}^*\|_2^2 + \sigma^2$. By the assumption that synthetic labels are generated via $\widetilde{y}_i = \widehat{\boldsymbol{\mu}}(\widetilde{\mathbf{x}}_i) + \widetilde{\epsilon}_i$, we have

$$\Phi_r(\widehat{\boldsymbol{\mu}}) \leq C_{\mathcal{X}}^2 \|\boldsymbol{\beta}^* - \widehat{\boldsymbol{\beta}}(\lambda_r)\|_2^2 \leq \frac{9C_{\mathcal{X}}^2 s \lambda_r^2}{4\kappa^2}, \quad (\text{S22})$$

with probability at least $1 - n^{-2}$ and $\lambda_r = \frac{8C_{\mathcal{X}} \sigma}{1-\alpha} \sqrt{\frac{\log p}{n}}$.

Note that \widehat{f}_{lasso} is also estimated from the real dataset and $f_{\mathcal{F}}^*(\mathbf{x}) = \mathbf{x}^T \boldsymbol{\beta}^*$. By assuming $\lambda_r \geq 2\|n^{-1} \sum_{i=1}^n \epsilon_i \mathbf{x}_i\|_{\infty}$, applying a similar argument as above yields

$$R_r(\widehat{f}_{lasso}) - R_r(f_{\mathcal{F}}^*) \leq C_{\mathcal{X}}^2 \|\boldsymbol{\beta}^* - \widehat{\boldsymbol{\beta}}(\lambda_r)\|_2^2 \leq \frac{9C_{\mathcal{X}}^2 s \lambda_r^2}{4\kappa^2}. \quad (\text{S23})$$

Next we proceed to bound $\widetilde{R}_r(\widetilde{f}_{lasso}) - \widetilde{R}_r(\widetilde{f}_{\mathcal{F}}^*)$. Here, it is worth noting that $\widetilde{f}_{\mathcal{F}}^*(\mathbf{x}) = \mathbf{x}^T \widehat{\boldsymbol{\beta}}(\lambda_r)$ is random and depends on $\widehat{\boldsymbol{\beta}}(\lambda_r)$. As proved in part 2, we have $\|\widehat{\boldsymbol{\beta}}(\lambda_r)\|_0 \leq \|\boldsymbol{\beta}^*\|_0 = s$. For any $\widehat{\boldsymbol{\beta}}(\lambda_r)$, applying similar arguments to \widetilde{f}_{lasso} yields that

$$\sup_{\widehat{\boldsymbol{\beta}}(\lambda_r): \widehat{\mathcal{A}} \subset \mathcal{A}} \left\{ \widetilde{R}_r(\widetilde{f}_{lasso}) - \widetilde{R}_r(\widetilde{f}_{\mathcal{F}}^*) \right\} \leq \sup_{\widehat{\boldsymbol{\beta}}(\lambda_r): \widehat{\mathcal{A}} \subset \mathcal{A}} C_{\mathcal{X}}^2 \|\widetilde{\boldsymbol{\beta}}(\widetilde{\lambda}_r) - \widehat{\boldsymbol{\beta}}(\lambda_r)\|_2^2 \leq \frac{9C_{\mathcal{X}}^2 s \widetilde{\lambda}_r^2}{4\kappa^2}, \quad (\text{S24})$$

for any $\widehat{\boldsymbol{\beta}}(\lambda_r)$, where $\widetilde{\lambda}_r \geq 2\|\widetilde{n}^{-1} \sum_{i=1}^{\widetilde{n}} \widetilde{\epsilon}_i \widetilde{\mathbf{x}}_i\|_\infty$. Clearly, the inequality in (S24) hold when

$$\begin{aligned} \widetilde{\lambda}_r &\geq 2\|\widetilde{n}^{-1} \sum_{i=1}^{\widetilde{n}} \widetilde{\epsilon}_i \widetilde{\mathbf{x}}_i\|_\infty, \\ \lambda_r &\geq 2 \max\left\{\|n^{-1} \sum_{i=1}^n \epsilon_i \mathbf{x}_i\|_\infty, \max_{j \in \mathcal{A}^c} \frac{2}{1-\alpha} |\mathbb{X}_j^T [I_n - \mathbb{X}_{\mathcal{A}}(\mathbb{X}_{\mathcal{A}}^T \mathbb{X}_{\mathcal{A}})^{-1} \mathbb{X}_{\mathcal{A}}^T] \boldsymbol{\epsilon}/n\right\}. \end{aligned}$$

Using the result in (S20), we get (S23) and (S24) hold simultaneously with probability at least $1 - n^{-2} - \widetilde{n}^{-2}$ with $\widetilde{\lambda}_r = 8C_{\mathcal{X}} \sqrt{\widetilde{n}^{-1} \log p}$.

4 Convergence of $D_{\mathcal{H}}(\mathbb{P}_{\mathbf{X}}, \mathbb{P}_{\widetilde{\mathbf{X}}})$. In this example, $D_{\mathcal{H}}(\mathbb{P}_{\mathbf{X}}, \mathbb{P}_{\widetilde{\mathbf{X}}})$ becomes

$$\begin{aligned} D_{\mathcal{H}}(\mathbb{P}_{\mathbf{X}}, \mathbb{P}_{\widetilde{\mathbf{X}}}) &= \max \left\{ \left| \int_{\mathcal{X}} \left[\widetilde{f}_{lasso}(\mathbf{x}) - \widehat{\mu}(\mathbf{x}) \right]^2 (P_{\mathbf{X}}(\mathbf{x}) - P_{\widetilde{\mathbf{X}}}(\mathbf{x})) d\mathbf{x} \right|, \right. \\ &\quad \left. \left| \int_{\mathcal{X}} [f^*(\mathbf{x}) - \widehat{\mu}(\mathbf{x})]^2 (P_{\mathbf{X}}(\mathbf{x}) - P_{\widetilde{\mathbf{X}}}(\mathbf{x})) d\mathbf{x} \right| \right\} \\ &\leq 2C_{\mathcal{X}}^2 \|\widetilde{\boldsymbol{\beta}}(\widetilde{\lambda}_r) - \widehat{\boldsymbol{\beta}}(\lambda_r)\|_2^2 + 2C_{\mathcal{X}}^2 \|\widehat{\boldsymbol{\beta}}(\lambda_r) - \boldsymbol{\beta}^*\|_2^2 \\ &\leq \frac{9C_{\mathcal{X}}^2 s \widetilde{\lambda}_r^2}{2\kappa^2} + \frac{9C_{\mathcal{X}}^2 s \lambda_r^2}{2\kappa^2}. \end{aligned} \tag{S25}$$

Next, we proceed to bound

$$2\left(\sqrt{\Phi_r(\widetilde{f}_{lasso})} + 2\sqrt{\Phi_r(\widetilde{f}_{\mathcal{F}}^*)} + \sqrt{\Phi_r(f_{\mathcal{F}}^*)}\right) \sqrt{\Phi_r(\widehat{\mu})} = 2\left(\sqrt{\Phi_r(\widetilde{f}_{lasso})} + 2\sqrt{\Phi_r(\widetilde{f}_{\mathcal{F}}^*)}\right) \sqrt{\Phi_r(\widehat{\mu})}.$$

Since $\widetilde{f}_{\mathcal{F}}^* = \widehat{\mu}$, using the inequality of arithmetic and geometric means gives

$$\begin{aligned} &2\left(\sqrt{\Phi_r(\widetilde{f}_{lasso})} + 2\sqrt{\Phi_r(\widetilde{f}_{\mathcal{F}}^*)}\right) \sqrt{\Phi_r(\widehat{\mu})} \leq \Phi_r(\widetilde{f}) + 5\Phi_r(\widehat{\mu}) \\ &\leq 2C_{\mathcal{X}}^2 \|\widetilde{\boldsymbol{\beta}}(\widetilde{\lambda}_r) - \widehat{\boldsymbol{\beta}}(\lambda_r)\|_2^2 + 7C_{\mathcal{X}}^2 \|\widehat{\boldsymbol{\beta}}(\lambda_r) - \boldsymbol{\beta}^*\|_2^2. \end{aligned} \tag{S26}$$

Combining (S22)-(S26) gives the upper bound for the utility metric as

$$\left| R_r(\widehat{f}_{lasso}) - R_r(\widetilde{f}_{lasso}) \right| \leq 20C_{\mathcal{X}}^2 \|\widetilde{\boldsymbol{\beta}}(\widetilde{\lambda}_r) - \widehat{\boldsymbol{\beta}}(\lambda_r)\|_2^2 + 11C_{\mathcal{X}}^2 \|\widehat{\boldsymbol{\beta}}(\lambda_r) - \boldsymbol{\beta}^*\|_2^2 \lesssim \frac{C_{\mathcal{X}}^2 s (\widetilde{\lambda}_r^2 + \lambda_r^2)}{\kappa^2}.$$

It then follows that

$$\left| R_r(\widehat{f}_{lasso}) - R_r(\widetilde{f}_{lasso}) \right| \lesssim \frac{C_{\mathcal{X}}^4 s \log p}{\kappa^2} \left(\frac{\sigma^2}{n} + \frac{\widetilde{\sigma}^2}{\widetilde{n}} \right),$$

with probability at least $1 - n^{-2} - \widetilde{n}^{-2}$. This completes the proof. \square

S.2.4 Proof of Theorem 4

This section aims to provide a complete proof for Theorem 4. First, we denote that $f_{\mathcal{F}_1}^* = \operatorname{argmin}_{f \in \mathcal{F}_1} R_r(f)$ and $f_{\mathcal{F}_2}^* = \operatorname{argmin}_{f \in \mathcal{F}_2} R_r(f)$. Given that $R_r(f_{\mathcal{F}_1}^*) > R_r(f_{\mathcal{F}_2}^*)$, we proceed to prove $R_r(\tilde{f}_{\mathcal{F}_1}^*) > R_r(\tilde{f}_{\mathcal{F}_2}^*)$, where $\tilde{f}_{\mathcal{F}_1}^* = \operatorname{argmin}_{f \in \mathcal{F}_1} \tilde{R}_r(f)$ and $\tilde{f}_{\mathcal{F}_2}^* = \operatorname{argmin}_{f \in \mathcal{F}_2} \tilde{R}_r(f)$. Notice that $R_r(\tilde{f}_{\mathcal{F}_1}^*) \geq R_r(f_{\mathcal{F}_1}^*)$, it suffices to prove $\Phi_r(f_{\mathcal{F}_1}^*) > \Phi_r(\tilde{f}_{\mathcal{F}_2}^*)$.

$$\sqrt{\Phi_r(\tilde{f}_{\mathcal{F}_2}^*)} = \sqrt{\int_{\mathcal{X}} \left(\mu(\mathbf{x}) - \tilde{f}_{\mathcal{F}_2}^*(\mathbf{x}) \right)^2 P_{\mathbf{X}}(\mathbf{x}) d\mathbf{x}} \leq \|\mu - \hat{\mu}\|_{L^2(\mathbb{P}_{\mathbf{X}})} + \sqrt{\int_{\mathcal{X}} \left(\hat{\mu}(\mathbf{x}) - \tilde{f}_{\mathcal{F}_2}^*(\mathbf{x}) \right)^2 P_{\mathbf{X}}(\mathbf{x}) d\mathbf{x}}.$$

Next, we decompose \mathcal{X} into two parts.

$$\mathcal{X} = \left\{ \mathbf{x} \in \mathcal{X} : \frac{P_{\mathbf{X}}(\mathbf{x})}{P_{\tilde{\mathbf{X}}}(\mathbf{x})} \leq C \right\} \cup \left\{ \mathbf{x} \in \mathcal{X} : \frac{P_{\mathbf{X}}(\mathbf{x})}{P_{\tilde{\mathbf{X}}}(\mathbf{x})} \geq C \right\} \triangleq \mathcal{X}_1 \cup \mathcal{X}_2.$$

With this, we have

$$\begin{aligned} & \int_{\mathcal{X}} \left(\hat{\mu}(\mathbf{x}) - \tilde{f}_{\mathcal{F}_2}^*(\mathbf{x}) \right)^2 P_{\mathbf{X}}(\mathbf{x}) d\mathbf{x} = \int_{\mathcal{X}_1} \left(\hat{\mu}(\mathbf{x}) - \tilde{f}_{\mathcal{F}_2}^*(\mathbf{x}) \right)^2 P_{\mathbf{X}}(\mathbf{x}) d\mathbf{x} + \int_{\mathcal{X}_2} \left(\hat{\mu}(\mathbf{x}) - \tilde{f}_{\mathcal{F}_2}^*(\mathbf{x}) \right)^2 P_{\mathbf{X}}(\mathbf{x}) d\mathbf{x} \\ & \leq C \int_{\mathcal{X}_1} \left(\hat{\mu}(\mathbf{x}) - \tilde{f}_{\mathcal{F}_2}^*(\mathbf{x}) \right)^2 P_{\tilde{\mathbf{X}}}(\mathbf{x}) d\mathbf{x} + \int_{\mathcal{X}_2} \left(\hat{\mu}(\mathbf{x}) - \tilde{f}_{\mathcal{F}_2}^*(\mathbf{x}) \right)^2 P_{\mathbf{X}}(\mathbf{x}) d\mathbf{x} \\ & \leq C \int_{\mathcal{X}} \left(\hat{\mu}(\mathbf{x}) - \tilde{f}_{\mathcal{F}_2}^*(\mathbf{x}) \right)^2 P_{\tilde{\mathbf{X}}}(\mathbf{x}) d\mathbf{x} + U^2 P_1 \leq C \tilde{\Phi}_r(\tilde{f}_{\mathcal{F}_2}^*) + U^2 P \leq C \tilde{\Phi}_r(f_{\mathcal{F}_2}^*) + U^2 P_1, \end{aligned}$$

where $P_1 = V \cdot C^{-d}$ and the last inequality follows from the fact that $\tilde{\Phi}_r(\tilde{f}_{\mathcal{F}_2}^*) \leq \tilde{\Phi}_r(f_{\mathcal{F}_2}^*)$. To sum up, we have

$$\int_{\mathcal{X}} \left(\hat{\mu}(\mathbf{x}) - \tilde{f}_{\mathcal{F}_2}^*(\mathbf{x}) \right)^2 P_{\mathbf{X}}(\mathbf{x}) d\mathbf{x} \leq \inf_{C > 0} \left\{ C \tilde{\Phi}_r(f_{\mathcal{F}_2}^*) + U^2 V C^{-d} \right\}.$$

Taking $C = \left(d V U^2 / \tilde{\Phi}_r(f_{\mathcal{F}_2}^*) \right)^{1/(d+1)}$ yields that

$$\int_{\mathcal{X}} \left(\hat{\mu}(\mathbf{x}) - \tilde{f}_{\mathcal{F}_2}^*(\mathbf{x}) \right)^2 P_{\mathbf{X}}(\mathbf{x}) d\mathbf{x} \leq \left(d^{\frac{1}{d+1}} + d^{-\frac{d}{d+1}} \right) V^{\frac{1}{d+1}} U^{\frac{2}{d+1}} \left(\tilde{\Phi}_r(f_{\mathcal{F}_2}^*) \right)^{\frac{d}{d+1}}. \quad (\text{S27})$$

Next, we turn to establish relation between $\tilde{\Phi}_r(f_{\mathcal{F}_2}^*)$ and $\Phi_r(f_{\mathcal{F}_2}^*)$. We first apply a similar treatment to \mathcal{X} by the decomposition as

$$\mathcal{X} = \left\{ \mathbf{x} \in \mathcal{X} : \frac{P_{\tilde{\mathbf{X}}}(\mathbf{x})}{P_{\mathbf{X}}(\mathbf{x})} \leq C \right\} \cup \left\{ \mathbf{x} \in \mathcal{X} : \frac{P_{\tilde{\mathbf{X}}}(\mathbf{x})}{P_{\mathbf{X}}(\mathbf{x})} \geq C \right\} \triangleq \mathcal{X}_3 \cup \mathcal{X}_4,$$

for some positive constants C . With this, it follows that

$$\begin{aligned}
\sqrt{\tilde{\Phi}_r(f_{\mathcal{F}_2}^*)} &= \sqrt{\int_{\mathcal{X}} (\hat{\mu}(\mathbf{x}) - f_{\mathcal{F}_2}^*(\mathbf{x}))^2 P_{\tilde{\mathcal{X}}}(\mathbf{x}) d\mathbf{x}} \\
&\leq \sqrt{\int_{\mathcal{X}_3} (\hat{\mu}(\mathbf{x}) - f_{\mathcal{F}_2}^*(\mathbf{x}))^2 P_{\tilde{\mathcal{X}}}(\mathbf{x}) d\mathbf{x}} + \sqrt{\int_{\mathcal{X}_4} (\hat{\mu}(\mathbf{x}) - f_{\mathcal{F}_2}^*(\mathbf{x}))^2 P_{\tilde{\mathcal{X}}}(\mathbf{x}) d\mathbf{x}} \\
&\leq C^{1/2} \sqrt{\int_{\mathcal{X}_3} (\hat{\mu}(\mathbf{x}) - f_{\mathcal{F}_2}^*(\mathbf{x}))^2 P_{\mathbf{X}}(\mathbf{x}) d\mathbf{x}} + \sqrt{\int_{\mathcal{X}_4} (\hat{\mu}(\mathbf{x}) - f_{\mathcal{F}_2}^*(\mathbf{x}))^2 P_{\tilde{\mathcal{X}}}(\mathbf{x}) d\mathbf{x}} \\
&\leq C^{1/2} \left(\|\hat{\mu} - \mu\|_{L^2(\mathbb{P}_{\mathbf{X}})} + \sqrt{\Phi_r(f_{\mathcal{F}_2}^*)} \right) + V^{1/2} U C^{-d/2}.
\end{aligned}$$

Similarly, by taking $C = \left(\frac{dV^{1/2}U}{\|\hat{\mu} - \mu\|_{L^2(\mathbb{P}_{\mathbf{X}})} + \sqrt{\Phi_r(f_{\mathcal{F}_2}^*)}} \right)^{\frac{2}{d+1}}$, we have

$$\sqrt{\tilde{\Phi}_r(f_{\mathcal{F}_2}^*)} \leq (d^{\frac{1}{d+1}} + d^{-\frac{d}{d+1}}) V^{\frac{1}{2(d+1)}} U^{\frac{1}{d+1}} \left(\|\hat{\mu} - \mu\|_{L^2(\mathbb{P}_{\mathbf{X}})} + \sqrt{\Phi_r(f_{\mathcal{F}_2}^*)} \right)^{\frac{d}{d+1}}. \quad (\text{S28})$$

Plugging (S28) into (S27), we get

$$\sqrt{\int_{\mathcal{X}} (\hat{\mu}(\mathbf{x}) - \tilde{f}_{\mathcal{F}_2}^*(\mathbf{x}))^2 P_{\mathbf{X}}(\mathbf{x}) d\mathbf{x}} \leq C_{d,V,U} \left(\|\hat{\mu} - \mu\|_{L^2(\mathbb{P}_{\mathbf{X}})} + \sqrt{\Phi_r(f_{\mathcal{F}_2}^*)} \right)^{\frac{d^2}{(d+1)^2}},$$

where $C_{d,V,U} = (d^{\frac{1}{d+1}} + d^{-\frac{d}{d+1}})^{\frac{3d+1}{2(d+1)}} V^{\frac{2d+1}{2(d+1)^2}} U^{\frac{2d+1}{(d+1)^2}}$. Therefore, we have

$$\begin{aligned}
\sqrt{\Phi_r(\tilde{f}_{\mathcal{F}_2}^*)} &\leq \|\mu - \hat{\mu}\|_{L^2(\mathbb{P}_{\mathbf{X}})} + C_{d,V,U} \left(\|\hat{\mu} - \mu\|_{L^2(\mathbb{P}_{\mathbf{X}})} + \sqrt{\Phi_r(f_{\mathcal{F}_2}^*)} \right)^{\frac{d^2}{(d+1)^2}} \\
&\leq \|\mu - \hat{\mu}\|_{L^2(\mathbb{P}_{\mathbf{X}})} + C_{d,V,U} \|\hat{\mu} - \mu\|_{L^2(\mathbb{P}_{\mathbf{X}})}^{\frac{d^2}{(d+1)^2}} + C_{d,V,U} \left(\sqrt{\Phi_r(f_{\mathcal{F}_2}^*)} \right)^{\frac{d^2}{(d+1)^2}}, \quad (\text{S29})
\end{aligned}$$

Hence, if the right-hand side of (S29) is smaller than $\sqrt{\Phi_r(f_{\mathcal{F}_1}^*)}$, we get $\sqrt{\Phi_r(\tilde{f}_{\mathcal{F}_2}^*)} < \sqrt{\Phi_r(\tilde{f}_{\mathcal{F}_1}^*)}$.

This completes the proof. \square

S.2.5 Proof of Theorem 5

First, by Theorem 4, we have consistent model comparison when the following holds true.

$$\|\mu - \hat{\mu}\|_{L^2(\mathbb{P}_{\mathbf{X}})} + C_{d,V,U} \|\hat{\mu} - \mu\|_{L^2(\mathbb{P}_{\mathbf{X}})}^{\frac{d^2}{(d+1)^2}} + C_{d,V,U} \left(\sqrt{\Phi_r(f_{\mathcal{F}_2}^*)} \right)^{\frac{d^2}{(d+1)^2}} \leq \sqrt{\Phi_r(f_{\mathcal{F}_1}^*)}.$$

Let $(\mathcal{F}_1, \mathcal{F}_2)$ denote any pair of function classes with $\sqrt{\Phi_r(f_{\mathcal{F}_1}^*)} - C_{d,V,U} (\Phi_r(f_{\mathcal{F}_2}^*))^{\frac{d^2}{2(d+1)^2}} = g_0 > 0$. Then we have

$$\begin{aligned} & \mathbb{P} \left((R_r(f_{\mathcal{F}_2}^*) - R_r(f_{\mathcal{F}_1}^*)) (R_r(\tilde{f}_{\mathcal{F}_2}^*) - R_r(\tilde{f}_{\mathcal{F}_1}^*)) < 0 \right) \\ & \leq \mathbb{P} \left(\|\mu - \hat{\mu}\|_{L^2(\mathbb{P}_{\mathbf{X}})} + C_{d,V,U} \|\hat{\mu} - \mu\|_{L^2(\mathbb{P}_{\mathbf{X}})}^{\frac{d^2}{(d+1)^2}} > g_0 \right). \end{aligned}$$

Next we consider two cases $\|\mu - \hat{\mu}\|_{L^2(\mathbb{P}_{\mathbf{X}})} > 1$ and $\|\mu - \hat{\mu}\|_{L^2(\mathbb{P}_{\mathbf{X}})} < 1$. Specifically,

$$\begin{aligned} & \mathbb{P} \left(\|\mu - \hat{\mu}\|_{L^2(\mathbb{P}_{\mathbf{X}})} + C_{d,V,U} \|\hat{\mu} - \mu\|_{L^2(\mathbb{P}_{\mathbf{X}})}^{\frac{d^2}{(d+1)^2}} > g_0 \right) \\ & = \mathbb{P} \left(\|\mu - \hat{\mu}\|_{L^2(\mathbb{P}_{\mathbf{X}})} + C_{d,V,U} \|\hat{\mu} - \mu\|_{L^2(\mathbb{P}_{\mathbf{X}})}^{\frac{d^2}{(d+1)^2}} > g_0 \mid \|\mu - \hat{\mu}\|_{L^2(\mathbb{P}_{\mathbf{X}})} > 1 \right) \mathbb{P} (\|\mu - \hat{\mu}\|_{L^2(\mathbb{P}_{\mathbf{X}})} > 1) \\ & + \mathbb{P} \left(\|\mu - \hat{\mu}\|_{L^2(\mathbb{P}_{\mathbf{X}})} + C_{d,V,U} \|\hat{\mu} - \mu\|_{L^2(\mathbb{P}_{\mathbf{X}})}^{\frac{d^2}{(d+1)^2}} > g_0 \mid \|\mu - \hat{\mu}\|_{L^2(\mathbb{P}_{\mathbf{X}})} < 1 \right) \mathbb{P} (\|\mu - \hat{\mu}\|_{L^2(\mathbb{P}_{\mathbf{X}})} < 1) \\ & \leq C_1 \exp(-C_2 a_n) + \mathbb{P} \left((C_{d,V,U} + 1) \|\hat{\mu} - \mu\|_{L^2(\mathbb{P}_{\mathbf{X}})}^{\frac{d^2}{(d+1)^2}} > g_0 \right) \\ & \leq C_1 \left\{ \exp(-C_2 a_n) + \exp\left(-C_2 a_n g_0^{\frac{(d+1)^2}{d^2}} (C_{d,V,U} + 1)^{-\frac{(d+1)^2}{d^2}}\right) \right\}. \end{aligned}$$

Clearly, for any $g_0 > 0$ and pair of $(\mathcal{F}_1, \mathcal{F}_2)$ with $\sqrt{\Phi_r(f_{\mathcal{F}_1}^*)} - C_{d,V,U} (\Phi_r(f_{\mathcal{F}_2}^*))^{\frac{d^2}{2(d+1)^2}} = g_0$, we have

$$\begin{aligned} & \mathbb{P} \left((R_r(f_{\mathcal{F}_2}^*) - R_r(f_{\mathcal{F}_1}^*)) (R_r(\tilde{f}_{\mathcal{F}_2}^*) - R_r(\tilde{f}_{\mathcal{F}_1}^*)) < 0 \right) \\ & \leq C_1 \left\{ \exp(-C_2 a_n) + \exp\left(-C_2 a_n g_0^{\frac{(d+1)^2}{d^2}} (C_{d,V,U} + 1)^{-\frac{(d+1)^2}{d^2}}\right) \right\}. \quad (\text{S30}) \end{aligned}$$

Notice that the right-hand side of (S30) only relies on (V, d) -fidelity level and the generalization difference. Therefore, it follows that

$$\begin{aligned} & \sup_{(\mathcal{F}_1, \mathcal{F}_2) \in \mathcal{H}(g)} \mathbb{P} \left((R_r(f_{\mathcal{F}_2}^*) - R_r(f_{\mathcal{F}_1}^*)) (R_r(\tilde{f}_{\mathcal{F}_2}^*) - R_r(\tilde{f}_{\mathcal{F}_1}^*)) < 0 \right) \\ & \leq C_1 \left\{ \exp(-C_2 a_n) + \exp\left(-C_2 a_n g_0^{\frac{(d+1)^2}{d^2}} (C_{d,V,U} + 1)^{-\frac{(d+1)^2}{d^2}}\right) \right\}. \end{aligned}$$

This completes the proof. \square

S.2.6 Proof of Theorem S6

In this section, we provide a complete proof of Theorem S6. First, by the triangle inequality, we have

$$U_c(\tilde{g}, \hat{g}) = |R_{0-1}(\tilde{g}) - R_{0-1}(\hat{g})| \leq |R_{0-1}(\tilde{g}) - R_{0-1}(g_G^*)| + |R_{0-1}(g_G^*) - R_{0-1}(\hat{g})|. \quad (\text{S31})$$

We first notice that for any $g \in \mathcal{G}$, we have

$$\begin{aligned} R_{0-1}(g) &= \int_{\mathcal{X}} \left[I(g(\mathbf{x}) < 0) \eta(\mathbf{x}) + I(g(\mathbf{x}) > 0) (1 - \eta(\mathbf{x})) \right] P_{\mathbf{X}}(\mathbf{x}) d\mathbf{x} \\ &= \int_{\mathcal{X}} |2\eta(\mathbf{x}) - 1| I(g(\mathbf{x})(\eta(\mathbf{x}) - 1/2) < 0) P_{\mathbf{X}}(\mathbf{x}) d\mathbf{x} + \int_{\mathcal{X}} \min\{\eta(\mathbf{x}), 1 - \eta(\mathbf{x})\} P_{\mathbf{X}}(\mathbf{x}) d\mathbf{x} \\ &= \Phi_{0-1}(g) + \mathbb{E}_{\mathbf{X}}[\min\{\eta(\mathbf{X}), 1 - \eta(\mathbf{X})\}] = \Phi_{0-1}(g) + R_{0-1}^*, \end{aligned}$$

where R_{0-1}^* is the Bayes risk. With this, the first term on the right-hand side of (S31) can be bounded by

$$\begin{aligned} R_{0-1}(\tilde{g}) - R_{0-1}(g_G^*) &= \Phi_{0-1}(\tilde{g}) - \Phi_{0-1}(g_G^*) \\ &= \Phi_{0-1}(\tilde{g}) - \tilde{\Phi}_{0-1}(\tilde{g}) + \tilde{\Phi}_{0-1}(\tilde{g}) - \tilde{\Phi}_{0-1}(\tilde{g}_G^*) + \tilde{\Phi}_{0-1}(\tilde{g}_G^*) - \Phi_{0-1}(\tilde{g}_G^*) + \Phi_{0-1}(\tilde{g}_G^*) - \Phi_{0-1}(g_G^*) \\ &\leq 2 \sup_{g \in \{\tilde{g}, \tilde{g}_G^*\}} \left| \tilde{\Phi}_{0-1}(g) - \Phi_{0-1}(g) \right| + \tilde{\Phi}_{0-1}(\tilde{g}) - \tilde{\Phi}_{0-1}(\tilde{g}_G^*) + \Phi_{0-1}(\tilde{g}_G^*) - \Phi_{0-1}(g_G^*) \\ &\triangleq T_1 + T_2 + T_3. \end{aligned}$$

Here $T_2 = \tilde{\Phi}_{0-1}(\tilde{g}) - \tilde{\Phi}_{0-1}(\tilde{g}_G^*) = \tilde{R}_{0-1}(\tilde{g}) - \tilde{R}_{0-1}(\tilde{g}_G^*)$ is the estimation error under the synthetic data distribution. It remains to bound T_1 and T_3 separately.

Bounding T_1 . For any $g \in \mathcal{G}$, we have

$$\begin{aligned}
& \left| \tilde{\Phi}_{0-1}(g) - \Phi_{0-1}(g) \right| \\
&= \left| \int_{\mathcal{X}} |2\hat{\eta}(\mathbf{x}) - 1| I(g(\mathbf{x})(\hat{\eta}(\mathbf{x}) - 1/2) < 0) P_{\tilde{\mathbf{X}}}(\mathbf{x}) d\mathbf{x} - \int_{\mathcal{X}} |2\eta(\mathbf{x}) - 1| I(g(\mathbf{x})(\eta(\mathbf{x}) - 1/2) < 0) P_{\mathbf{X}}(\mathbf{x}) d\mathbf{x} \right| \\
&\leq \left| \int_{\mathcal{X}} |2\hat{\eta}(\mathbf{x}) - 1| I(g(\mathbf{x})(\hat{\eta}(\mathbf{x}) - 1/2) < 0) P_{\tilde{\mathbf{X}}}(\mathbf{x}) d\mathbf{x} - \int_{\mathcal{X}} |2\hat{\eta}(\mathbf{x}) - 1| I(g(\mathbf{x})(\hat{\eta}(\mathbf{x}) - 1/2) < 0) P_{\mathbf{X}}(\mathbf{x}) d\mathbf{x} \right| \\
&+ \left| \int_{\mathcal{X}} |2\hat{\eta}(\mathbf{x}) - 1| I(g(\mathbf{x})(\hat{\eta}(\mathbf{x}) - 1/2) < 0) P_{\mathbf{X}}(\mathbf{x}) d\mathbf{x} - \int_{\mathcal{X}} |2\eta(\mathbf{x}) - 1| I(g(\mathbf{x})(\eta(\mathbf{x}) - 1/2) < 0) P_{\mathbf{X}}(\mathbf{x}) d\mathbf{x} \right| \\
&\triangleq A_1(g) + A_2(g).
\end{aligned}$$

To bound $|\tilde{\Phi}_{0-1}(g) - \Phi_{0-1}(g)|$, it remains to bound $A_1(g)$ and $A_2(g)$, respectively. $A_1(g)$ can be written as

$$A_1(g) = \left| \int_{\mathcal{X}} |2\hat{\eta}(\mathbf{x}) - 1| I(g(\mathbf{x})(\hat{\eta}(\mathbf{x}) - 1/2) < 0) \left(P_{\tilde{\mathbf{X}}}(\mathbf{x}) - P_{\mathbf{X}}(\mathbf{x}) \right) d\mathbf{x} \right|.$$

where the second last inequality follows from the Cauchy-Schwarz inequality. For $A_2(g)$, applying a similar argument yields that

$$\begin{aligned}
A_2(g) &= \left| \int_{\mathcal{X}} |2\hat{\eta}(\mathbf{x}) - 1| I(g(\mathbf{x})(\hat{\eta}(\mathbf{x}) - 1/2) < 0) P_{\mathbf{X}}(\mathbf{x}) d\mathbf{x} \right. \\
&\quad \left. - \int_{\mathcal{X}} |2\eta(\mathbf{x}) - 1| I(g(\mathbf{x})(\eta(\mathbf{x}) - 1/2) < 0) P_{\mathbf{X}}(\mathbf{x}) d\mathbf{x} \right| \\
&\leq \int_{\mathcal{X}} 2|\hat{\eta}(\mathbf{x}) - \eta(\mathbf{x})| I(g(\mathbf{x})(\hat{\eta}(\mathbf{x}) - 1/2) < 0) P_{\mathbf{X}}(\mathbf{x}) d\mathbf{x} + \\
&\quad \left| \int_{\mathcal{X}} |2\eta(\mathbf{x}) - 1| \left[I(g(\mathbf{x})(\hat{\eta}(\mathbf{x}) - 1/2) < 0) - I(g(\mathbf{x})(\eta(\mathbf{x}) - 1/2) < 0) \right] P_{\mathbf{X}}(\mathbf{x}) d\mathbf{x} \right| \\
&= 2\|\hat{\eta} - \eta\|_{L^2(\mathbb{P}_X)} C(g) + \Phi_{0-1}(\text{sign}(\hat{\eta}(\mathbf{x}) - 1/2)) \leq 4\|\hat{\eta} - \eta\|_{L^2(\mathbb{P}_X)}
\end{aligned}$$

where $C(g) = \sqrt{\mathbb{P}(g(\mathbf{X})(\hat{\eta}(\mathbf{X}) - 1/2) < 0)}$ and the inequality follows from the Cauchy-Schwarz inequality. Combining upper bounds of $A_1(g)$ and $A_2(g)$, $|\tilde{\Phi}_{0-1}(g) - \Phi_{0-1}(g)|$ can be upper bounded as

$$|\tilde{\Phi}_{0-1}(g) - \Phi_{0-1}(g)| \leq A_1(g) + 4\|\hat{\eta} - \eta\|_{L^2(\mathbb{P}_X)},$$

where the second inequality follows from the fact that $C(g) \leq 1$. Therefore, T_1 can be

bounded as

$$T_1 \leq 2D_{\mathcal{K}_1}(\mathbb{P}_{\mathbf{X}}, \mathbb{P}_{\widetilde{\mathbf{X}}}) + 8\|\widehat{\eta} - \eta\|_{L^2(\mathbb{P}_{\mathbf{X}})},$$

where $\mathcal{K}_1 = \{k(\mathbf{x}) = |2\widehat{\eta}(\mathbf{x}) - 1|I(g(\mathbf{x})(\widehat{\eta}(\mathbf{x}) - 1/2) < 0), g \in \{\widetilde{g}, \widetilde{g}_G^*\}\}$

Bounding T_3 . Next, we turn to bound $|\Phi_{0-1}(\widetilde{g}_G^*) - \Phi_{0-1}(g_G^*)|$. By the fact that g_G^* and \widetilde{g}_G^* minimizes $\Phi_{0-1}(g)$ and $\widetilde{\Phi}_{0-1}(g)$, respectively, it follows that

$$\begin{aligned} \left| \Phi_{0-1}(\widetilde{g}_G^*) - \Phi_{0-1}(g_G^*) \right| &= \Phi_{0-1}(\widetilde{g}_G^*) - \Phi_{0-1}(g_G^*) \leq (\Phi_{0-1}(\widetilde{g}_G^*) - \widetilde{\Phi}_{0-1}(\widetilde{g}_G^*)) - (\Phi_{0-1}(g_G^*) - \widetilde{\Phi}_{0-1}(g_G^*)) \\ &\leq |\Phi_{0-1}(\widetilde{g}_G^*) - \widetilde{\Phi}_{0-1}(\widetilde{g}_G^*)| + |\Phi_{0-1}(g_G^*) - \widetilde{\Phi}_{0-1}(g_G^*)|. \end{aligned}$$

Applying a similar argument as used in bounding T_1 , we can conclude that

$$\begin{aligned} U_c(\widetilde{g}, \widehat{g}) &\leq |R_{0-1}(\widehat{g}) - R_{0-1}(g_G^*)| + |\widetilde{R}'_{0-1}(\widehat{g}) - \widetilde{R}'_{0-1}(\widetilde{g}_G^*)| + |\Phi_{0-1}(\widehat{g}) - \widetilde{\Phi}_{0-1}(\widehat{g})| \\ &\quad + 2|\Phi_{0-1}(\widetilde{g}_G^*) - \widetilde{\Phi}_{0-1}(\widetilde{g}_G^*)| + |\Phi_{0-1}(g_G^*) - \widetilde{\Phi}_{0-1}(g_G^*)| \\ &\leq |R_{0-1}(\widehat{g}) - R_{0-1}(g_G^*)| + |\widetilde{R}_{0-1}(\widehat{g}) - \widetilde{R}_{0-1}(\widetilde{g}_G^*)| \\ &\quad + 16\|\widehat{\eta} - \eta\|_{L^2(\mathbb{P}_{\mathbf{X}})} + 4D_{\mathcal{K}}(\mathbb{P}_{\mathbf{X}}, \mathbb{P}_{\widetilde{\mathbf{X}}}), \end{aligned}$$

where $\mathcal{K} = \{k(\mathbf{x}) = |2\widehat{\eta}(\mathbf{x}) - 1|I(g(\mathbf{x})(\widehat{\eta}(\mathbf{x}) - 1/2) < 0), g \in \{\widetilde{g}, g_G^*, \widetilde{g}_G^*\}\}$. This completes the proof. \square

S.2.7 Proof of Theorem S7

First, by Theorem S6, the utility bound in this example is given as

$$\begin{aligned} U_c(\widetilde{g}_{log}, \widehat{g}_{log}) &\leq |R_{0-1}(\widehat{g}_{log}) - R_{0-1}(g_G^*)| + |\widetilde{R}_{0-1}(\widetilde{g}_{log}) - \widetilde{R}_{0-1}(\widetilde{g}_G^*)| + 16\|\widehat{\eta} - \eta\|_{L^2(\mathbb{P}_{\mathbf{X}})} \\ &\quad + 4D_{\mathcal{K}}(\mathbb{P}_{\mathbf{X}}, \mathbb{P}_{\widetilde{\mathbf{X}}}). \end{aligned} \tag{S32}$$

where $\mathcal{K} = \{k(\mathbf{x}) = |2\widehat{\eta}(\mathbf{x}) - 1|I(g(\mathbf{x})(\widehat{\eta}(\mathbf{x}) - 1/2) < 0), g \in \{\widetilde{g}, g_G^*, \widetilde{g}_G^*\}\}$. To prove the convergence of $U_c(\widetilde{g}_{log}, \widehat{g}_{log})$, it suffices to prove the convergence of each component of the upper bound in (S32). Note that $\widehat{\beta}$ is a maximum likelihood estimator, therefore it follows from

asymptotic normality of M -estimator that $\|\widehat{\boldsymbol{\beta}} - \boldsymbol{\beta}^*\|_2 = o_p(1)$. The model specification is $\mathcal{G} = \{g(\mathbf{x}) = \mathbf{x}^T \boldsymbol{\beta} : \boldsymbol{\beta} \in [-B, B]^p\}$ and $\|\boldsymbol{\beta}^*\|_\infty < B/2$. Therefore, the model specification \mathcal{G} asymptotically includes $\widehat{\boldsymbol{\beta}}^T \mathbf{x}$. For example, if $\|\widehat{\boldsymbol{\beta}} - \boldsymbol{\beta}^*\|_2 \leq B/2$, then we get $\|\widehat{\boldsymbol{\beta}}\|_\infty \leq \|\boldsymbol{\beta}^*\|_\infty + B/2 < B$, which implies $\widehat{\boldsymbol{\beta}}^T \mathbf{x} \in \mathcal{G}$. Let $\mathcal{E} = \{\widehat{\boldsymbol{\beta}} \notin [-B, B]^p\}$ denotes the event that $\widehat{\boldsymbol{\beta}}$ falls into $[-B, B]^p$. There exist some positive constants C_1, C_2 such that $\mathbb{P}(\mathcal{E}) \geq 1 - C_1 \exp(-C_2 n)$.

1. Convergence of $|R_{0-1}(\widehat{g}_{log}) - R_{0-1}(g_G^*)|$. Conditional on the event \mathcal{E} , we have $R_{0-1}(g_G^*) = R_{0-1}(g^*)$ and $\widehat{\eta}(\mathbf{x}) = 1/(1 + \exp(-\widehat{g}_{log}(\mathbf{x})))$, where $g^*(\mathbf{x}) = \mathbf{x}^T \boldsymbol{\beta}^*$.

$$\begin{aligned} R_{0-1}(\widehat{g}_{log}) - R_{0-1}(g_G^*) &= \int_{\mathcal{X}} |2\eta(\mathbf{x}) - 1| I(\text{sign}(\widehat{g}_{log}(\mathbf{x})) \neq \text{sign}(g^*(\mathbf{x}))) P_{\mathbf{X}}(\mathbf{x}) d\mathbf{x} \\ &= \int_{\mathcal{X}} |2\eta(\mathbf{x}) - 1| I(\text{sign}(\widehat{\eta}(\mathbf{x}) - 1/2) \neq \text{sign}(\eta(\mathbf{x}) - 1/2)) P_{\mathbf{X}}(\mathbf{x}) d\mathbf{x} \\ &\leq 2 \int_{\mathcal{X}} |\eta(\mathbf{x}) - \widehat{\eta}(\mathbf{x})| P_{\mathbf{X}}(\mathbf{x}) d\mathbf{x} \leq 2 \|\widehat{\eta} - \eta\|_{L^2(\mathbb{P}_{\mathbf{X}})}, \end{aligned}$$

where the second last inequality follows from the fact that $\text{sign}(\widehat{\eta}(\mathbf{x}) - 1/2) \neq \text{sign}(\eta(\mathbf{x}) - 1/2)$ implies that $|2\eta(\mathbf{x}) - 1| \leq 2|\eta(\mathbf{x}) - \widehat{\eta}(\mathbf{x})|$. Then, $|\eta(\mathbf{x}) - \widehat{\eta}(\mathbf{x})|$ can be further bounded as

$$|\widehat{\eta}(\mathbf{x}) - \eta(\mathbf{x})| = \left| \frac{1}{1 + \exp(-\mathbf{x}^T \widehat{\boldsymbol{\beta}})} - \frac{1}{1 + \exp(-\mathbf{x}^T \boldsymbol{\beta}^*)} \right| \leq \frac{1}{4} \|\mathbf{x}\|_2 \cdot \|\widehat{\boldsymbol{\beta}} - \boldsymbol{\beta}^*\|_2. \quad (\text{S33})$$

With (S33), it follows that

$$\|\widehat{\eta} - \eta\|_{L^2(\mathbb{P}_{\mathbf{X}})}^2 \leq \frac{1}{16} \mathbb{E}_{\mathbf{X}}(\|\mathbf{X}\|_2^2) \|\widehat{\boldsymbol{\beta}} - \boldsymbol{\beta}^*\|_2^2.$$

Therefore, we get $R_{0-1}(\widehat{g}_{log}) - R_{0-1}(g_G^*) = \|\widehat{\eta} - \eta\|_{L^2(\mathbb{P}_{\mathbf{X}})} = o_p(1)$ given that $\|\widehat{\boldsymbol{\beta}} - \boldsymbol{\beta}^*\|_2 = o_p(1)$.

2. Convergence of $|\widetilde{R}_{0-1}(\widetilde{g}_{log}) - \widetilde{R}_{0-1}(\widetilde{g}_G^*)|$. Here it is worth noting that $|\widetilde{R}_{0-1}(\widetilde{g}_{log}) - \widetilde{R}_{0-1}(\widetilde{g}_G^*)|$ consists of two sources of randomness from the real dataset and synthetic dataset. Additionally, since the model specification is correct, we have $\widetilde{\Phi}_{0-1}(\widetilde{g}_{log}) = |\widetilde{R}_{0-1}(\widetilde{g}_{log}) - \widetilde{R}_{0-1}(\widetilde{g}_G^*)|$. Then it suffices to prove the convergence of $\widetilde{\Phi}_{0-1}(\widetilde{g}_{log})$. We define

$$\mathcal{V} = \left\{ \eta(\mathbf{x}) = \frac{1}{1 + \exp(-g(\mathbf{x}))} : g \in \mathcal{G} \right\} \text{ and } \mathcal{L} = \left\{ \mathbb{P}_{\widetilde{\mathbf{X}}, \widetilde{\mathcal{Z}}} : \mathbb{P}(\widetilde{\mathcal{Z}} = 1 | \mathbf{X}) = \eta(\mathbf{X}), \eta \in \mathcal{V} \right\}.$$

Here all distributions in \mathcal{L} have the same marginal distribution $\mathbb{P}_{\widetilde{\mathbf{X}}}$ by assumption. Moreover,

conditional on the event \mathcal{E} , \mathcal{L} consists of all possible synthetic distributions. Therefore, we consider bounding the following term.

$$\sup_{\mathbb{P}_{\tilde{\mathbf{x}}, \tilde{\mathbf{z}} \in \mathcal{L}}} \tilde{\Phi}_{0-1}(\tilde{g}_{log}) = \sup_{\mathbb{P}_{\tilde{\mathbf{x}}, \tilde{\mathbf{z}} \in \mathcal{L}}} \left| \tilde{R}_{0-1}(\tilde{g}_{log}) - \tilde{R}_{0-1}(\tilde{g}_G^*) \right|.$$

We first prove the convergence of $\tilde{\Phi}_{0-1}(\tilde{g}_{log})$ under any fixed synthetic distribution. By Theorem 2.1 of Zhang (2004), for any synthetic distribution $\mathbb{P}_{\tilde{\mathbf{x}}, \tilde{\mathbf{z}}}$, we have

$$\tilde{\Phi}_{0-1}(\tilde{g}_{log}) \lesssim \sqrt{\tilde{R}_{log}(\tilde{g}_{log}) - \tilde{R}_{log}(\tilde{g}_G^*)}, \quad (\text{S34})$$

where $\tilde{R}_{log}(g)$ is defined as

$$\begin{aligned} \tilde{R}_{log}(g) &= \int_{\mathcal{X}} \left[\hat{\eta}(\mathbf{x}) \log(1 + e^{-g(\mathbf{x})}) + (1 - \hat{\eta}(\mathbf{x})) \log(1 + e^{g(\mathbf{x})}) \right] P_{\tilde{\mathbf{X}}}(\mathbf{x}) d\mathbf{x} \\ &= \int_{\mathcal{X}} \left[\log(1 + e^{g(\mathbf{x})}) - \hat{\eta}(\mathbf{x}) g(\mathbf{x}) \right] P_{\tilde{\mathbf{X}}}(\mathbf{x}) d\mathbf{x}. \end{aligned}$$

Then the convergence of $\tilde{R}_{log}(\tilde{g}_{log}) - \tilde{R}_{log}(\tilde{g}_G^*)$ can be proved by a uniform convergence argument as follow.

$$\tilde{R}_{log}(\tilde{g}_{log}) - \tilde{R}_{log}(\tilde{g}_G^*) \leq 2 \sup_{g \in \mathcal{G}} \left| \hat{\tilde{R}}_{log}(g) - \tilde{R}_{log}(g) \right|,$$

where $\hat{\tilde{R}}_{log}(g) = \frac{1}{\tilde{n}} \sum_{i=1}^{\tilde{n}} \log(1 + \exp(-\tilde{z}_i g(\tilde{\mathbf{x}}_i)))$.

Conditional on the event \mathcal{E} , for two different samples $(\tilde{\mathbf{x}}_i, \tilde{z}_i)$ and $(\tilde{\mathbf{x}}'_i, \tilde{z}'_i)$, we have

$$\left| \frac{1}{\tilde{n}} \log(1 + e^{-\tilde{z}'_i g(\tilde{\mathbf{x}}'_i)}) - \frac{1}{\tilde{n}} \log(1 + e^{-\tilde{z}_i g(\tilde{\mathbf{x}}_i)}) \right| \leq \frac{1}{\tilde{n}} |g(\tilde{\mathbf{x}}'_i) - g(\tilde{\mathbf{x}}_i)| \leq \frac{2pBC_0}{\tilde{n}},$$

where C_0 is the upper bound for each dimension of \mathbf{x} . Using the McDiarmid's inequality, we have

$$\mathbb{P} \left(\sup_{g \in \mathcal{G}} \left| \hat{\tilde{R}}_{log}(g) - \tilde{R}_{log}(g) \right| - \mathbb{E} \left[\sup_{g \in \mathcal{G}} \left| \hat{\tilde{R}}_{log}(g) - \tilde{R}_{log}(g) \right| \right] \geq \epsilon \right) \leq \exp(-C_1 \tilde{n} \epsilon^2), \quad (\text{S35})$$

for some constant $C_1 > 0$.

Next, we provide an upper bound for $\mathbb{E} \left[\sup_{g \in \mathcal{G}} \left| \hat{\tilde{R}}_{log}(g) - \tilde{R}_{log}(g) \right| \right]$. Let $\mathcal{D}'_c = \{(\mathbf{x}'_i, y'_i)\}_{i=1}^{\tilde{n}}$

denote a ghost dataset and denote $l(g(\tilde{\mathbf{x}}_i), \tilde{z}_i) = \log(1 + e^{-\tilde{z}_i g(\tilde{\mathbf{x}}_i)})$.

$$\begin{aligned}
& \mathbb{E} \left[\sup_{g \in \mathcal{G}} |\widehat{R}_{\log}(g) - \widetilde{R}_{\log}(g)| \right] = \mathbb{E} \left[\sup_{g \in \mathcal{G}} \left| \mathbb{E}_{\mathcal{D}'_c} \left(\widehat{R}_{\log}(g) - \widetilde{R}'_{\log}(g) \right) \right| \right] \\
& \leq \mathbb{E} \left[\sup_{g \in \mathcal{G}} \left| \left(\widehat{R}_{\log}(g) - \widetilde{R}'_{\log}(g) \right) \right| \right] = \mathbb{E} \left[\sup_{g \in \mathcal{G}} \left| \frac{1}{n} \sum_{i=1}^n \sigma_i (l(g(\tilde{\mathbf{x}}_i), \tilde{z}_i) - l(g(\tilde{\mathbf{x}}'_i), \tilde{z}'_i)) \right| \right] \\
& \leq 2 \mathbb{E} \left[\sup_{g \in \mathcal{G}} \left| \frac{1}{\tilde{n}} \sum_{i=1}^{\tilde{n}} \sigma_i l(g(\tilde{\mathbf{x}}_i), \tilde{z}_i) \right| \right].
\end{aligned}$$

By the fact that $l(g(\tilde{\mathbf{x}}_i), \tilde{z}_i)$ is a 1-Lipschitz, we have

$$\mathbb{E} \left[\sup_{g \in \mathcal{G}} \left| \frac{1}{\tilde{n}} \sum_{i=1}^{\tilde{n}} \sigma_i l(g(\tilde{\mathbf{x}}_i), \tilde{z}_i) \right| \right] \leq \mathbb{E} \left[\sup_{g \in \mathcal{G}} \left| \frac{1}{\tilde{n}} \sum_{i=1}^{\tilde{n}} \sigma_i g(\tilde{\mathbf{x}}_i) \right| \right] \lesssim \frac{1}{\sqrt{\tilde{n}}}. \quad (\text{S36})$$

Combining (S35) and (S36), it follows that

$$\mathbb{P} \left(\sup_{g \in \mathcal{G}} \left| \widehat{R}_{\log}(g) - \widetilde{R}_{\log}(g) \right| \geq \log^{1/2}(\tilde{n}) \tilde{n}^{-1/2} + C_3 \tilde{n}^{-1/2} \right) \lesssim n^{-C_1}. \quad (\text{S37})$$

Therefore, for any fixed synthetic distribution $\mathbb{P}_{\tilde{\mathbf{X}}, \tilde{\mathbf{Z}}}$, it follows that

$$\widetilde{R}_{\log}(\tilde{g}_{\log}) - \widetilde{R}_{\log}(\tilde{g}_{\log}^*) = o_p(1). \quad (\text{S38})$$

With (S38), we turn to develop a uniform convergence argument for $\sup_{\mathbb{P}_{\tilde{\mathbf{X}}, \tilde{\mathbf{Z}}} \in \mathcal{K}} \widetilde{R}_{\log}(\tilde{g}_{\log}) - \widetilde{R}_{\log}(\tilde{g}_{\log}^*)$. To this end, we need to measure the complexity of \mathcal{L} . Let $\widetilde{R}'_{\log}(g)$ denote the risk under the the distribution $\mathbb{P}'_{\tilde{\mathbf{X}}, \tilde{\mathbf{Z}}} \in \mathcal{L}$. For any pair of synthetic distributions $\mathbb{P}_{\tilde{\mathbf{X}}, \tilde{\mathbf{Z}}}, \mathbb{P}'_{\tilde{\mathbf{X}}, \tilde{\mathbf{Z}}} \in \mathcal{K}$,

$$\begin{aligned}
& \left| \sup_{g \in \mathcal{G}} \left| \widehat{R}_{\log}(g) - \widetilde{R}_{\log}(g) \right| - \sup_{g \in \mathcal{G}} \left| \widetilde{R}'_{\log}(g) - \widetilde{R}_{\log}(g) \right| \right| \leq \sup_{g \in \mathcal{G}} \left| \widetilde{R}_{\log}(g) - \widetilde{R}'_{\log}(g) \right| \\
& = \sup_{g \in \mathcal{G}} \left| \int_{\mathcal{X}} \left\{ [\eta(\mathbf{x}) - \eta'(\mathbf{x})] \log(1 + \exp(-g(\mathbf{x}))) + [\eta'(\mathbf{x}) - \eta(\mathbf{x})] \log(1 + \exp(g(\mathbf{x}))) \right\} \mathbb{P}_{\tilde{\mathbf{X}}}(\mathbf{x}) d\mathbf{x} \right| \\
& \leq \sup_{g \in \mathcal{G}} \mathbb{E}_{\mathbf{X}} [|\eta(\mathbf{X}) - \eta'(\mathbf{X})|] \cdot \sup_{\mathbf{x} \in \mathcal{X}} |g(\mathbf{x})| \leq \sup_{g \in \mathcal{G}, \mathbf{x} \in \mathcal{X}} |g(\mathbf{x})| \cdot \|\eta - \eta'\|_{L^2(\mathbb{P}_{\tilde{\mathbf{X}}})}. \quad (\text{S39})
\end{aligned}$$

Let $\mathcal{C}(\xi, \mathcal{V}, \|\cdot\|_{L^2(\mathbb{P}_{\tilde{\mathbf{X}}})})$ denote an ξ -covering set of \mathcal{V} and $\mathcal{L}_{\mathcal{C}} = \left\{ \mathbb{P}_{\tilde{\mathbf{X}}, \tilde{\mathbf{Z}}} : \mathbb{P}(\tilde{\mathbf{Z}} = 1 | \mathbf{X}) = \eta(\mathbf{X}), \eta \in \mathcal{C}(\xi, \mathcal{V}, \|\cdot\|_{L^2(\mathbb{P}_{\tilde{\mathbf{X}}})}) \right\}$. Furthermore, we define

$$\mathcal{S} = \left\{ \sup_{g \in \mathcal{G}} \left| \widehat{R}_{\log}(g) - \widetilde{R}_{\log}(g) \right| : \mathbb{P}_{\tilde{\mathbf{X}}, \tilde{\mathbf{Z}}} \in \mathcal{K} \right\} \text{ and } \mathcal{B} = \left\{ \sup_{g \in \mathcal{G}} \left| \widehat{R}_{\log}(g) - \widetilde{R}_{\log}(g) \right| : \mathbb{P}_{\tilde{\mathbf{X}}, \tilde{\mathbf{Z}}} \in \mathcal{K}_{\mathcal{C}} \right\}.$$

From (S39), we can see that \mathcal{B} is an $\sup_{g \in \mathcal{G}, \mathbf{x} \in \mathcal{X}} |g(\mathbf{x})| \xi$ -covering set of \mathcal{S} . For ease of notation, we denote $Q(\mathbb{P}_{\widetilde{\mathbf{X}}, \widetilde{\mathbf{Z}}}) = \sup_{g \in \mathcal{G}} |\widehat{R}_{\log}(g) - \widetilde{R}_{\log}(g)|$. For any $\mathbb{P}_{\widetilde{\mathbf{X}}, \widetilde{\mathbf{Z}}} \in \mathcal{K}$, there exists $\mathbb{P}'_{\widetilde{\mathbf{X}}, \widetilde{\mathbf{Z}}} \in \mathcal{K}_C$ such that

$$\begin{aligned} \sup_{\mathbb{P}_{\widetilde{\mathbf{X}}, \widetilde{\mathbf{Z}}} \in \mathcal{K}} Q(\mathbb{P}_{\widetilde{\mathbf{X}}, \widetilde{\mathbf{Z}}}) &\leq \sup_{\mathbb{P}_{\widetilde{\mathbf{X}}, \widetilde{\mathbf{Z}}} \in \mathcal{K}} \left| Q(\mathbb{P}_{\widetilde{\mathbf{X}}, \widetilde{\mathbf{Z}}}) - Q(\mathbb{P}'_{\widetilde{\mathbf{X}}, \widetilde{\mathbf{Z}}}) \right| + \sup_{\mathbb{P}'_{\widetilde{\mathbf{X}}, \widetilde{\mathbf{Z}}} \in \mathcal{B}} Q(\mathbb{P}'_{\widetilde{\mathbf{X}}, \widetilde{\mathbf{Z}}}) \\ &\leq \sup_{g \in \mathcal{G}, \mathbf{x} \in \mathcal{X}} |g(\mathbf{x})| \xi + \sup_{\mathbb{P}'_{\widetilde{\mathbf{X}}, \widetilde{\mathbf{Z}}} \in \mathcal{B}} Q(\mathbb{P}'_{\widetilde{\mathbf{X}}, \widetilde{\mathbf{Z}}}). \end{aligned} \quad (\text{S40})$$

With this, it holds that for any $\epsilon > 0$,

$$\mathbb{P} \left(\sup_{\mathbb{P}_{\widetilde{\mathbf{X}}, \widetilde{\mathbf{Z}}} \in \mathcal{K}} Q(\mathbb{P}_{\widetilde{\mathbf{X}}, \widetilde{\mathbf{Z}}}) > \epsilon \right) \leq \mathbb{P} \left(\sup_{\mathbb{P}'_{\widetilde{\mathbf{X}}, \widetilde{\mathbf{Z}}} \in \mathcal{B}} Q(\mathbb{P}'_{\widetilde{\mathbf{X}}, \widetilde{\mathbf{Z}}}) > \epsilon - \sup_{g \in \mathcal{G}, \mathbf{x} \in \mathcal{X}} |g(\mathbf{x})| \xi \right). \quad (\text{S41})$$

From (S33), we have $|\mathcal{B}| = |\mathcal{C}(\xi, \mathcal{V}, \|\cdot\|_{L^2(\mathbb{P}_{\widetilde{\mathbf{X}}})})| \asymp \xi^{-p}$. By setting $\epsilon = 2 \sup_{g \in \mathcal{G}, \mathbf{x} \in \mathcal{X}} |g(\mathbf{x})| \xi$, there exists constants $C_4, C_5 > 0$ such that

$$\mathbb{P} \left(\sup_{\mathbb{P}_{\widetilde{\mathbf{X}}, \widetilde{\mathbf{Z}}} \in \mathcal{B}} Q(\mathbb{P}_{\widetilde{\mathbf{X}}, \widetilde{\mathbf{Z}}}) > \epsilon \right) \leq C_4 \exp(-C_5(\tilde{n}\epsilon^2 - p \log(1/\epsilon))),$$

where the right-hand side converges to 0 as \tilde{n} goes to infinity provided that $\epsilon \asymp \sqrt{p/\tilde{n} \log(\tilde{n}/p)}$.

Therefore, we have $\sup_{\mathbb{P}_{\widetilde{\mathbf{X}}, \widetilde{\mathbf{Z}}} \in \mathcal{K}} Q(\mathbb{P}_{\widetilde{\mathbf{X}}, \widetilde{\mathbf{Z}}}) = o_p(1)$. This combined with (S34) implies that for any $\delta > 0$,

$$\lim_{\tilde{n} \rightarrow \infty} \mathbb{P} \left(\sup_{\mathbb{P}_{\widetilde{\mathbf{X}}, \widetilde{\mathbf{Z}}} \in \mathcal{K}} \widetilde{\Phi}_{0-1}(\widetilde{g}_{\log}) > \delta \right) = 0. \quad (\text{S42})$$

3. Convergence of $D_{\mathcal{K}}(\mathbb{P}_{\mathbf{X}}, \mathbb{P}_{\widetilde{\mathbf{X}}})$. In this example, $D_{\mathcal{K}}(\mathbb{P}_{\mathbf{X}}, \mathbb{P}_{\widetilde{\mathbf{X}}})$ can be written as

$$\begin{aligned} D_{\mathcal{K}}(\mathbb{P}_{\mathbf{X}}, \mathbb{P}_{\widetilde{\mathbf{X}}}) &\leq \left| \int_{\mathcal{X}} |2\widehat{\eta}(\mathbf{x}) - 1| I(\widetilde{g}_{\log}(\mathbf{x})(\widehat{\eta}(\mathbf{x}) - 1/2) < 0) [P_{\mathbf{X}}(\mathbf{x}) - P_{\widetilde{\mathbf{X}}}(\mathbf{x})] d\mathbf{x} \right| \\ &\quad + \left| \int_{\mathcal{X}} |2\widehat{\eta}(\mathbf{x}) - 1| I(g_{\mathcal{G}}^*(\mathbf{x})(\widehat{\eta}(\mathbf{x}) - 1/2) < 0) [P_{\mathbf{X}}(\mathbf{x}) - P_{\widetilde{\mathbf{X}}}(\mathbf{x})] d\mathbf{x} \right|. \end{aligned}$$

By the assumption that $M_1 \leq P_{\widetilde{\mathbf{X}}}(\mathbf{x})/P_{\mathbf{X}}(\mathbf{x}) \leq M_2$, we have

$$D_{\mathcal{K}}(\mathbb{P}_{\mathbf{X}}, \mathbb{P}_{\widetilde{\mathbf{X}}}) \leq 2(M_2 + 1) \|\widehat{\eta} - \eta\|_{L^2(\mathbb{P}_{\mathbf{X}})} + (M_1^{-1} + 1) \widetilde{\Phi}_{0-1}(\widetilde{g}_{\log}).$$

To sum up, we have

$$\begin{aligned}\mathbb{P}(U_c(\tilde{g}, \hat{g}) > \delta) &= \mathbb{P}(U_c(\tilde{g}, \hat{g}) > \delta | \mathcal{E}) \mathbb{P}(\mathcal{E}) + \mathbb{P}(U_c(\tilde{g}, \hat{g}) > \delta | \mathcal{E}^c) \mathbb{P}(\mathcal{E}^c) \\ &\leq \mathbb{P}(U_c(\tilde{g}, \hat{g}) > \delta | \mathcal{E}) + \mathbb{P}(\mathcal{E}^c) \leq \mathbb{P}(U_c(\tilde{g}, \hat{g}) > \delta | \mathcal{E}) + C_1 \exp(-C_2 n).\end{aligned}$$

It remains to bound $\mathbb{P}(U_c(\tilde{g}, \hat{g}) > \delta | \mathcal{E})$.

$$\mathbb{P}(U_c(\tilde{g}, \hat{g}) > \delta | \mathcal{E}) \leq \mathbb{P}(4(M_1^{-1} + 2)\tilde{\Phi}_{0-1}(\tilde{g}_{log}) > \delta | \mathcal{E}) + \mathbb{P}(4(M_2 + 7)\|\hat{\eta} - \eta\|_{L^2(\mathbb{P}_X)} > \delta | \mathcal{E}).$$

This completes the proof. \square

S.2.8 Proof of Theorem S8

The proof for the classification case is similar to that for the regression case. We first denote that $g_{\mathcal{G}_1}^* = \operatorname{argmin}_{g \in \mathcal{G}_1} R_{0-1}(g)$ and $g_{\mathcal{G}_2}^* = \operatorname{argmin}_{g \in \mathcal{G}_2} R_{0-1}(g)$. Next, we proceed to find a sufficient condition for $R_{0-1}(\tilde{g}_{\mathcal{G}_1}^*) > R_{0-1}(\tilde{g}_{\mathcal{G}_2}^*)$. Notice that $R_{0-1}(\tilde{g}_{\mathcal{G}_1}^*) \geq R_{0-1}(g_{\mathcal{G}_1}^*)$, it suffices to prove $\Phi_{0-1}(g_{\mathcal{G}_1}^*) > \Phi_{0-1}(\tilde{g}_{\mathcal{G}_2}^*)$.

$$\begin{aligned}\Phi_{0-1}(\tilde{g}_{\mathcal{G}_2}^*) &= \int_{\mathcal{X}} I(\operatorname{sign}(\tilde{g}_{\mathcal{G}_2}^*(\mathbf{x})) \neq \operatorname{sign}(\eta(\mathbf{x}) - 1/2)) |2\eta(\mathbf{x}) - 1| P_{\mathbf{X}}(\mathbf{x}) d\mathbf{x} \\ &\leq \int_{\mathcal{X}} I(\operatorname{sign}(\tilde{g}_{\mathcal{G}_2}^*(\mathbf{x})) \neq \operatorname{sign}(\hat{\eta}(\mathbf{x}) - 1/2)) |2\eta(\mathbf{x}) - 1| P_{\mathbf{X}}(\mathbf{x}) d\mathbf{x} \\ &\quad + \int_{\mathcal{X}} I(\operatorname{sign}(\eta(\mathbf{x}) - 1/2) \neq \operatorname{sign}(\hat{\eta}(\mathbf{x}) - 1/2)) |2\eta(\mathbf{x}) - 1| P_{\mathbf{X}}(\mathbf{x}) d\mathbf{x} \\ &\leq \int_{\mathcal{X}} I(\operatorname{sign}(\tilde{g}_{\mathcal{G}_2}^*(\mathbf{x})) \neq \operatorname{sign}(\hat{\eta}(\mathbf{x}) - 1/2)) |2\eta(\mathbf{x}) - 1| P_{\mathbf{X}}(\mathbf{x}) d\mathbf{x} + 2 \int_{\mathcal{X}} |\eta(\mathbf{x}) - \hat{\eta}(\mathbf{x})| P_{\mathbf{X}}(\mathbf{x}) d\mathbf{x} \\ &\leq \int_{\mathcal{X}} I(\operatorname{sign}(\tilde{g}_{\mathcal{G}_2}^*(\mathbf{x})) \neq \operatorname{sign}(\hat{\eta}(\mathbf{x}) - 1/2)) |2\eta(\mathbf{x}) - 1| P_{\mathbf{X}}(\mathbf{x}) d\mathbf{x} + 2\|\hat{\eta} - \eta\|_{L^2(\mathbb{P}_X)} \\ &\leq \int_{\mathcal{X}} I(\operatorname{sign}(\tilde{g}_{\mathcal{G}_2}^*(\mathbf{x})) \neq \operatorname{sign}(\hat{\eta}(\mathbf{x}) - 1/2)) |2\hat{\eta}(\mathbf{x}) - 1| P_{\mathbf{X}}(\mathbf{x}) d\mathbf{x} + 4\|\hat{\eta} - \eta\|_{L^2(\mathbb{P}_X)}.\end{aligned}$$

Next, we decompose \mathcal{X} into two parts.

$$\mathcal{X} = \left\{ \mathbf{x} \in \mathcal{X} : \frac{P_{\mathbf{X}}(\mathbf{x})}{P_{\tilde{\mathbf{X}}}(\mathbf{x})} \leq C \right\} \cup \left\{ \mathbf{x} \in \mathcal{X} : \frac{P_{\mathbf{X}}(\mathbf{x})}{P_{\tilde{\mathbf{X}}}(\mathbf{x})} \geq C \right\} \triangleq \mathcal{X}_1 \cup \mathcal{X}_2.$$

For ease of notation, we denote $J(g_1(\mathbf{x}), g_2(\mathbf{x})) = I(\text{sign}(g_1(\mathbf{x})) \neq \text{sign}(g_2(\mathbf{x})))$.

$$\begin{aligned}
& \int_{\mathcal{X}} J(\tilde{g}_{\mathcal{G}_2}^*(\mathbf{x}), \hat{\eta}(\mathbf{x}) - 1/2) |2\hat{\eta}(\mathbf{x}) - 1| P_{\mathbf{X}}(\mathbf{x}) d\mathbf{x} \\
&= \int_{\mathcal{X}_1} J(\tilde{g}_{\mathcal{G}_2}^*(\mathbf{x}), \hat{\eta}(\mathbf{x}) - 1/2) |2\hat{\eta}(\mathbf{x}) - 1| P_{\mathbf{X}}(\mathbf{x}) d\mathbf{x} + \int_{\mathcal{X}_2} J(\tilde{g}_{\mathcal{G}_2}^*(\mathbf{x}), \hat{\eta}(\mathbf{x}) - 1/2) |2\hat{\eta}(\mathbf{x}) - 1| P_{\mathbf{X}}(\mathbf{x}) d\mathbf{x} \\
&\leq C \int_{\mathcal{X}_1} J(\tilde{g}_{\mathcal{G}_2}^*(\mathbf{x}), \hat{\eta}(\mathbf{x}) - 1/2) |2\hat{\eta}(\mathbf{x}) - 1| P_{\tilde{\mathbf{X}}}(\mathbf{x}) d\mathbf{x} + V \cdot C^{-d} \leq C \tilde{\Phi}_{0-1}(\tilde{g}_{\mathcal{G}_2}^*) + V \cdot C^{-d}.
\end{aligned}$$

By the fact that $f(x) = ax + bx^{-d}$ attains its minimum at $x = (db/a)^{1/(d+1)}$, we set $C = (dV/\tilde{\Phi}_{0-1}(\tilde{g}_{\mathcal{G}_2}^*))^{\frac{1}{d+1}}$, which yields that

$$\begin{aligned}
& \int_{\mathcal{X}} J(\tilde{g}_{\mathcal{G}_2}^*(\mathbf{x}), \hat{\eta}(\mathbf{x}) - 1/2) |2\hat{\eta}(\mathbf{x}) - 1| P_{\mathbf{X}}(\mathbf{x}) d\mathbf{x} \\
&\leq (d^{\frac{1}{d+1}} + d^{-\frac{d}{d+1}}) V^{\frac{1}{d+1}} \left(\tilde{\Phi}_{0-1}(g_{\mathcal{G}_2}^*) \right)^{\frac{d}{d+1}} + \leq (d^{\frac{1}{d+1}} + d^{-\frac{d}{d+1}}) V^{\frac{1}{d+1}} \left(\tilde{\Phi}_{0-1}(g_{\mathcal{G}_2}^*) \right)^{\frac{d}{d+1}}. \quad (\text{S43})
\end{aligned}$$

Next, we turn to establish relation between $\tilde{\Phi}_{0-1}(g_{\mathcal{G}_2}^*)$ and $\Phi_{0-1}(g_{\mathcal{G}_2}^*)$. We first apply a similar treatment to \mathcal{X} by the decomposition as

$$\mathcal{X} = \left\{ \mathbf{x} \in \mathcal{X} : \frac{P_{\tilde{\mathbf{X}}}(\mathbf{x})}{P_{\mathbf{X}}(\mathbf{x})} \leq C \right\} \cup \left\{ \mathbf{x} \in \mathcal{X} : \frac{P_{\tilde{\mathbf{X}}}(\mathbf{x})}{P_{\mathbf{X}}(\mathbf{x})} \geq C \right\} \triangleq \mathcal{X}_3 \cup \mathcal{X}_4,$$

for some positive constants C . With this, it follows that

$$\begin{aligned}
\tilde{\Phi}_{0-1}(g_{\mathcal{G}_2}^*) &= \int_{\mathcal{X}} J(g_{\mathcal{G}_2}^*(\mathbf{x}), \hat{\eta}(\mathbf{x}) - 1/2) |2\hat{\eta}(\mathbf{x}) - 1| P_{\tilde{\mathbf{X}}}(\mathbf{x}) d\mathbf{x} \\
&\leq \int_{\mathcal{X}_3} J(g_{\mathcal{G}_2}^*(\mathbf{x}), \hat{\eta}(\mathbf{x}) - 1/2) |2\hat{\eta}(\mathbf{x}) - 1| P_{\tilde{\mathbf{X}}}(\mathbf{x}) d\mathbf{x} \\
&\quad + \int_{\mathcal{X}_4} J(g_{\mathcal{G}_2}^*(\mathbf{x}), \hat{\eta}(\mathbf{x}) - 1/2) |2\hat{\eta}(\mathbf{x}) - 1| P_{\tilde{\mathbf{X}}}(\mathbf{x}) d\mathbf{x} \\
&\leq C \int_{\mathcal{X}} J(g_{\mathcal{G}_2}^*(\mathbf{x}), \hat{\eta}(\mathbf{x}) - 1/2) |2\hat{\eta}(\mathbf{x}) - 1| P_{\mathbf{X}}(\mathbf{x}) d\mathbf{x} + V \cdot C^{-d}.
\end{aligned}$$

Similarly, taking $C = (Vd/\int_{\mathcal{X}} J(g_{\mathcal{G}_2}^*(\mathbf{x}), \hat{\eta}(\mathbf{x}) - 1/2) |2\hat{\eta}(\mathbf{x}) - 1| P_{\mathbf{X}}(\mathbf{x}) d\mathbf{x})^{\frac{1}{d+1}}$ yields that

$$\tilde{R}_{0-1}(g_{\mathcal{G}_2}^*) \leq (d^{\frac{1}{d+1}} + d^{-\frac{d}{d+1}}) V^{\frac{1}{d+1}} \left(\int_{\mathcal{X}} J(g_{\mathcal{G}_2}^*(\mathbf{x}), \hat{\eta}(\mathbf{x}) - 1/2) |2\hat{\eta}(\mathbf{x}) - 1| P_{\mathbf{X}}(\mathbf{x}) d\mathbf{x} \right)^{\frac{d}{d+1}}. \quad (\text{S44})$$

Next, we proceed to bound the right-hand side.

$$\begin{aligned}
& \int_{\mathcal{X}} J(g_{\mathcal{G}_2}^*(\mathbf{x}), \widehat{\eta}(\mathbf{x}) - 1/2) |2\widehat{\eta}(\mathbf{x}) - 1| P_{\mathbf{X}}(\mathbf{x}) d\mathbf{x} \\
& \leq \int_{\mathcal{X}} J(g_{\mathcal{G}_2}^*(\mathbf{x}), \eta(\mathbf{x}) - 1/2) |2\widehat{\eta}(\mathbf{x}) - 1| P_{\mathbf{X}}(\mathbf{x}) d\mathbf{x} + \int_{\mathcal{X}} J(\eta(\mathbf{x}) - 1/2, \widehat{\eta}(\mathbf{x}) - 1/2) |2\widehat{\eta}(\mathbf{x}) - 1| P_{\mathbf{X}}(\mathbf{x}) d\mathbf{x} \\
& \leq \int_{\mathcal{X}} J(g_{\mathcal{G}_2}^*(\mathbf{x}), \eta(\mathbf{x}) - 1/2) (|2\widehat{\eta}(\mathbf{x}) - 1| - |2\eta(\mathbf{x}) - 1|) P_{\mathbf{X}}(\mathbf{x}) d\mathbf{x} + 2\|\widehat{\eta} - \eta\|_{L^2(\mathbb{P}_{\mathbf{X}})} \\
& \quad + \int_{\mathcal{X}} J(g_{\mathcal{G}_2}^*(\mathbf{x}), \eta(\mathbf{x}) - 1/2) |2\eta(\mathbf{x}) - 1| P_{\mathbf{X}}(\mathbf{x}) d\mathbf{x} \\
& \leq \Phi_{0-1}(g_{\mathcal{G}_2}^*) + 4\|\widehat{\eta} - \eta\|_{L^2(\mathbb{P}_{\mathbf{X}})}. \tag{S45}
\end{aligned}$$

Combining (S44) and (S45), we get

$$\widetilde{\Phi}_{0-1}(g_{\mathcal{G}_2}^*) \leq (d^{\frac{1}{d+1}} + d^{-\frac{d}{d+1}}) V^{\frac{1}{d+1}} (\Phi_{0-1}(g_{\mathcal{G}_2}^*) + 4\|\widehat{\eta} - \eta\|_{L^2(\mathbb{P}_{\mathbf{X}})})^{\frac{d}{d+1}}. \tag{S46}$$

Plugging (S46) into (S43)

$$\begin{aligned}
& \int_{\mathcal{X}} J(\widetilde{g}_{\mathcal{G}_2}^*(\mathbf{x}), \widehat{\eta}(\mathbf{x}) - 1/2) |2\widehat{\eta}(\mathbf{x}) - 1| P_{\mathbf{X}}(\mathbf{x}) d\mathbf{x} \\
& \leq (d^{\frac{1}{d+1}} + d^{-\frac{d}{d+1}})^{\frac{2d+1}{d+1}} V^{\frac{2d+1}{(d+1)^2}} (\Phi_{0-1}(g_{\mathcal{G}_2}^*) + 4\|\widehat{\eta} - \eta\|_{L^2(\mathbb{P}_{\mathbf{X}})})^{\frac{d^2}{(d+1)^2}}.
\end{aligned}$$

To sum up, we get

$$\begin{aligned}
\Phi_{0-1}(\widetilde{g}_{\mathcal{G}_2}^*) & \leq (d^{\frac{1}{d+1}} + d^{-\frac{d}{d+1}})^{\frac{2d+1}{d+1}} V^{\frac{2d+1}{(d+1)^2}} (\Phi_{0-1}(g_{\mathcal{G}_2}^*) + 4\|\widehat{\eta} - \eta\|_{L^2(\mathbb{P}_{\mathbf{X}})})^{\frac{d^2}{(d+1)^2}} + 4\|\widehat{\eta} - \eta\|_{L^2(\mathbb{P}_{\mathbf{X}})} \\
& \leq K_{d,V} (\Phi_{0-1}(g_{\mathcal{G}_2}^*))^{\frac{d^2}{(d+1)^2}} + 4K_{d,V} \|\widehat{\eta} - \eta\|_{L^2(\mathbb{P}_{\mathbf{X}})}^{\frac{d^2}{(d+1)^2}} + 4\|\widehat{\eta} - \eta\|_{L^2(\mathbb{P}_{\mathbf{X}})},
\end{aligned}$$

where $K_{d,V} = (d^{\frac{1}{d+1}} + d^{-\frac{d}{d+1}})^{\frac{2d+1}{d+1}} V^{\frac{2d+1}{(d+1)^2}}$. Clearly, we have $\Phi_{0-1}(\widetilde{g}_{\mathcal{G}_2}^*) < \Phi_{0-1}(\widetilde{g}_{\mathcal{G}_1}^*)$ if the following inequality holds true.

$$K_{d,V} (\Phi_{0-1}(g_{\mathcal{G}_2}^*))^{\frac{d^2}{(d+1)^2}} + 4K_{d,V} \|\widehat{\eta} - \eta\|_{L^2(\mathbb{P}_{\mathbf{X}})}^{\frac{d^2}{(d+1)^2}} + 4\|\widehat{\eta} - \eta\|_{L^2(\mathbb{P}_{\mathbf{X}})} < \Phi_{0-1}(g_{\mathcal{G}_1}^*).$$

This completes the proof of Theorem S8. □

S.2.9 Proof of Theorem S9

We first note that $\widehat{\eta}(\mathbf{x}), \eta(\mathbf{x}) \in [0, 1]$. Therefore, $\|\widehat{\eta} - \eta\|_{L^2(\mathbb{P}_{\mathbf{X}})} \leq \|\widehat{\eta} - \eta\|_{L^2(\mathbb{P}_{\mathbf{X}})}^{\frac{d^2}{(d+1)^2}}$. This indicates a sufficient condition to achieve condition (b) in Theorem S8 is

$$4(K_{d,V} + 1)\|\widehat{\eta} - \eta\|_{L^2(\mathbb{P}_{\mathbf{X}})}^{\frac{d^2}{(d+1)^2}} < \Phi_{0-1}(g_{\mathcal{G}_1}^*) - K_{d,V} (\Phi_{0-1}(g_{\mathcal{G}_2}^*))^{\frac{d^2}{(d+1)^2}}.$$

Then for any $(\mathcal{G}_1, \mathcal{G}_2) \in \mathcal{H}_c(u)$, we have

$$\begin{aligned} & \mathbb{P} \left((R_{0-1}(g_{\mathcal{G}_2}^*) - R_{0-1}(g_{\mathcal{G}_1}^*)) (R_{0-1}(\widetilde{g}_{\mathcal{G}_2}^*) - R_{0-1}(\widetilde{g}_{\mathcal{G}_1}^*)) > 0 \right) \\ & \geq \mathbb{P} \left(4(K_{d,V} + 1)\|\widehat{\eta} - \eta\|_{L^2(\mathbb{P}_{\mathbf{X}})}^{\frac{d^2}{(d+1)^2}} \leq u \right) \geq 1 - C_1 \exp \left(-C_2 a_n u^{\frac{(d+1)^2}{d^2}} (4K_{d,V} + 4)^{-\frac{(d+1)^2}{d^2}} \right). \end{aligned}$$

This completes the proof. □

S.3 Proof of Lemma 1

In the first example, $P_{\mathbf{X}}(\mathbf{x}) = P_{\widetilde{\mathbf{X}}}(\mathbf{x})$ for any $\mathbf{x} \in \mathcal{X}$. It follows that

$$\int_{\mathcal{X}'_C} P_{\widetilde{\mathbf{X}}}(\mathbf{x}) d\mathbf{x} = \int_{\mathcal{X}_C} P_{\mathbf{X}}(\mathbf{x}) d\mathbf{x} = \begin{cases} 1, C \in [0, 1], \\ 0, C \in (1, +\infty). \end{cases}$$

The desired result immediately follows by setting $V = 1$ and $d = \infty$.

For the second example, the density ratio $P_{\mathbf{X}}(\mathbf{x})/P_{\widetilde{\mathbf{X}}}(\mathbf{x})$ is upper bounded by M_2 and lower bounded by M_1 . Therefore, we can verify that

$$\int_{\mathcal{X}_C} P_{\mathbf{X}}(\mathbf{x}) d\mathbf{x} = \begin{cases} 1, C \in [0, M_1], \\ \text{unknown}, C \in (M_1, M_2), \\ 0, C \in [M_2, +\infty). \end{cases}$$

Note that the value of $\int_{\mathcal{X}_C} P_{\mathbf{X}}(\mathbf{x}) d\mathbf{x}$ is unknown on the interval (M_1, M_2) , depending on the explicit distributions of \mathbf{X} and $\widetilde{\mathbf{X}}$. Therefore, we consider the worst case that $\int_{\mathcal{X}_C} P_{\mathbf{X}}(\mathbf{x}) d\mathbf{x} \equiv 1$ for $C \in (M_1, M_2)$. Then by setting $V = M_2^d$, we can verify that

$$\int_{\mathcal{X}_C} P_{\mathbf{X}}(\mathbf{x}) d\mathbf{x} \leq M_2^d \cdot C^{-d}, \text{ for any } C > 0.$$

Applying a similar argument to $M_2^{-1} \leq P_{\tilde{\mathbf{X}}}(\mathbf{x})/P_{\mathbf{X}}(\mathbf{x}) \leq M_1^{-1}$ yields that

$$\int_{\mathcal{X}'_C} P_{\tilde{\mathbf{X}}}(\mathbf{x}) d\mathbf{x} \leq (M_1 C)^{-d}, \text{ for any } C > 0.$$

To sum up, we get

$$\max \left\{ \int_{\mathcal{X}_C} P_{\mathbf{X}}(\mathbf{x}) d\mathbf{x}, \int_{\mathcal{X}'_C} P_{\tilde{\mathbf{X}}}(\mathbf{x}) d\mathbf{x} \right\} \leq \max\{M_2^d, M_1^{-d}\} \cdot C^{-d}, \text{ for any } C > 0.$$

This completes the proof for the second example. \square

S.4 Proof of Corollary 1

The proof of Corollary 1 is a direct application of Theorem 5. First, applying similar steps as in the proof of Theorem 4, we have consistent model comparison if

$$\|\mu - \hat{\mu}\|_{L^2(\mathbb{P}_{\mathbf{X}})} + C_{d,V,U} \|\hat{\mu} - \mu\|_{L^2(\mathbb{P}_{\mathbf{X}})}^{\frac{d^2}{(d+1)^2}} \leq \sqrt{\Phi_r(f_{\mathcal{F}_1}^*)},$$

where the inequality utilizes the fact that $\Phi_r(f_{\mathcal{F}_2}^*) = 0$. Then we have

$$\begin{aligned} & \mathbb{P} \left((R_r(f_{\mathcal{F}_2}^*) - R_r(f_{\mathcal{F}_1}^*)) (R_r(\tilde{f}_{\mathcal{F}_2}^*) - R_r(\tilde{f}_{\mathcal{F}_1}^*)) < 0 \right) \\ & \leq \mathbb{P} \left(\|\mu - \hat{\mu}\|_{L^2(\mathbb{P}_{\mathbf{X}})} + C_{d,V,U} \|\hat{\mu} - \mu\|_{L^2(\mathbb{P}_{\mathbf{X}})}^{\frac{d^2}{(d+1)^2}} > \sqrt{\Phi_r(f_{\mathcal{F}_1}^*)} \right) \\ & = \mathbb{P} \left(\|\mu - \hat{\mu}\|_{L^2(\mathbb{P}_{\mathbf{X}})} + C_{d,V,U} \|\hat{\mu} - \mu\|_{L^2(\mathbb{P}_{\mathbf{X}})}^{\frac{d^2}{(d+1)^2}} > \sqrt{\Phi_r(f_{\mathcal{F}_1}^*)} \mid \{\|\mu - \hat{\mu}\|_{L^2(\mathbb{P}_{\mathbf{X}})} > 1\} \right) \mathbb{P}(\|\mu - \hat{\mu}\|_{L^2(\mathbb{P}_{\mathbf{X}})} > 1) \\ & + \mathbb{P} \left(\|\mu - \hat{\mu}\|_{L^2(\mathbb{P}_{\mathbf{X}})} + C_{d,V,U} \|\hat{\mu} - \mu\|_{L^2(\mathbb{P}_{\mathbf{X}})}^{\frac{d^2}{(d+1)^2}} > \sqrt{\Phi_r(f_{\mathcal{F}_1}^*)} \mid \{\|\mu - \hat{\mu}\|_{L^2(\mathbb{P}_{\mathbf{X}})} < 1\} \right) \mathbb{P}(\|\mu - \hat{\mu}\|_{L^2(\mathbb{P}_{\mathbf{X}})} < 1) \\ & \leq C_1 \exp(-C_2 a_n) + \mathbb{P} \left((C_{d,V,U} + 1) \|\hat{\mu} - \mu\|_{L^2(\mathbb{P}_{\mathbf{X}})}^{\frac{d^2}{(d+1)^2}} > \sqrt{\Phi_r(f_{\mathcal{F}_1}^*)} \right) \\ & \leq C_1 \left\{ \exp(-C_2 a_n) + \exp\left(-C_2 a_n [\Phi_r(f_{\mathcal{F}_1}^*)]^{\frac{(d+1)^2}{2d^2}} (C_{d,V,U} + 1)^{-\frac{(d+1)^2}{d^2}}\right) \right\}. \end{aligned}$$

This completes the proof. \square